High Performance Visible & Infrared Sensors for Exoplanet Astronomy

James W. Beletic
Teledyne Imaging Sensors

19 August 2010

Teledyne

Providing the best images of the Universe

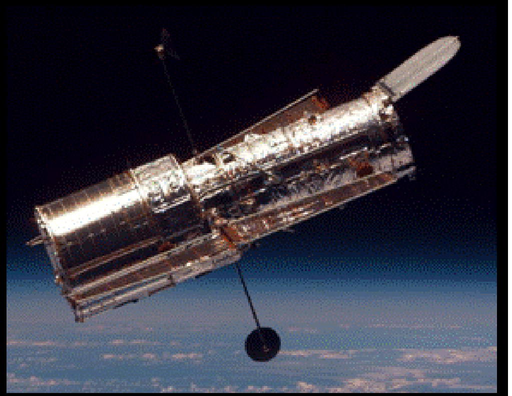

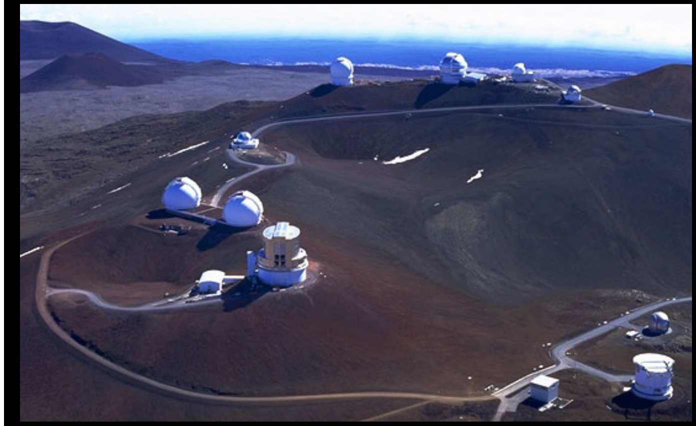

Credits and sincere thanks for information provided by the following organizations

e2v technologies

Peter Pool
Paul Jorden

MIT Lincoln Laboratory

Barry Burke
Vyshnavi Suntharalingham

Fairchild Imaging

Paul Vu

Semiconductor Technology Associates

Dick Bredthauer

Sarnoff

James Janesick

Disclaimer

All information presented in this slide set is accurate according to the best knowledge of James Beletic. Any errors in content or presentation are solely due to the author, and not the persons listed above.

The Ideal Detector for High Resolution Spectroscopy

• Detect 100% of photons	✓ Up to 98% quantum efficiency
• Each photon detected as a delta function	✓ One electron for each photon
• Large number of pixels	✓ 2K×2K, 2K×4K, 4K×4K, 10K×10K Gigapixel mosaics possible
• All pixels of equal size	✓ Mostly true (watch for stitch boundaries)
• Record charge where detected (i.e. no blurring within detector)	☒ Charge diffusion, charge transfer inefficiency (CTI), electrical crosstalk
• No noise other than photon noise	☒ Dark current, readout noise
• Time tag for each photon	☒ No – framing detectors
• Measure photon wavelength	☒ No – defined by filter
• Measure photon polarization	☒ No – defined by filter

Plus numerous other "features": poorly operating pixels (cosmetics), hot pixels, charge traps, persistence (latency), etc.

Basic Types of Imaging Sensors

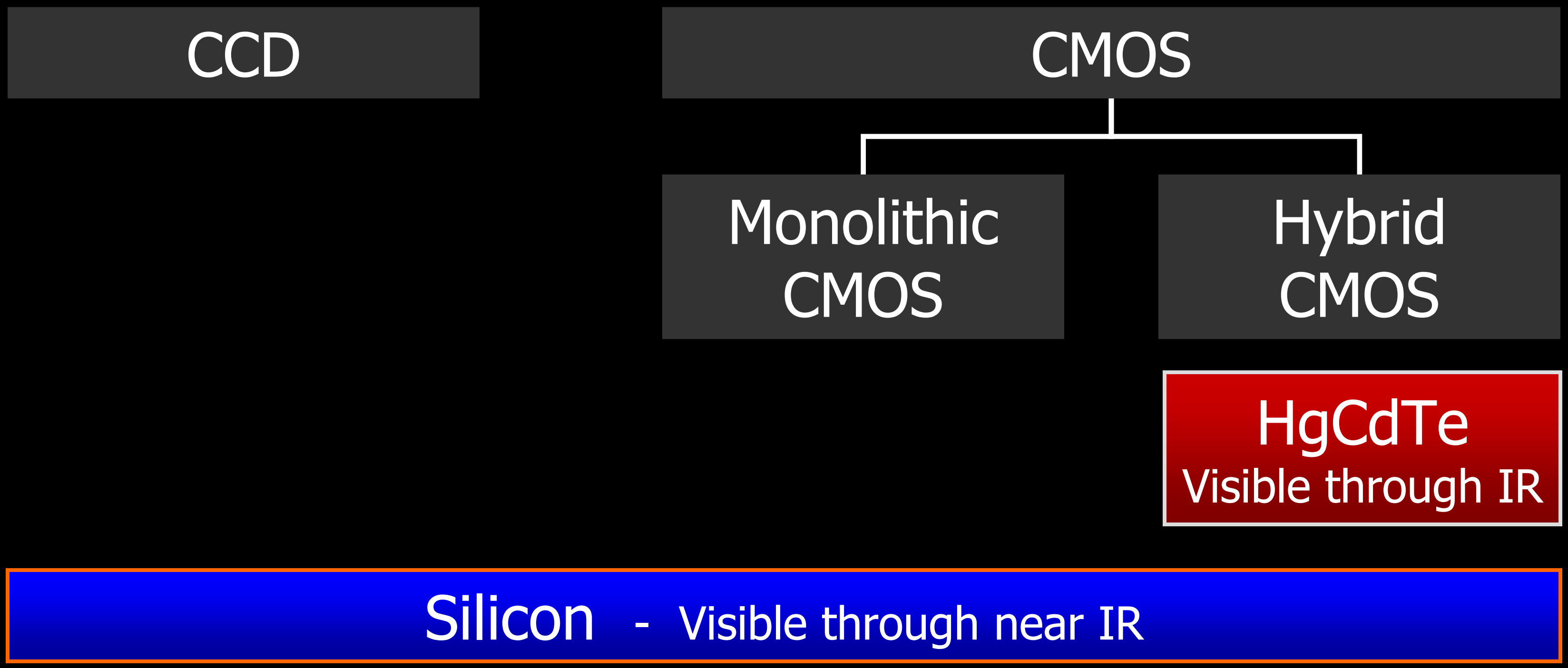

CCD

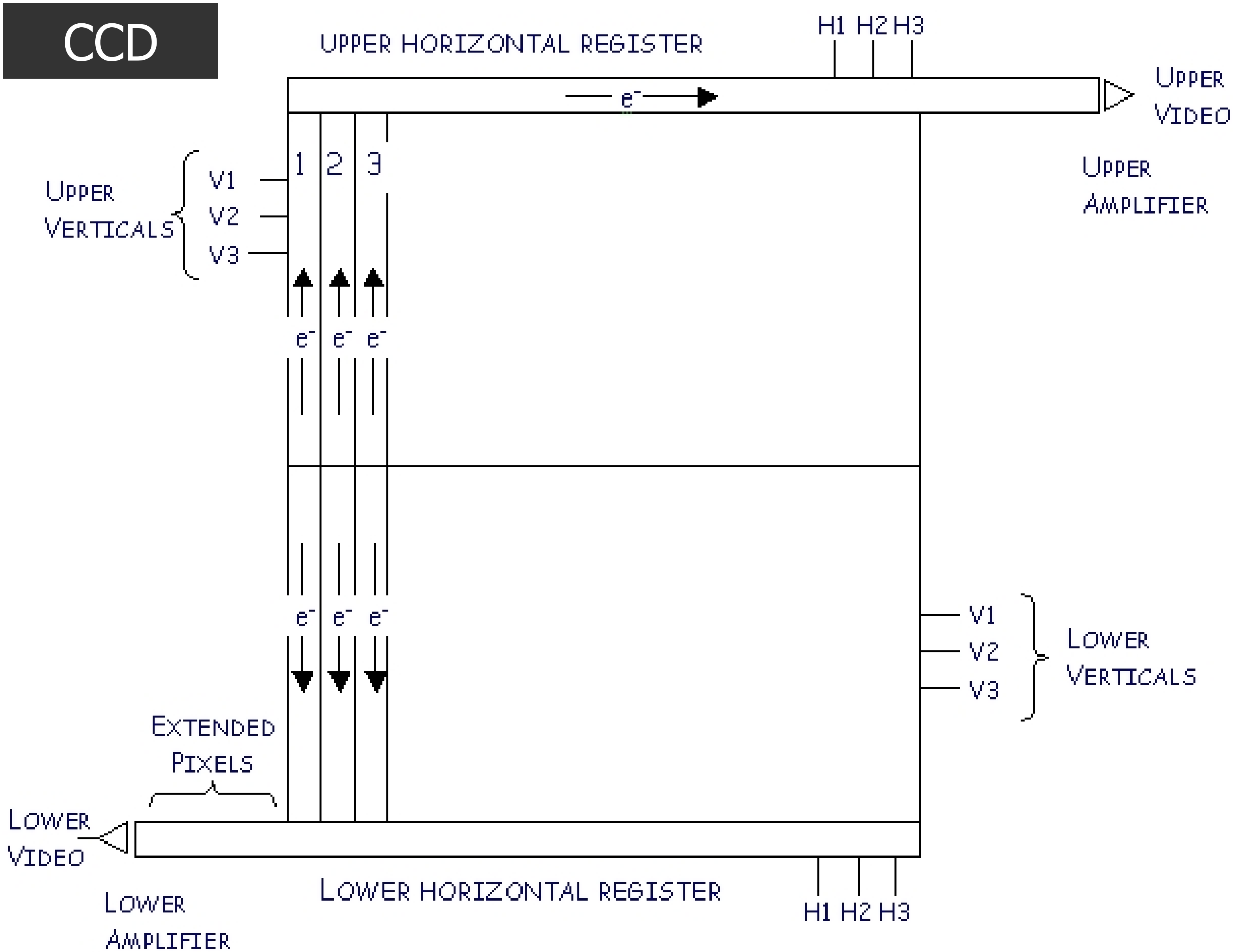

UPPER HORIZONTAL REGISTER
H1 H2 H3
e-
UPPER VIDEO
UPPER AMPLIFIER
UPPER VERTICALS
V1
V2
V3
1 2 3
e- e- e-
e- e- e-
V1
V2
V3
LOWER VERTICALS
EXTENDED PIXELS
LOWER VIDEO
LOWER AMPLIFIER
LOWER HORIZONTAL REGISTER
H1 H2 H3

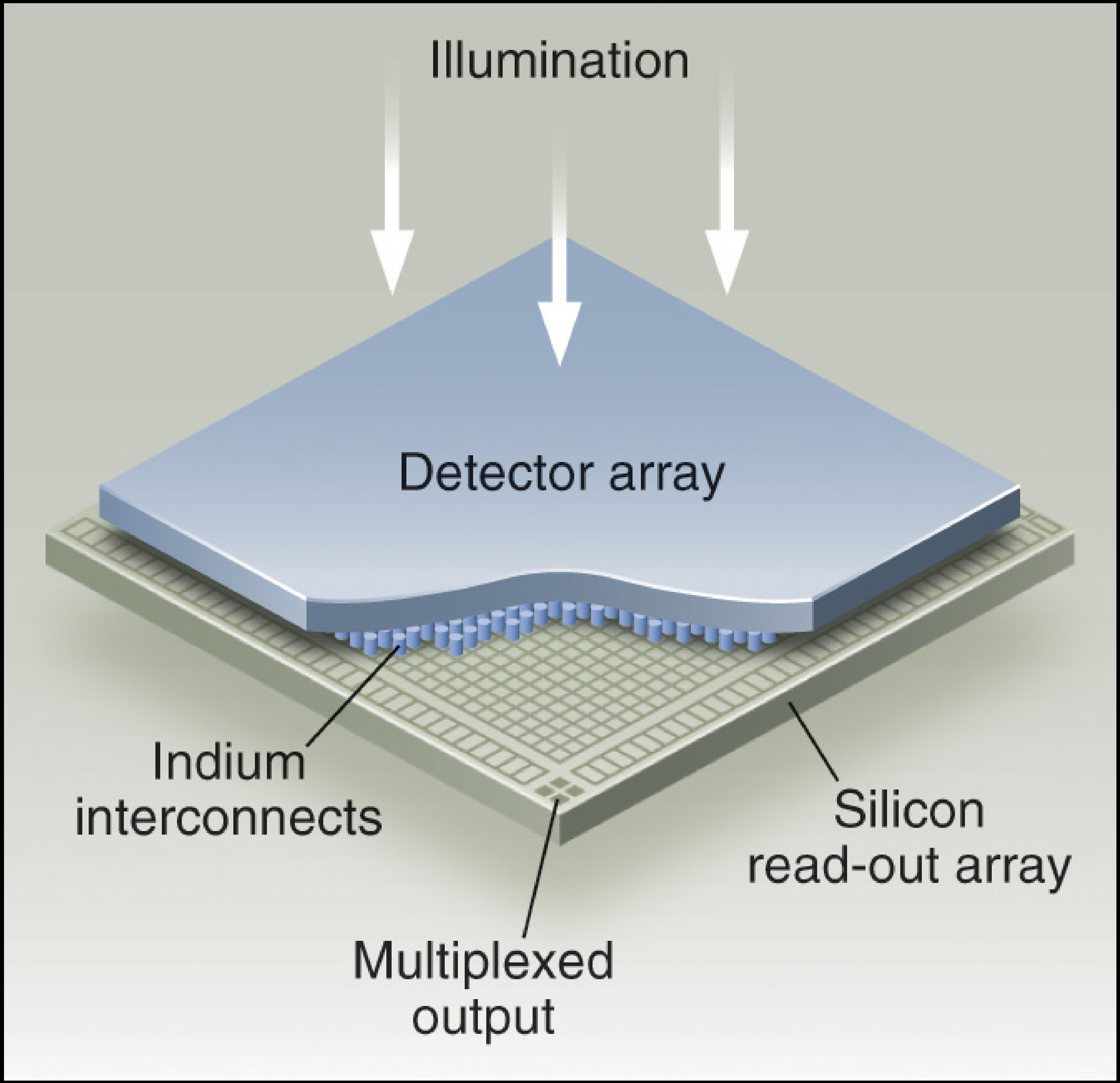
Illumination
Detector array
Indium interconnects
Silicon read-out array
Multiplexed output

Hybrid CMOS

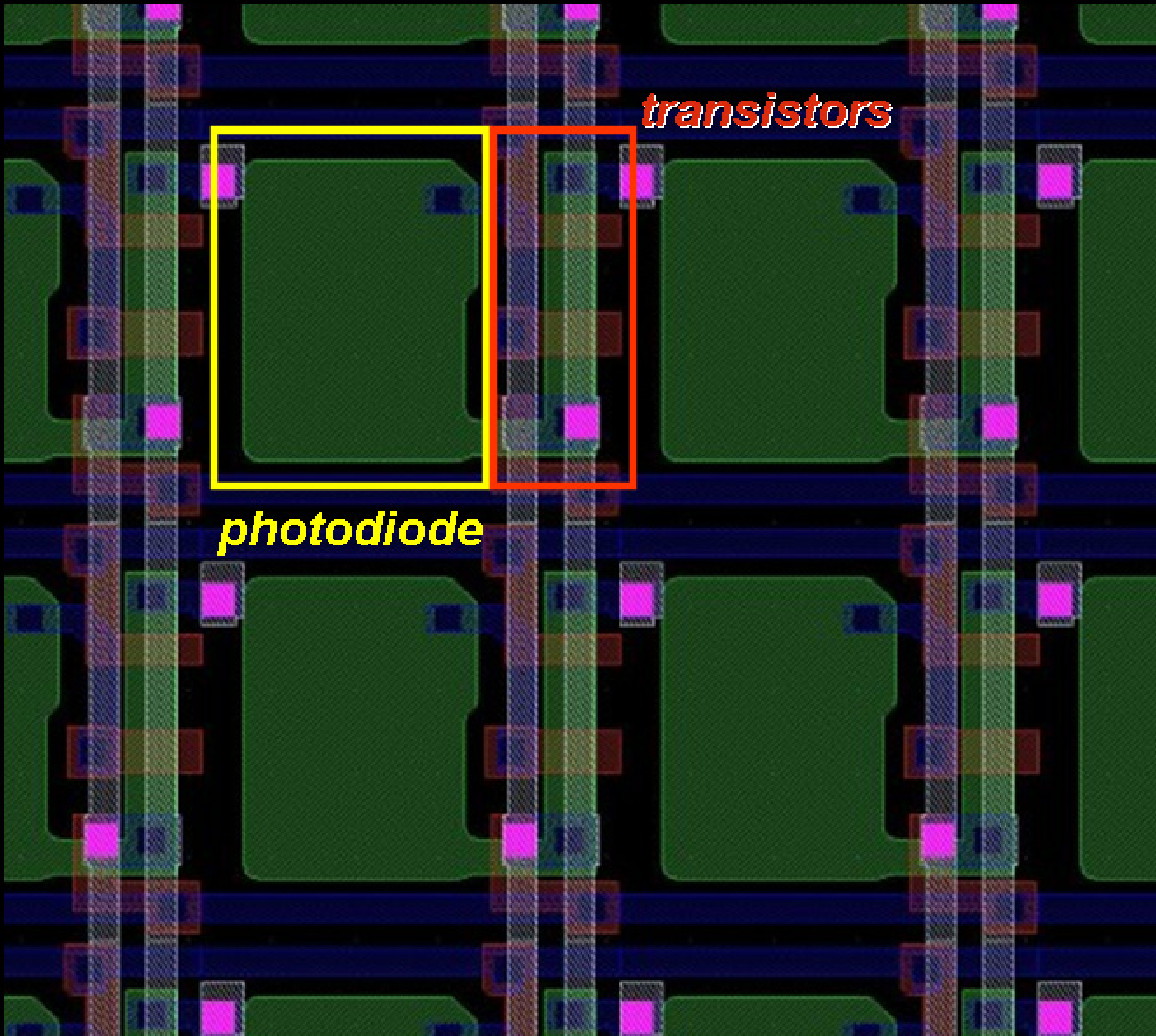

Monolithic CMOS

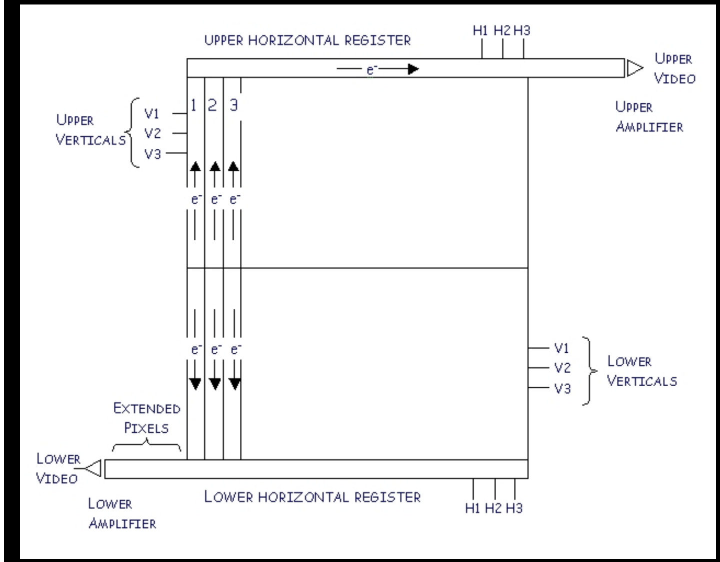

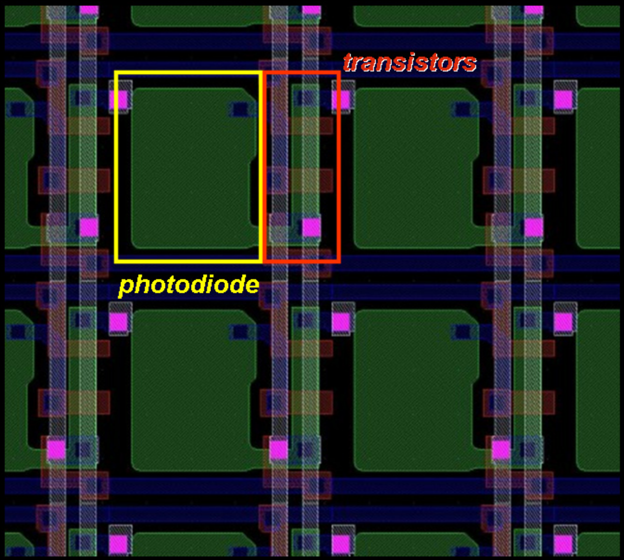

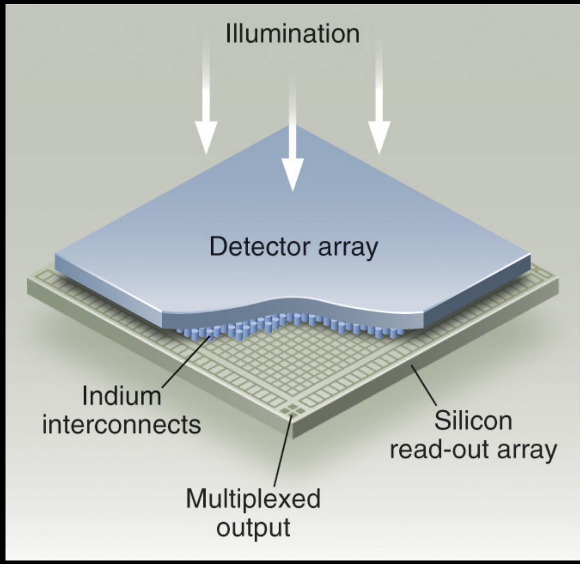

CCD

Monolithic CMOS

Hybrid CMOS

HgCdTe
Visible through IR

Silicon - Visible through near IR

Two main parts of an imaging detector

Detector material & Solid state electronics

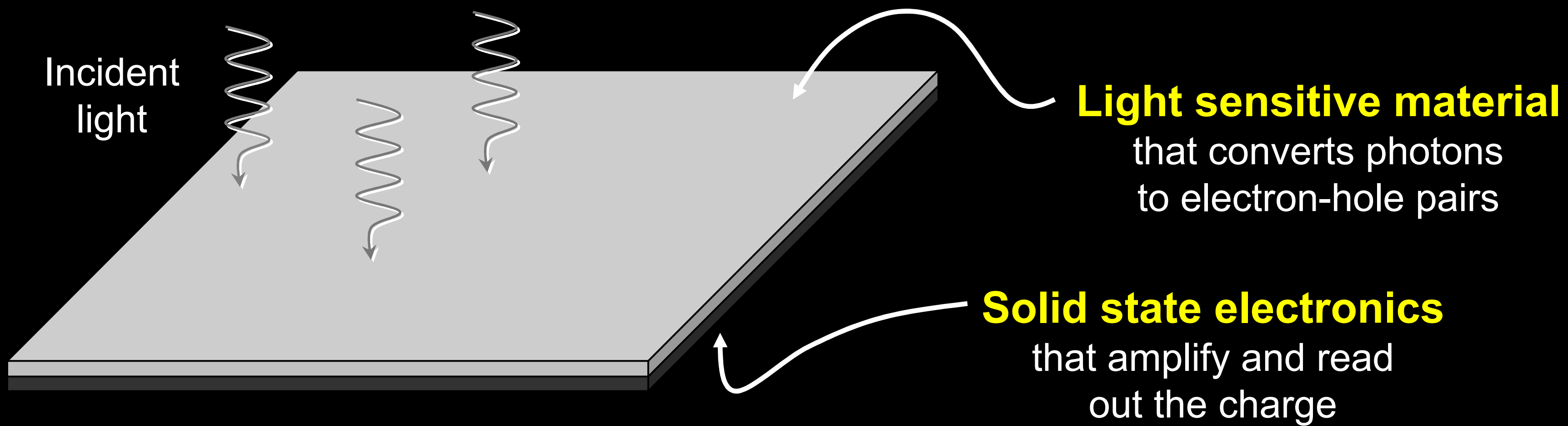

Charge Collection

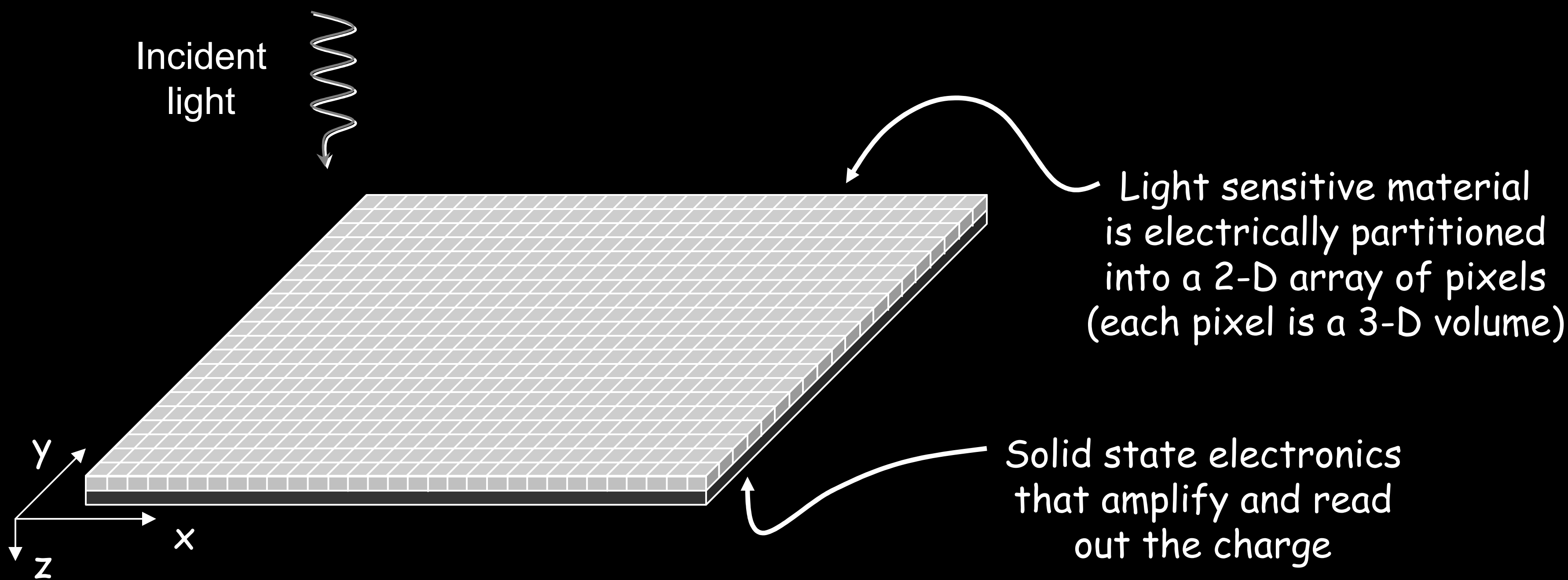

- Intensity image is generated by collecting photocharge generated in 3-D volume into 2-D array of pixels.
- Optical and IR focal plane arrays both collect charges via electric fields.
- In the z-direction, optical and IR use a p-n junction to "sweep" charge toward pixel collection nodes.

6 steps of optical / IR photon detection

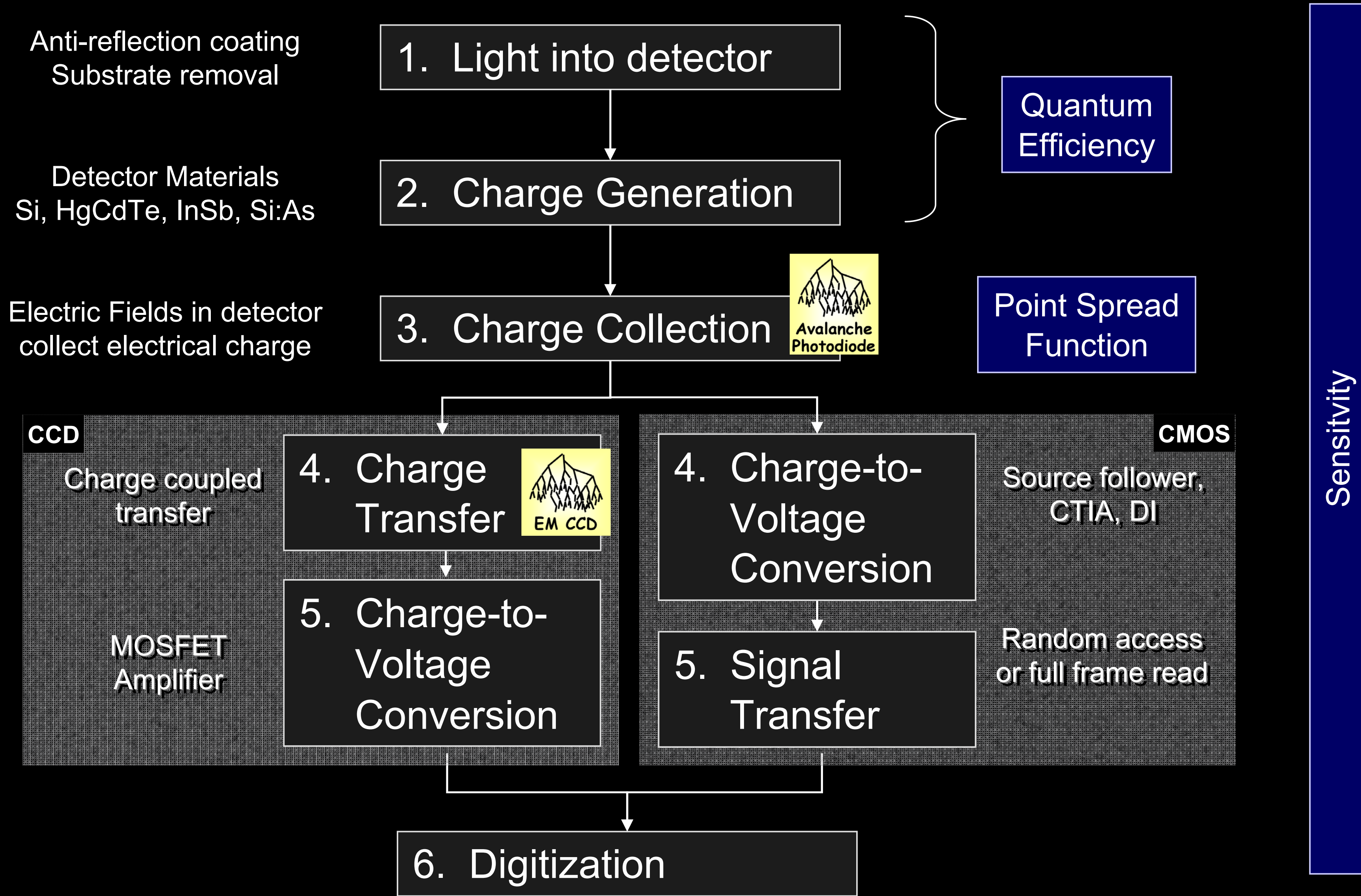

Crystals are excellent detectors of light

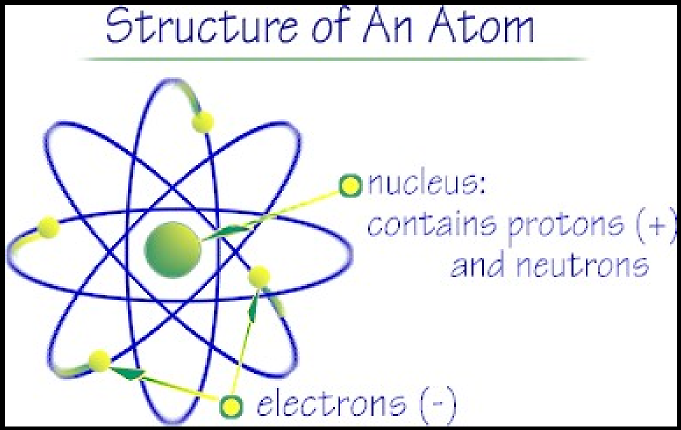

- Simple model of atom
  - Protons (+) and neutrons in the nucleus with electrons orbiting

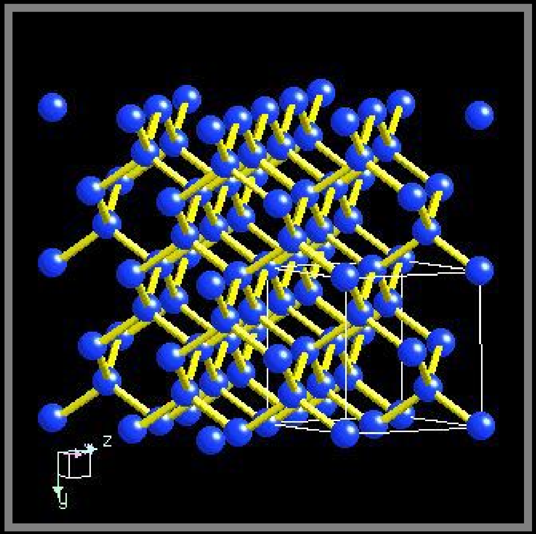

Silicon crystal lattice

- Electrons are trapped in the crystal lattice
  - by electric field of protons
- Light energy can free an electron from the grip of the protons, allowing the electron to roam about the crystal
  - creates an "electron-hole" pair.
- The photocharge can be collected and amplified, so that light is detected
- The light energy required to free an electron depends on the material.

Periodic Table

1 H Hydrogen 1.0																	2 He Helium 4.0
3 Li Lithium 6.9	4 Be Beryllium 9.0											5 B Boron 10.8	6 C Carbon 12.0	7 N Nitrogen 14.0	8 O Oxygen 16.0	9 F Fluorine 19.0	10 Ne Neon 20.2
11 Na Sodium 23.0	12 Mg Magnesium 9.0											13 Al Aluminum 27.0	14 Si Silicon 28.1	15 P Phosphorus 31.0	16 S Sulfur 32.1	17 Cl Chlorine 35.5	18 Ar Argon 40.0
19 K Potassium 39.1	20 Ca Calcium 40.2	21 Sc Scandium 45.0	22 Ti Titanium 47.9	23 V Vanadium 50.9	24 Cr Chromium 52.0	25 Mn Manganese 54.9	26 Fe Iron 55.9	27 Co Colbalt 58.9	28 Ni Nickel 58.7	29 Cu Copper 63.5	30 Zn Zinc 65.4	31 Ga Gallium 69.7	32 Ge Germanium 72.6	33 As Arsenic 74.9	34 Se Selenium 79.0	35 Br Bromine 79.9	36 Kr Krypton 83.8
37 Rb Rubidium 85.5	38 Sr Strontium 87.6	39 Y Yttrium 88.9	40 Zr Zirconium 91.2	41 Nb Niobium 92.9	42 Mo Molybdenum 95.9	43 Tc Technetium 99	44 Ru Ruthenium 101.0	45 Rh Rhodium 102.9	46 Pd Palladium 106.4	47 Ag Silver 107.9	48 Cd Cadmium 112.4	49 In Indium 114.8	50 Sn Tin 118.7	51 Sb Antimony 121.8	52 Te Tellurium 127.6	53 I Iodine 126.9	54 Xe Xenon 131.3
55 Cs Caesium 132.9	56 Ba Barium 137.4	57-71	72 Hf Hafnium 178.5	73 Ta Tantalum 181.0	74 W Tungsten 183.9	75 Re Rhenium 186.2	76 Os Osmium 190.2	77 Ir Iridium 192.2	78 Pt Platinum 195.1	79 Au Gold 197.0	80 Hg Mercury 200.6	81 Tl Thallium 204.4	82 Pb Lead 207.2	83 Bi Bismuth 209.0	84 Po Polonium 210.0	85 At Astatine 210.0	86 Rn Radon 222.0
87 Fr Francium 223.0	88 Ra Radium 226.0	89-103	104 Rf Rutherfordium 261	105 Db Dubnium 262	106 Sg Seaborgium 263	107 Bh Bohrium 262	108 Hs Hassium 265	109 Mt Meitnerium 266	110 Uun Ununnilium 272								

57 La Lanthanum 138.9	58 Ce Cerium 140.1	59 Pr Praseodymium 140.9	60 Nd Neodymium 144.2	61 Pm Promethium 147.0	62 Sm Samarium 150.4	63 Eu Europium 152.0	64 Gd Gadolinium 157.3	65 Tb Terbium 158.9	66 Dy Dysprosium 162.5	67 Ho Holmium 164.9	68 Er Erbium 167.3	69 Tm Thulium 168.9	70 Yb Ytterbium 173.0	71 Lu Lutetium 175.0
89 Ac Actinium 132.9	90 Th Thorium 232.0	91 Pa Protactinium 231.0	92 U Uranium 238.0	93 Np Neptunium 237.0	94 Pu Plutonium 242.0	95 Am Americium 243.0	96 Cm Curium 247.0	97 Bk Berkelium 247.0	98 Cf Californium 251.0	99 Es Einsteinium 254.0	100 Fm Fermium 253.0	101 Md Mendelevium 256.0	102 No Nobelium 254.0	103 Lr Lawrencium 257.0

Types of Elements Key:

- Alkali metals
- Alkaline earth metals
- Transition metals
- Lanthanides
- Actinides
- Poor metals
- Semi-metals
- Non-metals
- Noble gases

The Astronomer's Periodic Table

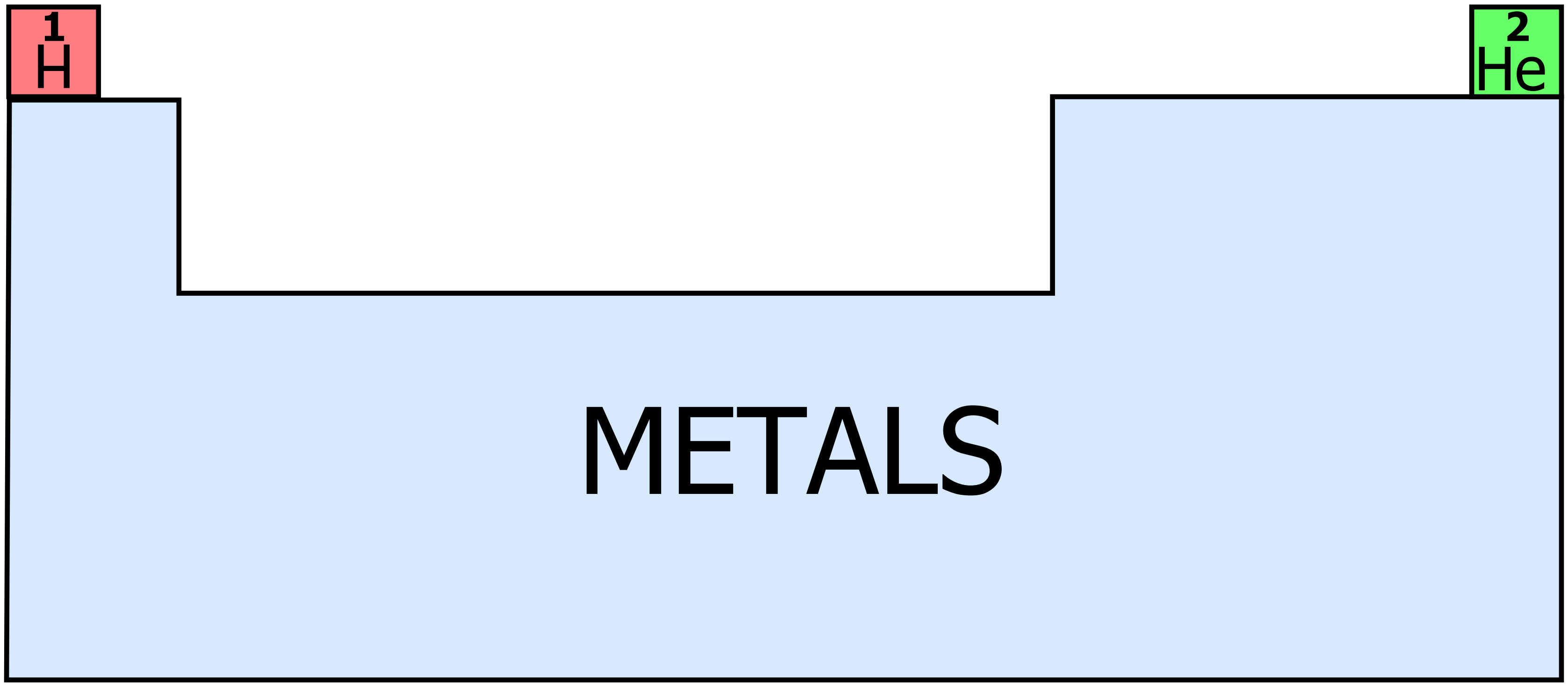

Periodic Table

1 H Hydrogen 1.0																	2 He Helium 4.0
3 Li Lithium 6.9	4 Be Beryllium 9.0											5 B Boron 10.8	6 C Carbon 12.0	7 N Nitrogen 14.0	8 O Oxygen 16.0	9 F Fluorine 19.0	10 Ne Neon 20.2
11 Na Sodium 23.0	12 Mg Magnesium 9.0											13 Al Aluminum 27.0	14 Si Silicon 28.1	15 P Phosphorus 31.0	16 S Sulfur 32.1	17 Cl Chlorine 35.5	18 Ar Argon 40.0
19 K Potassium 39.1	20 Ca Calcium 40.2	21 Sc Scandium 45.0	22 Ti Titanium 47.9	23 V Vanadium 50.9	24 Cr Chromium 52.0	25 Mn Manganese 54.9	26 Fe Iron 55.9	27 Co Colbalt 58.9	28 Ni Nickel 58.7	29 Cu Copper 63.5	30 Zn Zinc 65.4	31 Ga Gallium 69.7	32 Ge Germanium 72.6	33 As Arsenic 74.9	34 Se Selenium 79.0	35 Br Bromine 79.9	36 Kr Krypton 83.8
37 Rb Rubidium 85.5	38 Sr Strontium 87.6	39 Y Yttrium 88.9	40 Zr Zirconium 91.2	41 Nb Niobium 92.9	42 Mo Molybdenum 95.9	43 Tc Technetium 99	44 Ru Ruthenium 101.0	45 Rh Rhodium 102.9	46 Pd Palladium 106.4	47 Ag Silver 107.9	48 Cd Cadmium 112.4	49 In Indium 114.8	50 Sn Tin 118.7	51 Sb Antimony 121.8	52 Te Tellurium 127.6	53 I Iodine 126.9	54 Xe Xenon 131.3
55 Cs Caesium 132.9	56 Ba Barium 137.4	57-71	72 Hf Hafnium 178.5	73 Ta Tantalum 181.0	74 W Tungsten 183.9	75 Re Rhenium 186.2	76 Os Osmium 190.2	77 Ir Iridium 192.2	78 Pt Platinum 195.1	79 Au Gold 197.0	80 Hg Mercury 200.6	81 Tl Thallium 204.4	82 Pb Lead 207.2	83 Bi Bismuth 209.0	84 Po Polonium 210.0	85 At Astatine 210.0	86 Rn Radon 222.0
87 Fr Francium 223.0	88 Ra Radium 226.0	89-103	104 Rf Rutherfordium 261	105 Db Dubnium 262	106 Sg Seaborgium 263	107 Bh Bohrium 262	108 Hs Hassium 265	109 Mt Meitnerium 266	110 Uun Ununnilium 272								

57 La Lanthanum 138.9	58 Ce Cerium 140.1	59 Pr Praseodymium 140.9	60 Nd Neodymium 144.2	61 Pm Promethium 147.0	62 Sm Samarium 150.4	63 Eu Europium 152.0	64 Gd Gadolinium 157.3	65 Tb Terbium 158.9	66 Dy Dysprosium 162.5	67 Ho Holmium 164.9	68 Er Erbium 167.3	69 Tm Thulium 168.9	70 Yb Ytterbium 173.0	71 Lu Lutetium 175.0
89 Ac Actinium 132.9	90 Th Thorium 232.0	91 Pa Protactinium 231.0	92 U Uranium 238.0	93 Np Neptunium 237.0	94 Pu Plutonium 242.0	95 Am Americium 243.0	96 Cm Curium 247.0	97 Bk Berkelium 247.0	98 Cf Californium 251.0	99 Es Einsteinium 254.0	100 Fm Fermium 253.0	101 Md Mendelevium 256.0	102 No Nobelium 254.0	103 Lr Lawrencium 257.0

Types of Elements Key:

- Alkali metals
- Alkaline earth metals
- Transition metals
- Lanthanides
- Actinides
- Poor metals
- Semi-metals
- Non-metals
- Noble gases

Periodic Table

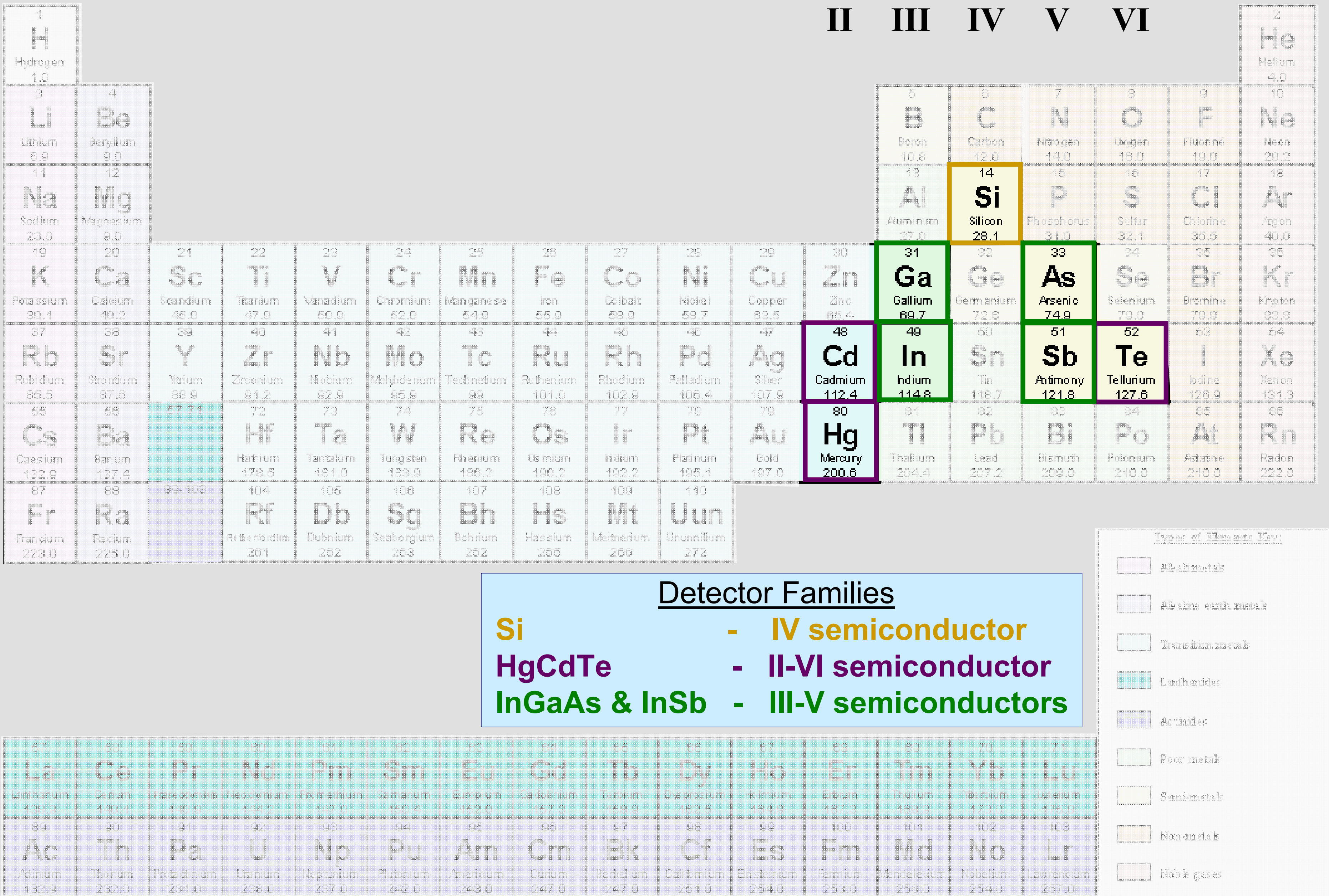

Photon Detection

For an electron to be excited from the conduction band to the valence band

$$h\nu > E_g$$

h = Planck constant (6.6310^{-34} Joule•sec)
ν = frequency of light (cycles/sec) = λ/c
E_g = energy gap of material (electron-volts)

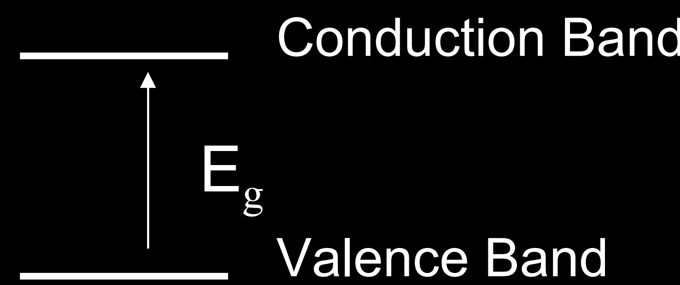

$\lambda_c = 1.238 / E_g$ (eV)

Material Name	Symbol	E_g (eV)	λ_c (μm)
Silicon	Si	1.12	1.1
Indium Antimonide	InSb	0.23	5.5
Mer-Cad-Tel	HgCdTe	1.00 – 0.07	1.24 – 18

Tunable Wavelength: Valuable property of HgCdTe

$Hg_{1-x}Cd_xTe$ Modify ratio of Mercury and Cadmium to “tune” the bandgap energy

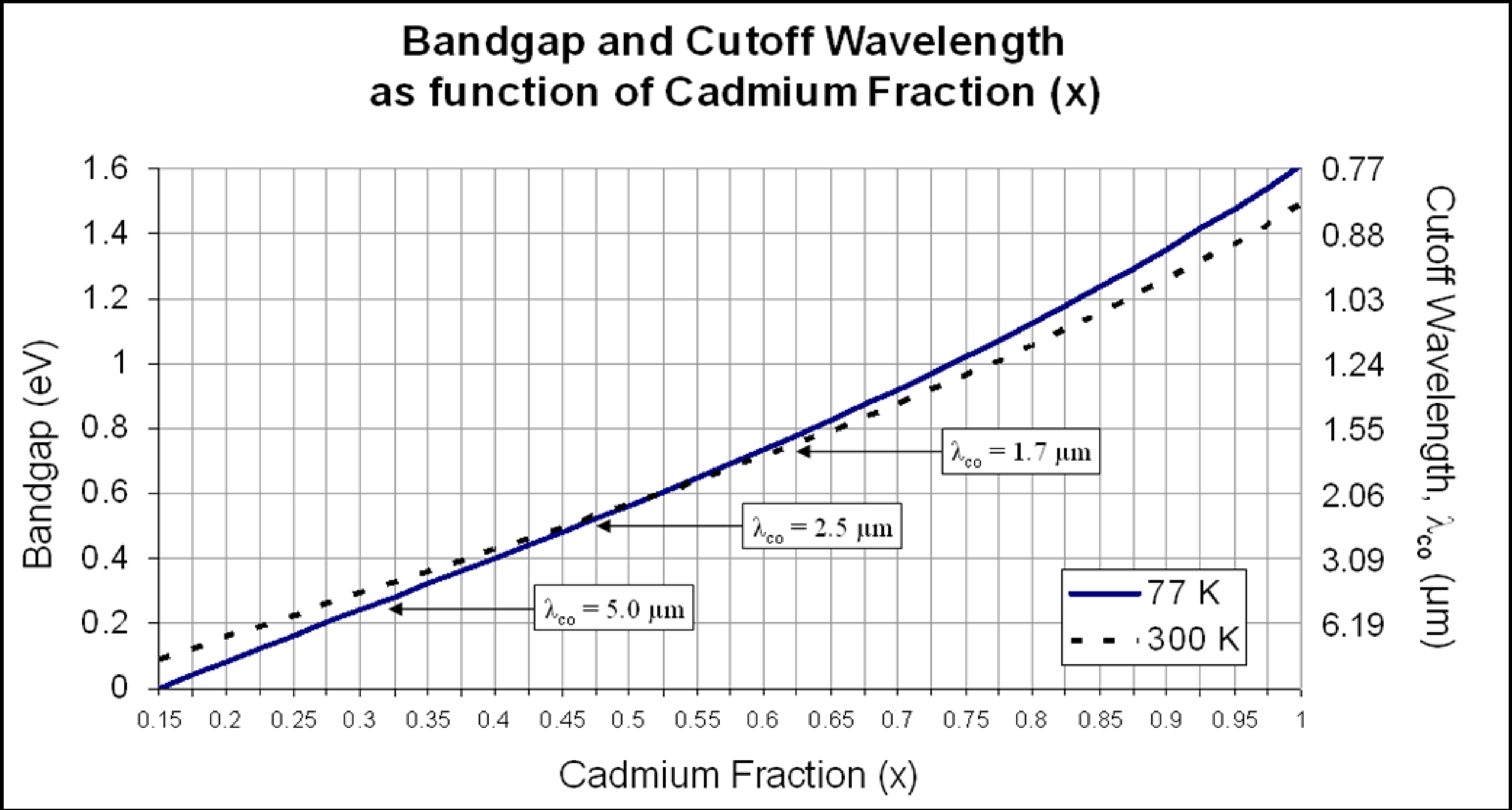

$$E_g = -0.302 + 1.93x - 0.81x^2 + 0.832x^3 + 5.35\times10^{-4}T(1-2x)$$

G. L. Hansen, J. L. Schmidt, T. N. Casselman, J. Appl. Phys. 53(10), 1982, p. 7099

Absorption Depth

The depth of detector material that absorbs 63.2% of the radiation

(1-1/e) of the energy is absorbed

1 absorption depth(s)	63.2% of light absorbed
2	86.5%
3	95.0%
4	98.2%

For high QE, thickness of detector material should be ≥ 3 absorption depths

Silicon is an indirect bandgap material and is a poor absorber of light as the photon energy approaches the bandgap energy. For an indirect bandgap material, both the laws of conservation of energy and momentum must be observed. To excite an electron from the valence band to the conduction band, silicon must simultaneously absorb a photon and a phonon that compensates for the missing momentum vector.

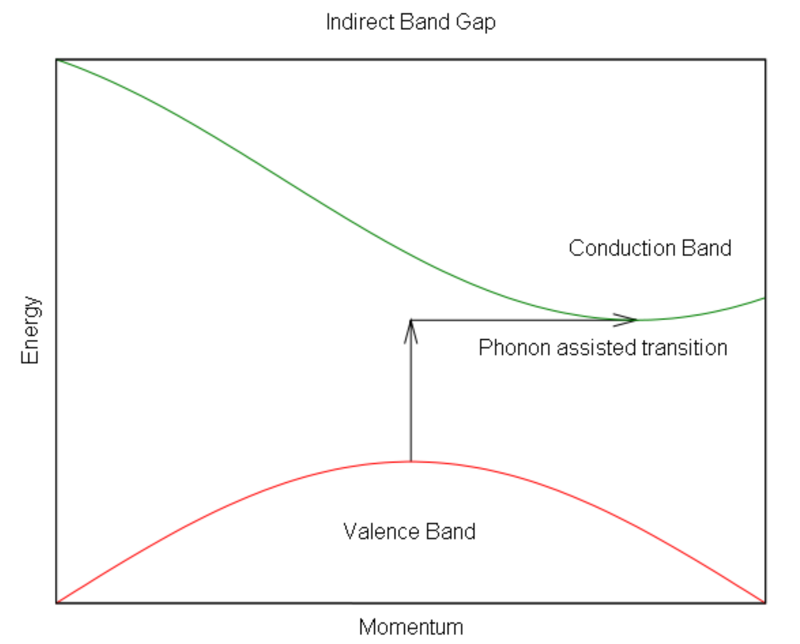

Absorption Depth of Light in Silicon

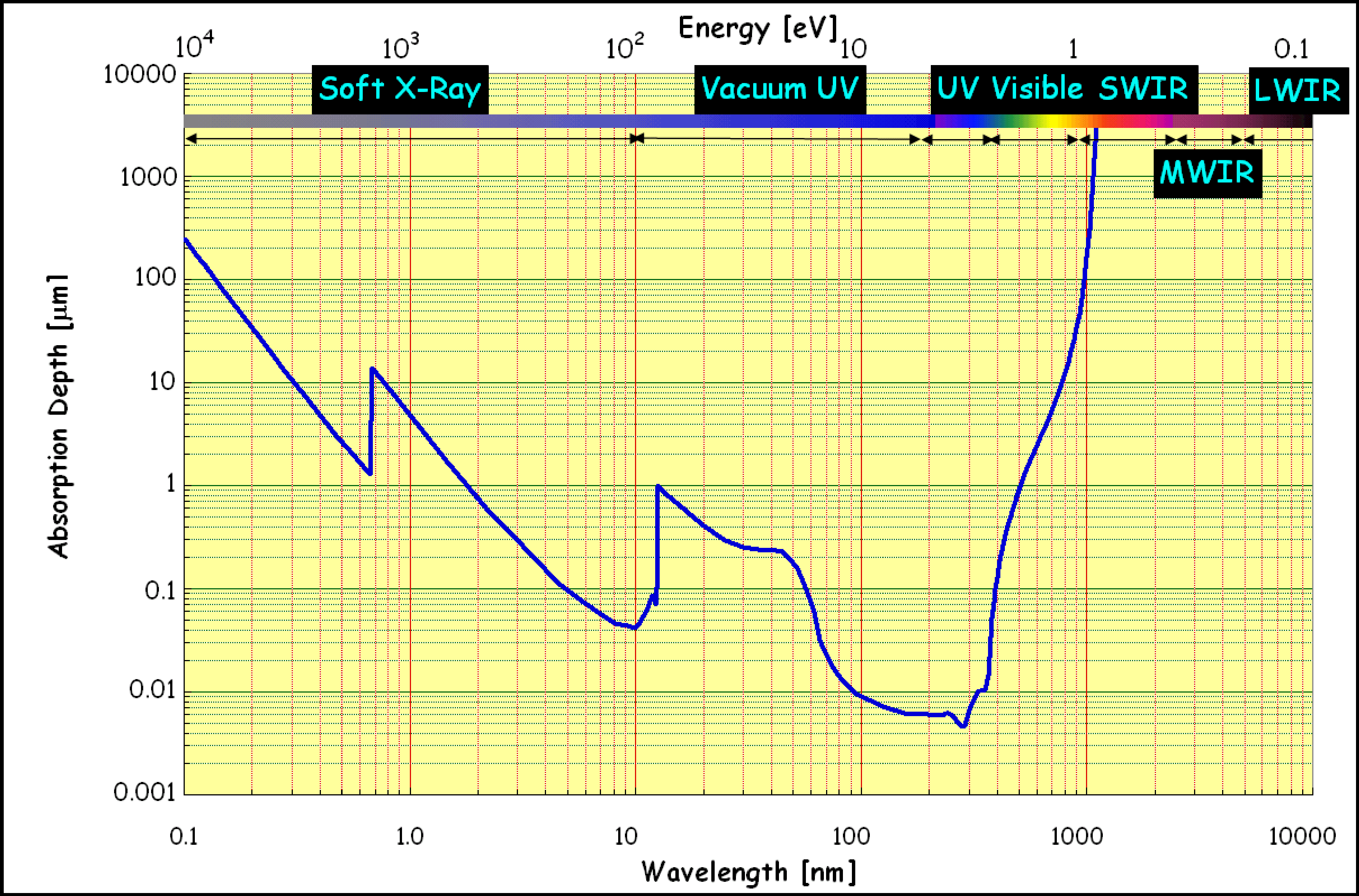

Absorption Depth of Silicon

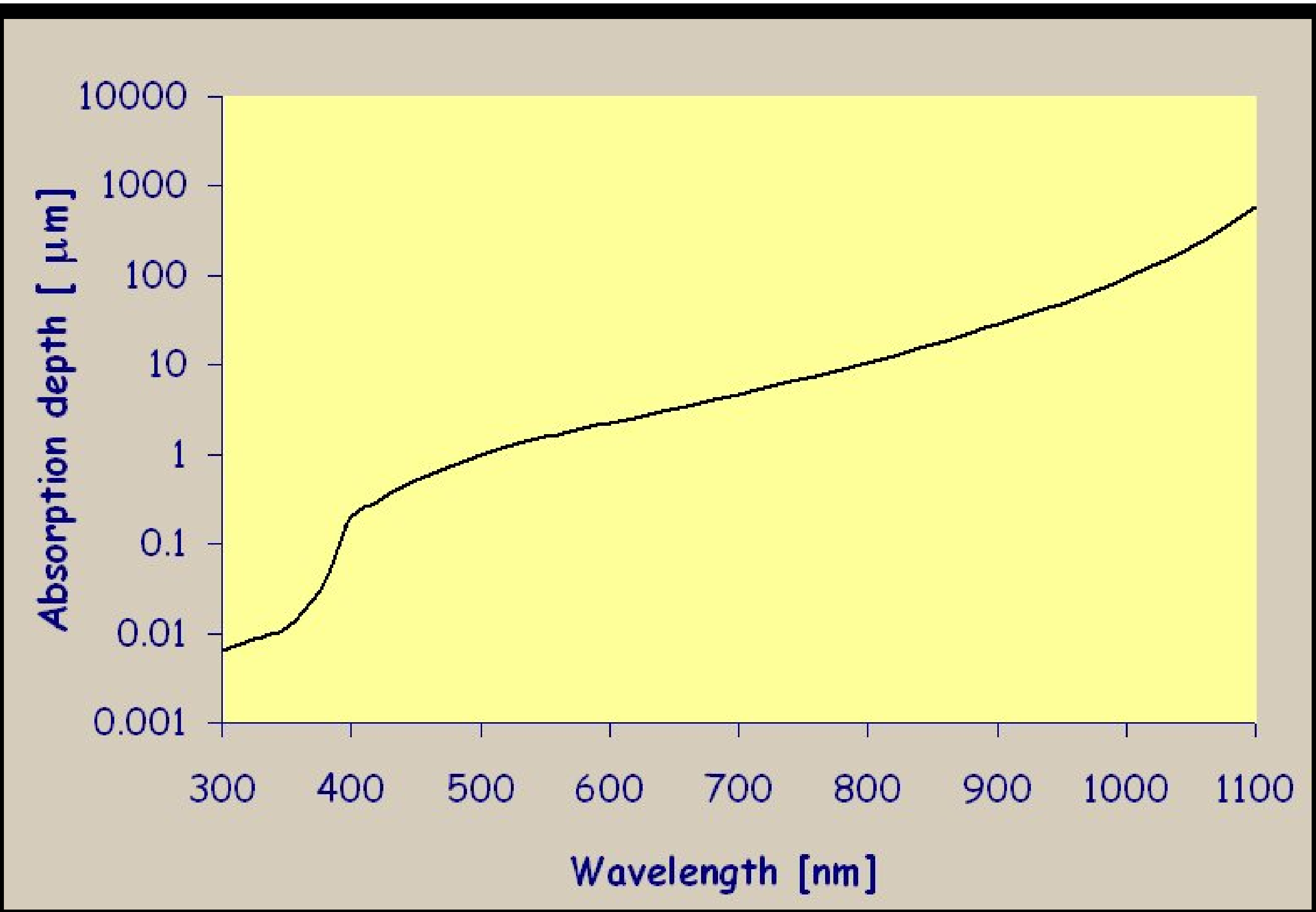

- For high QE in the near infrared, need very thick (up to 300 microns) silicon detector layer.
- For high QE in the ultraviolet, need to be able to capture photocharge created within 10 nm of the surface where light enters the detector.
- In addition, the index of refraction of silicon varies over wavelength – a challenge for anti-reflection coatings.

Boron Implant / Laser Anneal

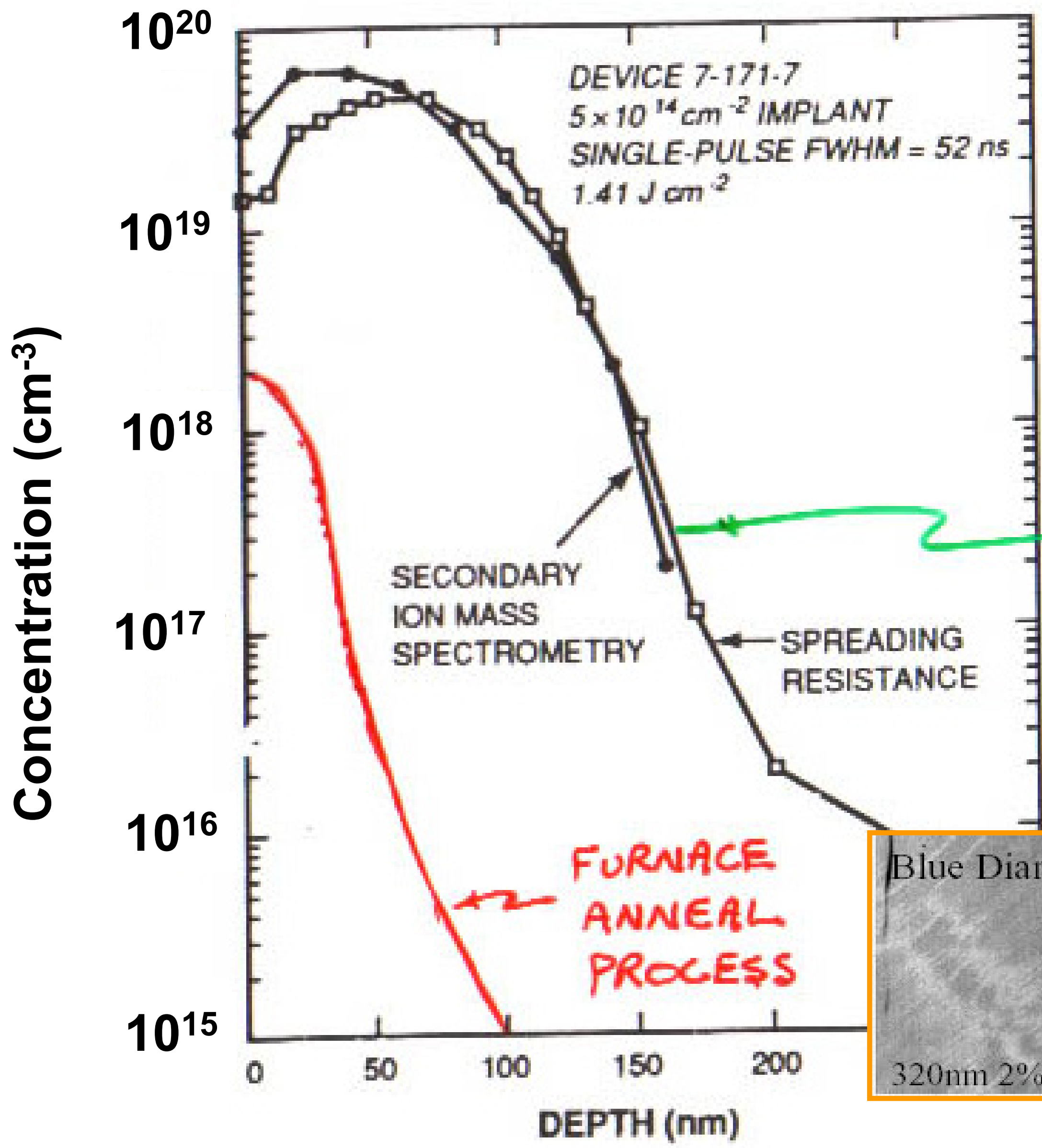

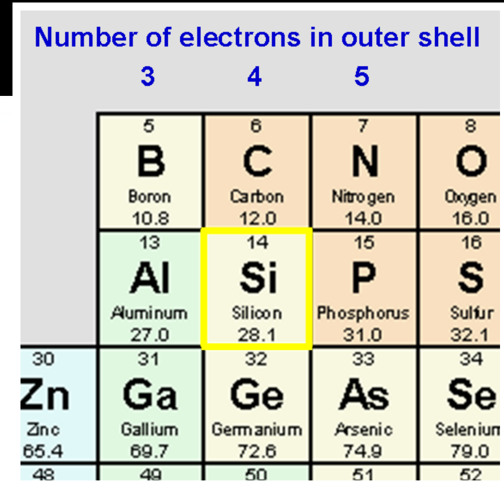

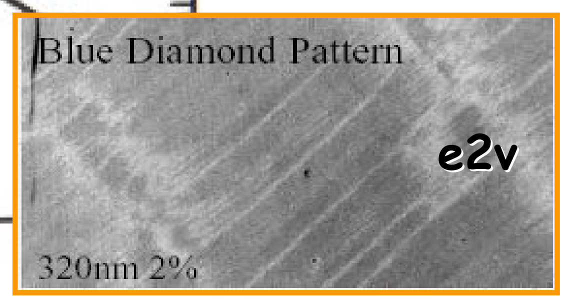

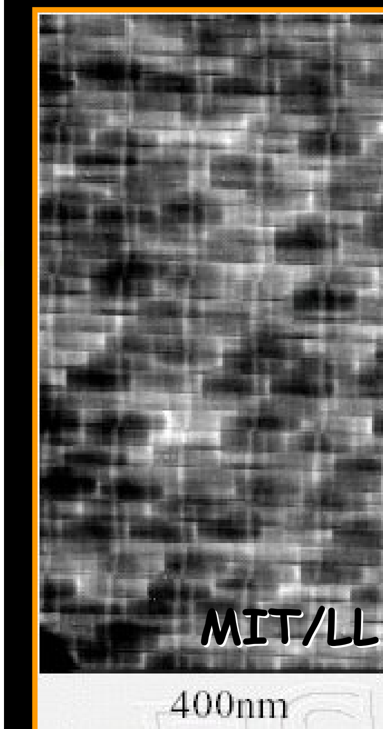

Cyril Cavadore, ESO

Molecular Beam Epitaxy growth of very thin (~5 nm) thick backside Si layer with boron

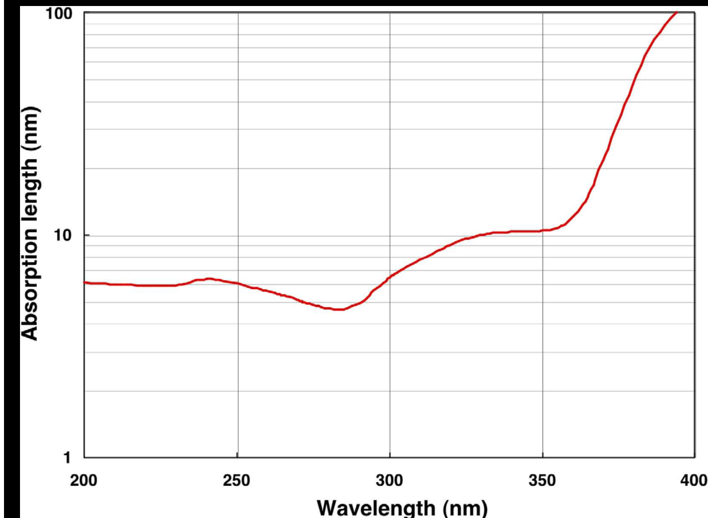

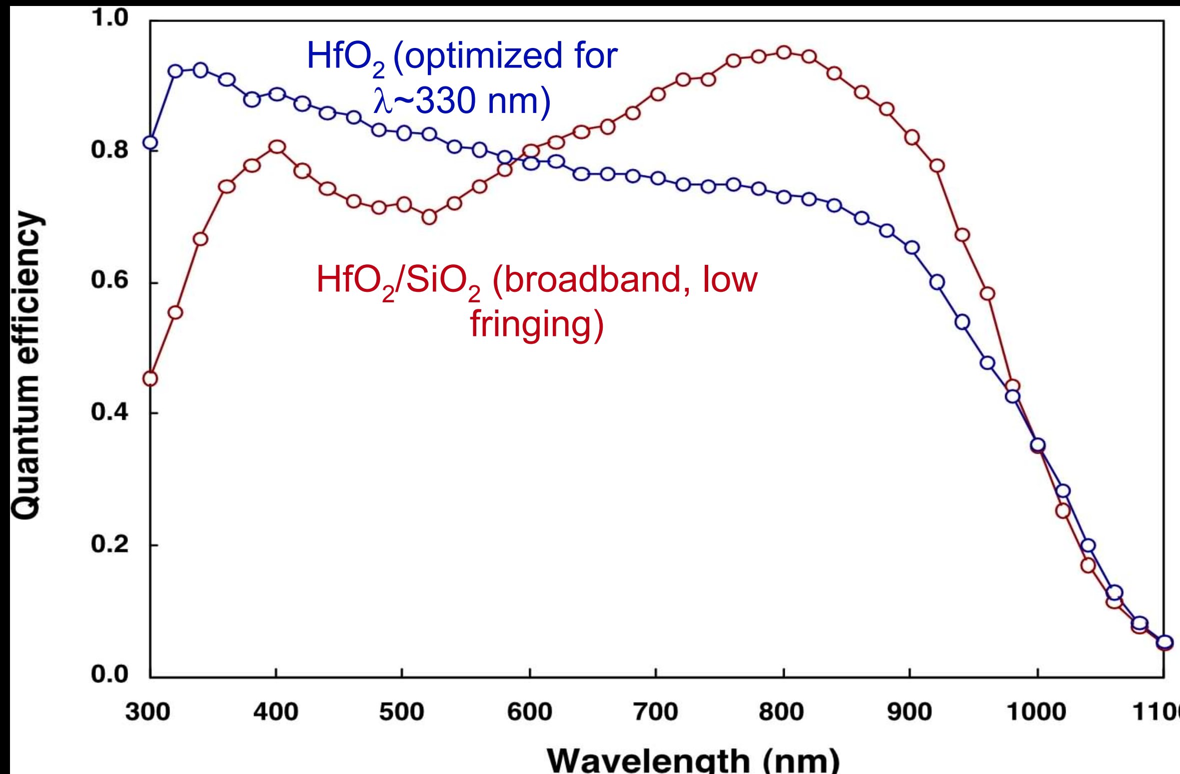

- UV (<400 nm) is challenging
  - Shallow penetration depth of radiation (<10 nm at λ=200-350 nm)
  - Requires extremely thin, doped surface layer

MBE processed
Device thickness = 45μm, T = 20°C

Plots from Barry Burke, MIT/LL

Jet Propulsion Laboratory (JPL) has similar process which they call "delta doping"

HIRES CCDs

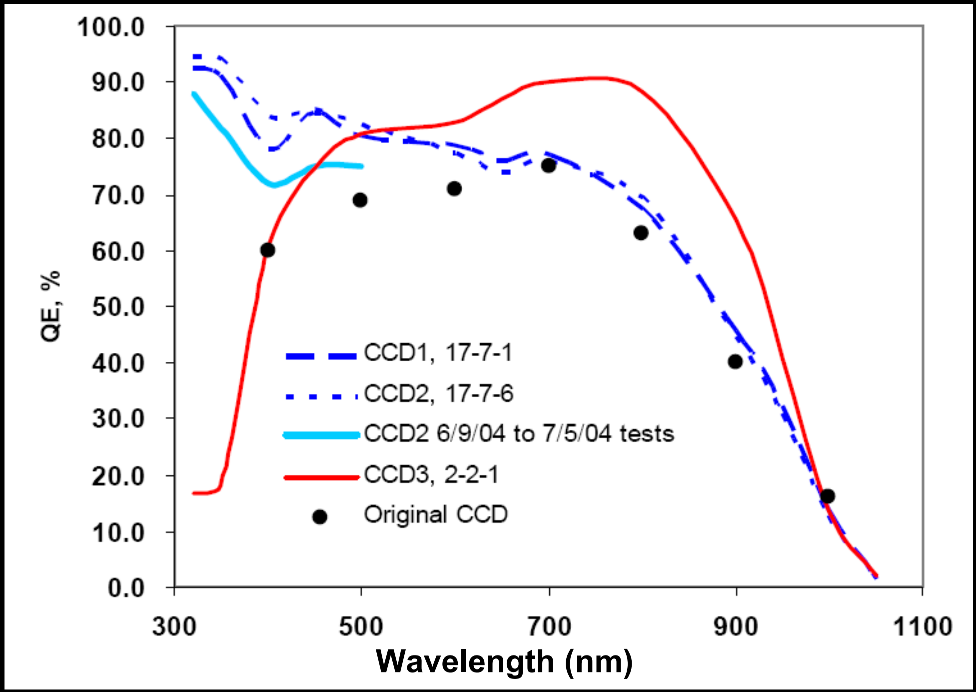

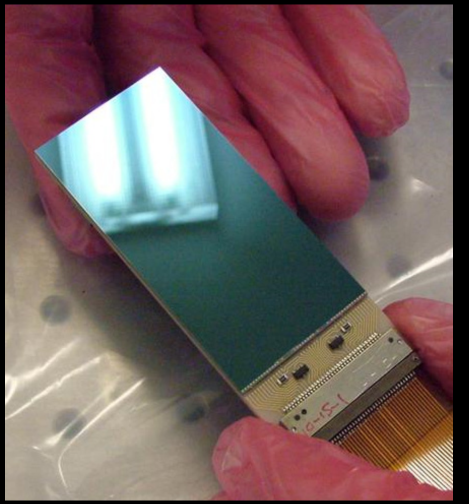

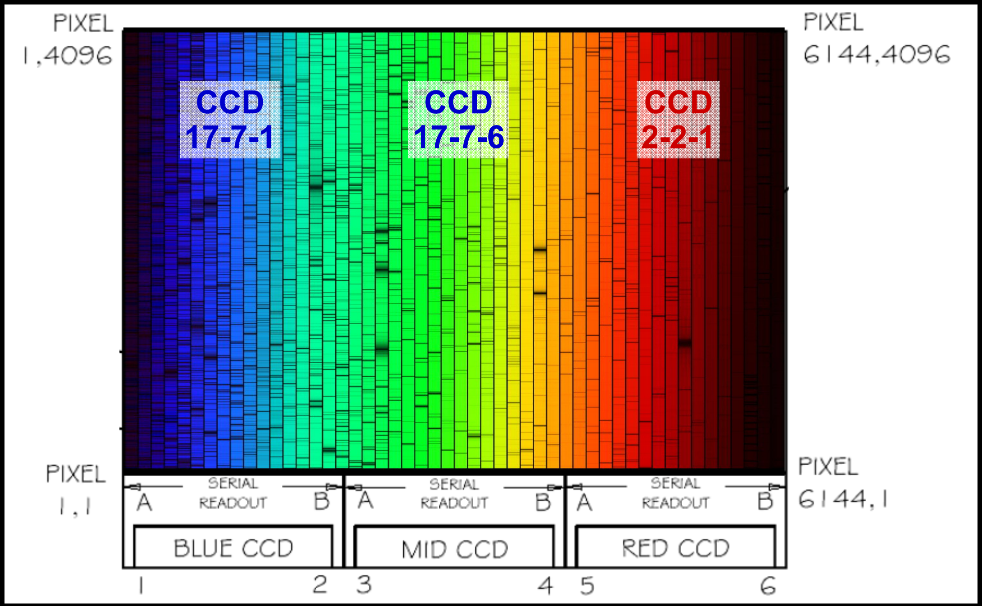

MIT Lincoln Laboratory 2K×4K CCDs

- Two CCDs with U. Arizona **chemisorption** backside process for high blue/UV QE
- The “red” CCD has boron implant & laser anneal

QE variations

Boron implant / laser anneal (blue end), and fringing (red)

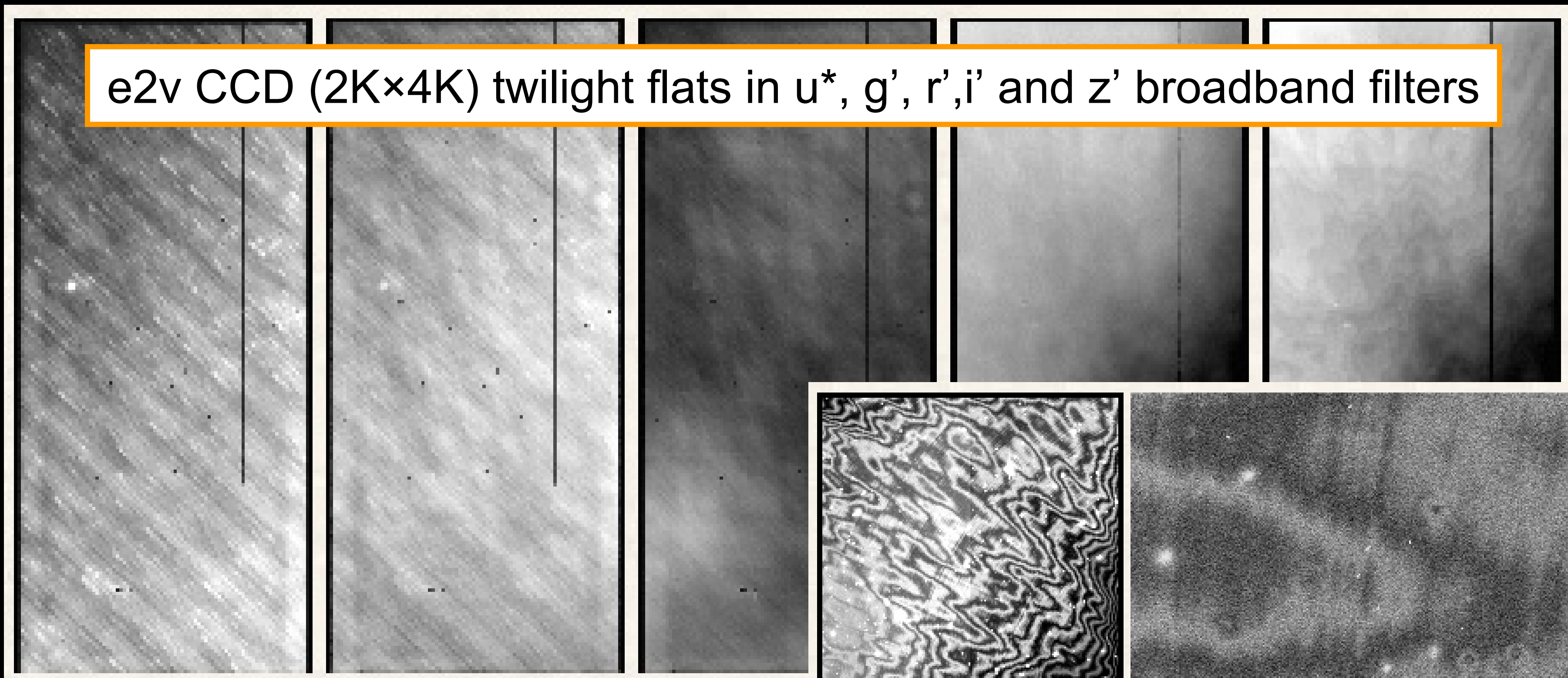

e2v CCD (2K×4K) twilight flats in u*, g’, r’,i’ and z’ broadband filters

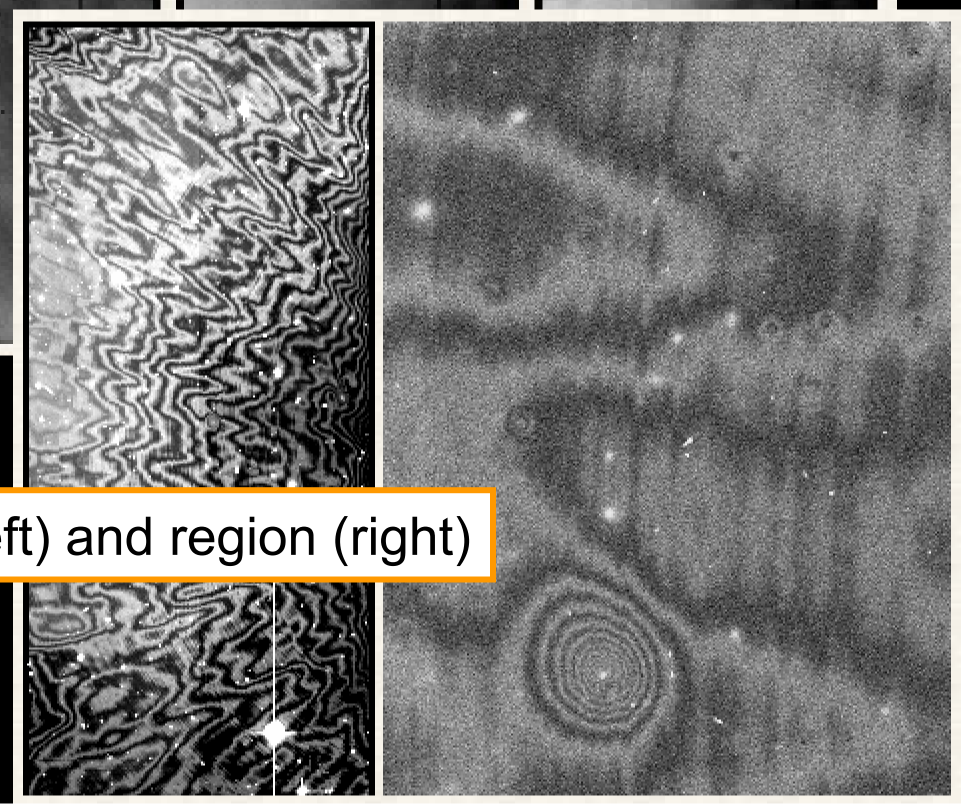

Fringes in the i’ band: full CCD (left) and region (right)

Photovoltaic Detector Potential Well

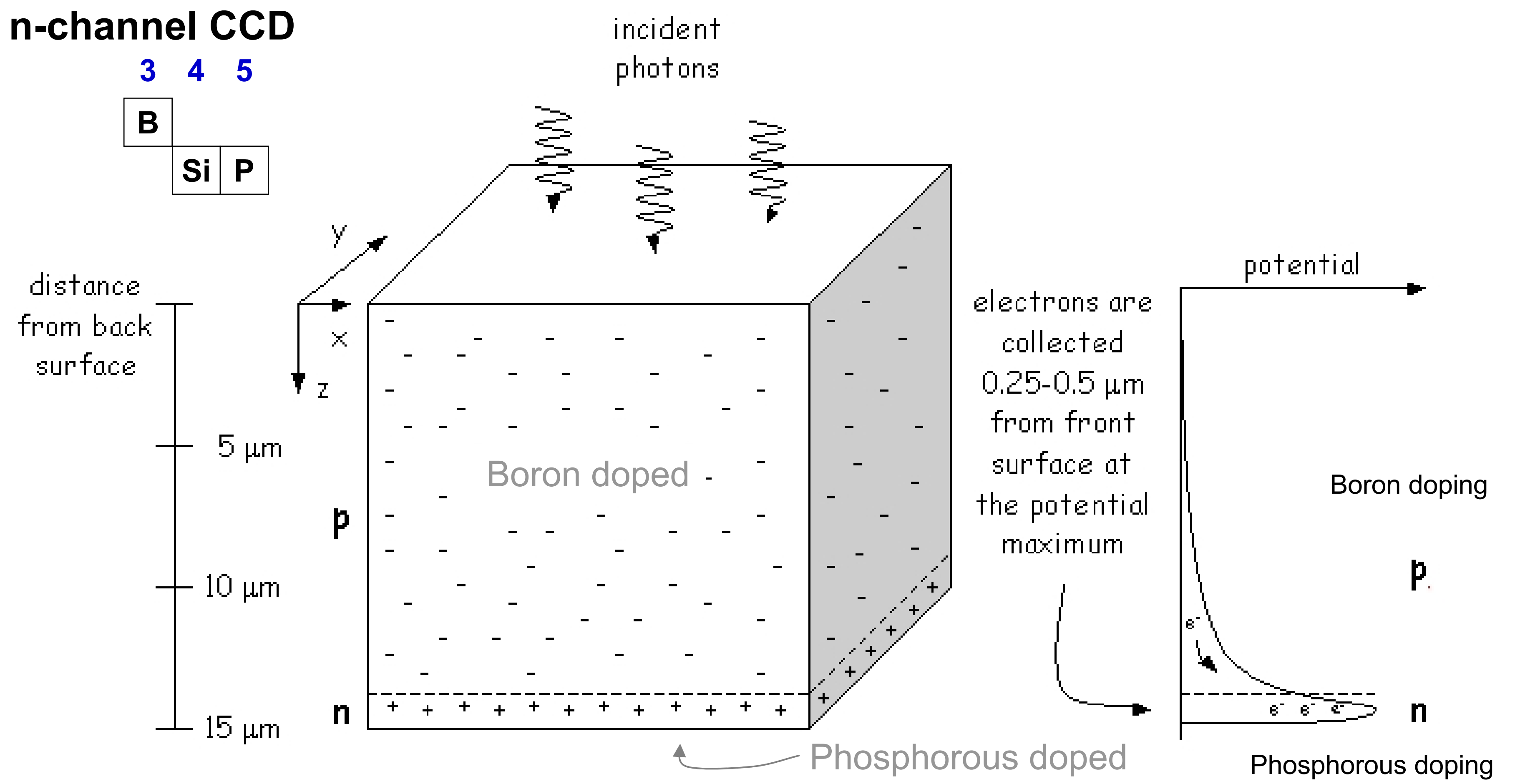

Silicon, HgCdTe and InSb are photovoltaic detectors. All use a pn-junction to generate E-field in the z-direction of each pixel. This electric field separates the electron-hole pairs generated by a photon.

Tradeoff: High Near-IR QE vs. Imager Resolution

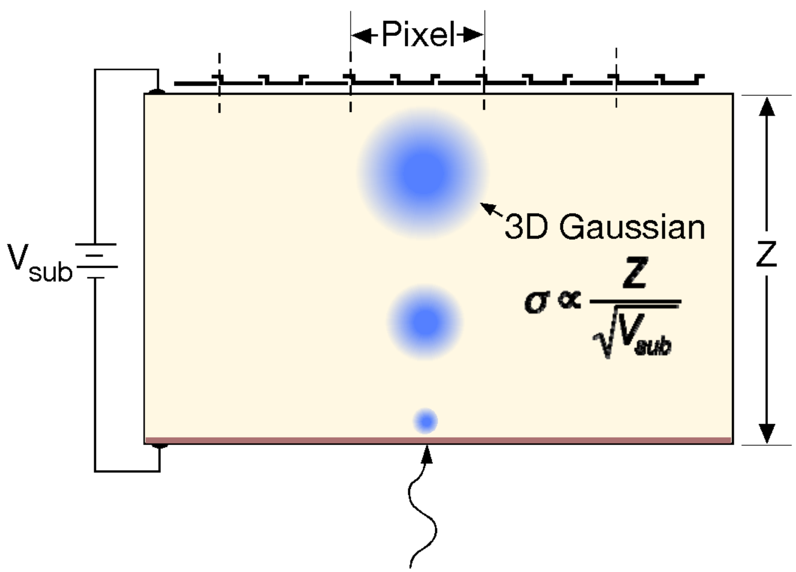

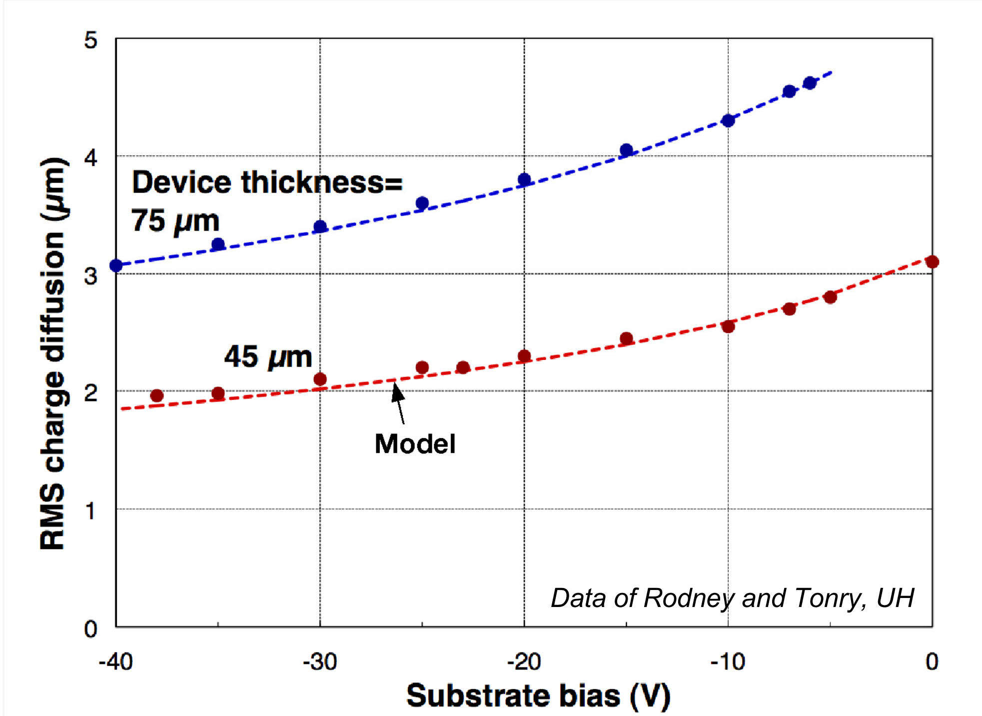

Thermal diffusion of photoelectrons reduces resolution

Substrate bias helps counteract effects of thermal diffusion

High resolution in thick imagers => bias across sensor

Quantum Efficiency

- **Thicker devices: higher near-infrared quantum efficiency**

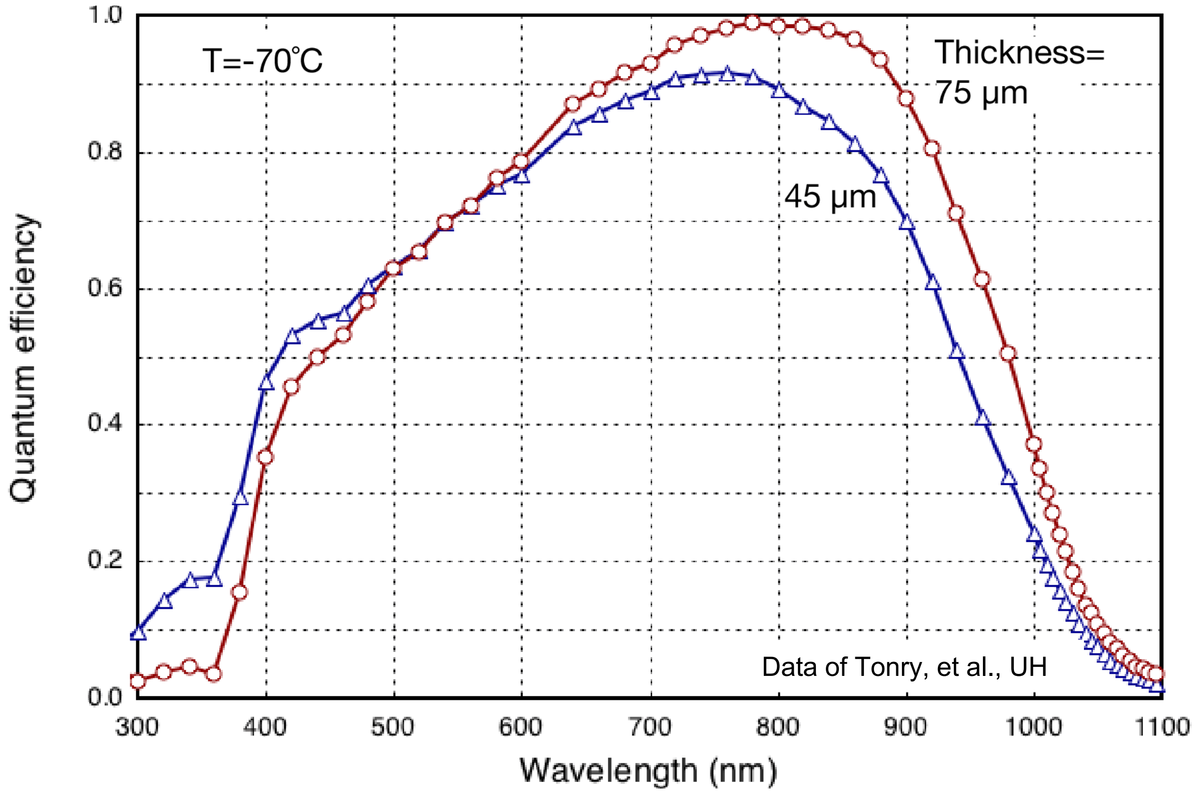

Available CCD performance

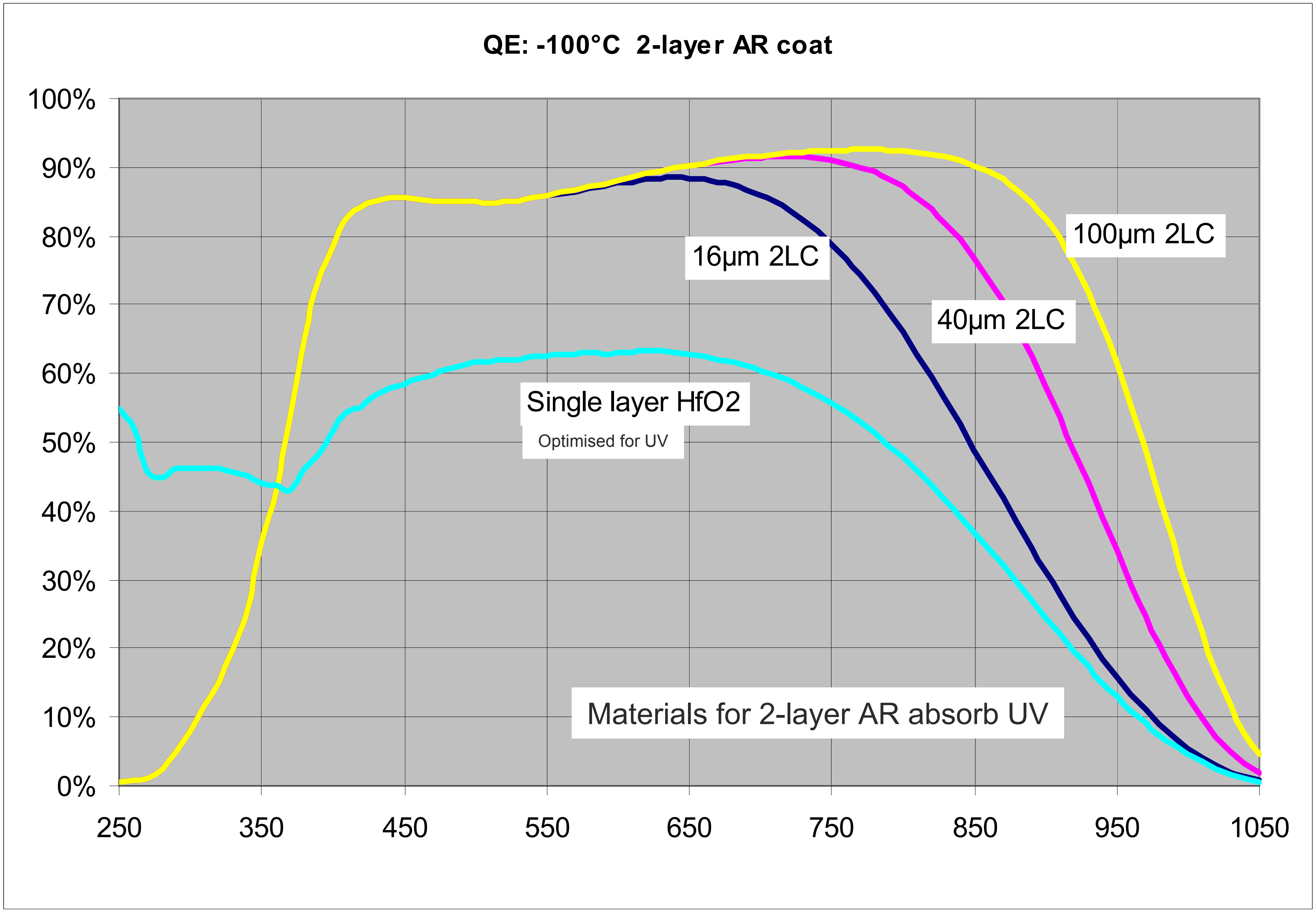

Dark Current

Undesirable byproduct of light detecting materials

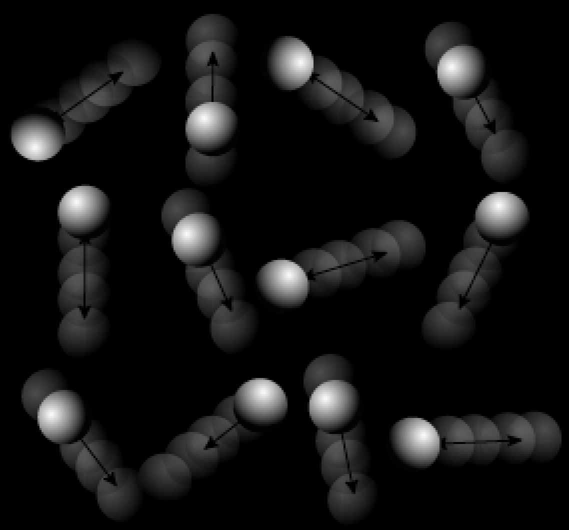

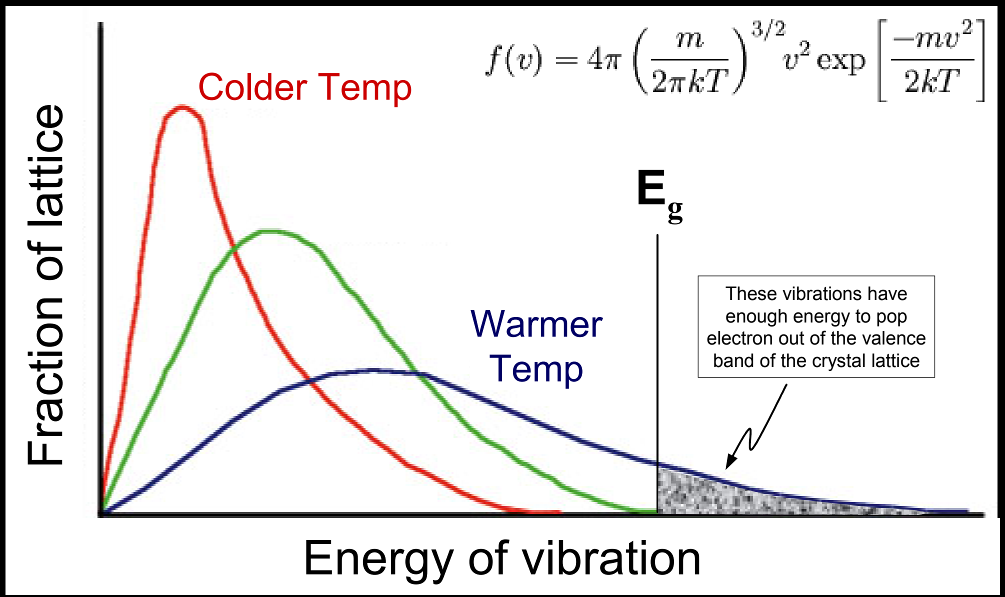

- The vibration of particles (includes crystal lattice phonons, electrons and holes) has energies described by the Maxwell-Boltzmann distribution. Above absolute zero, some vibration energies may be larger than the bandgap energy, and will cause electron transitions from valence to conduction band.
- Need to cool detectors to limit the flow of electrons due to temperature, i.e. the **dark current** that exists in the absence of light.
- The smaller the bandgap, the colder the required temperature to limit dark current below other noise sources (e.g. readout noise)

Dark Current of Silicon-based Detectors

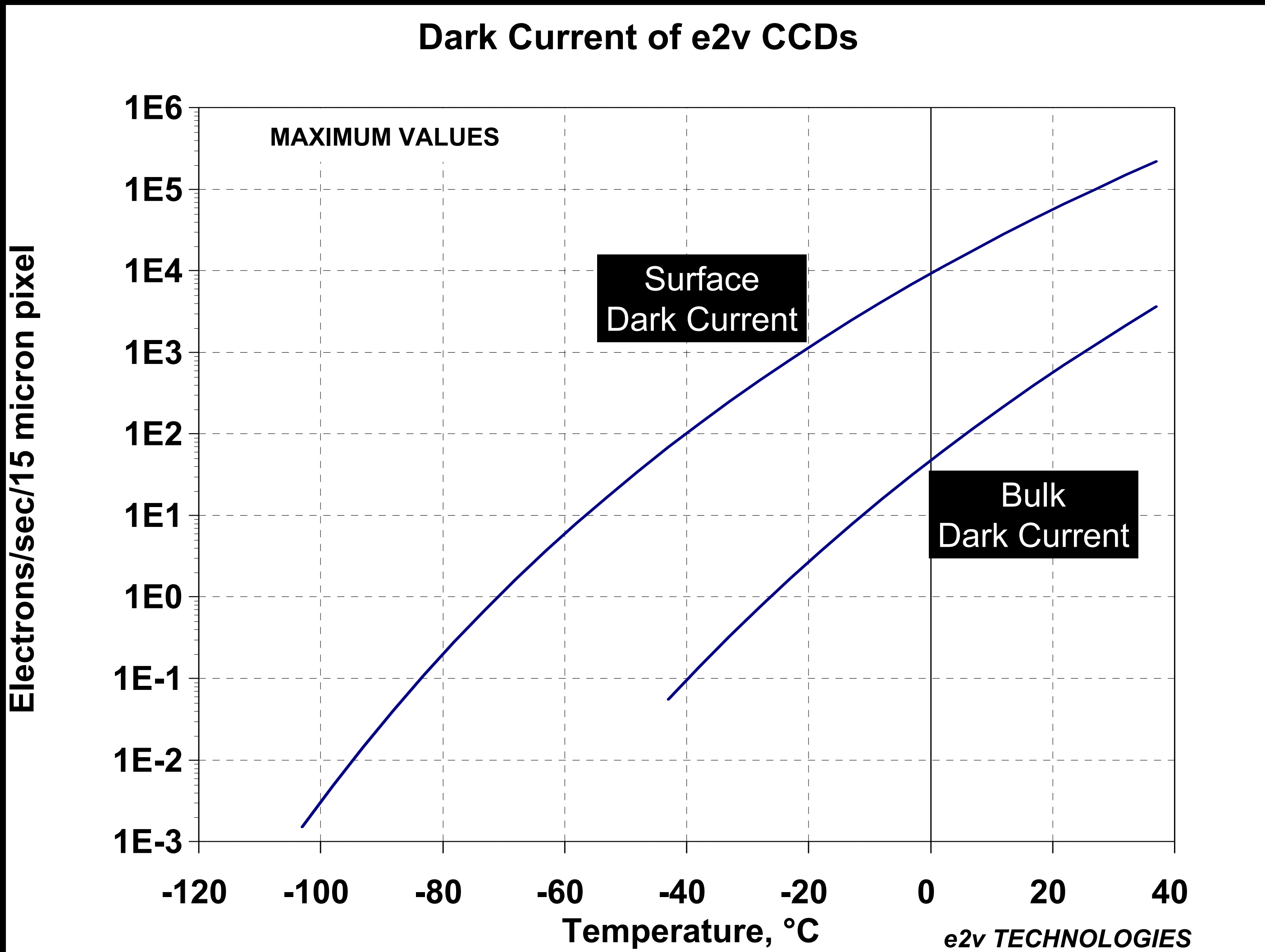

In silicon, dark current usually dominated by surface defects

e2v technologies

CCD Architecture

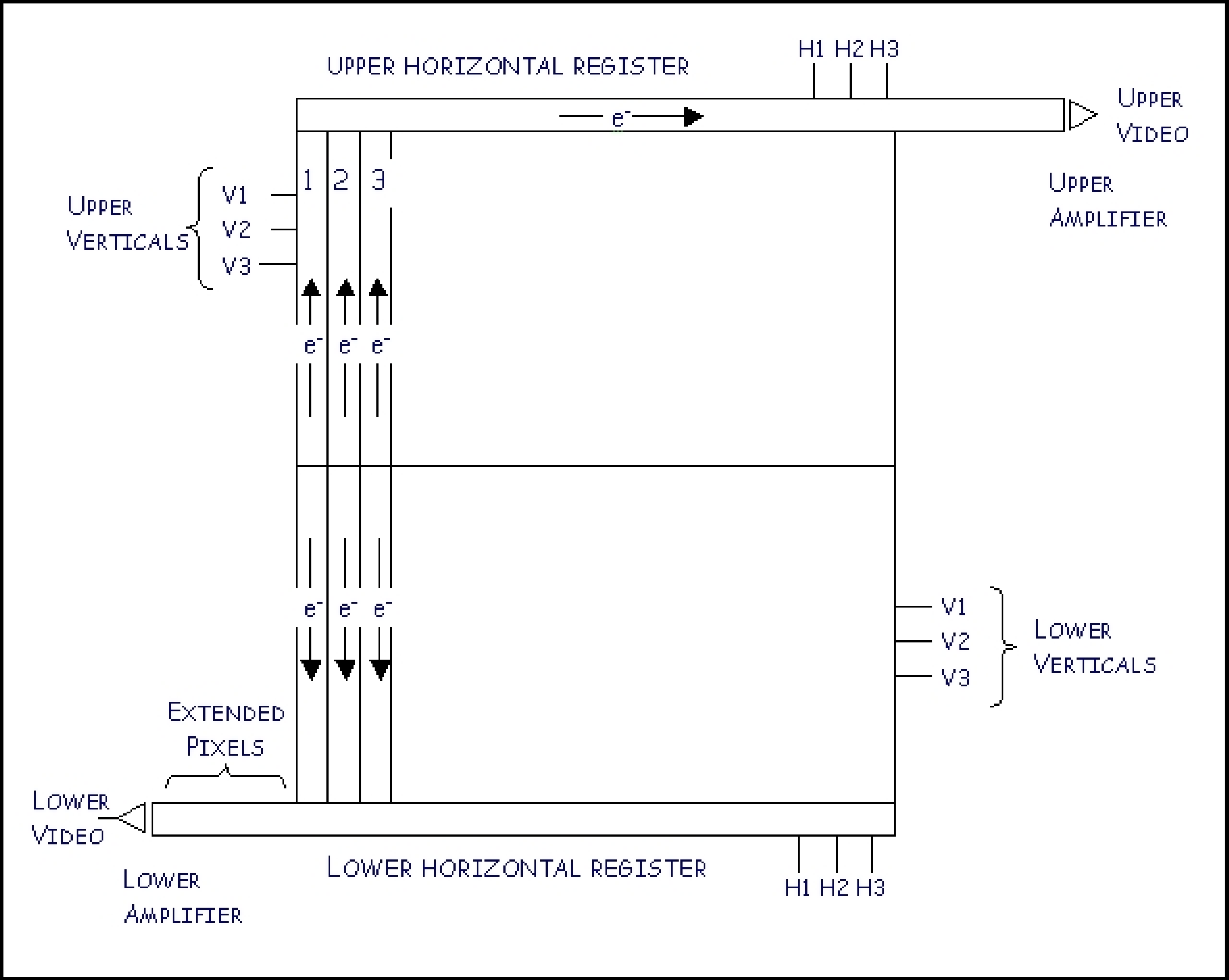

CCD Timing

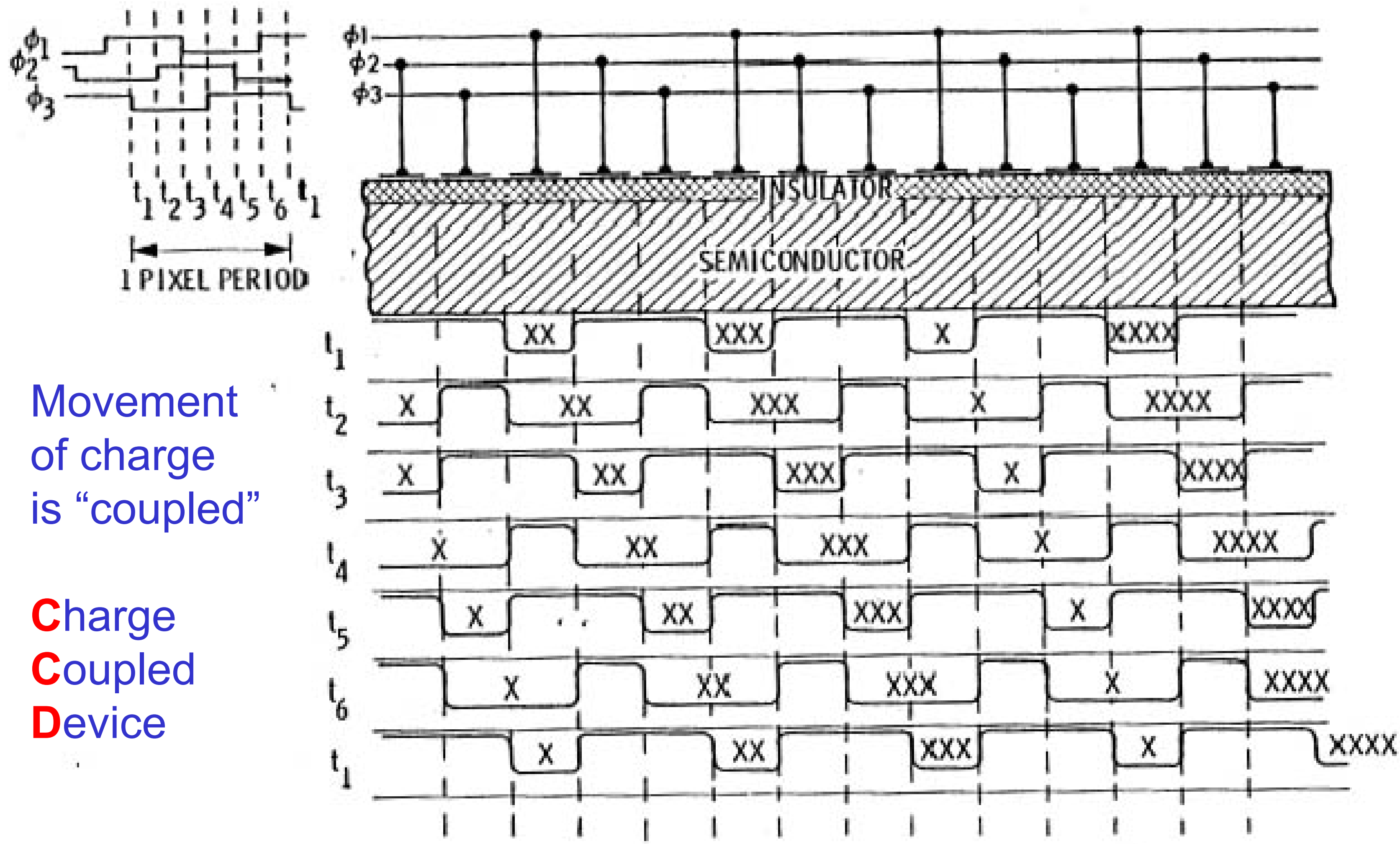

Movement of charge is "coupled"

Charge
Coupled
Device

CCD – 3 Phase Serial Register

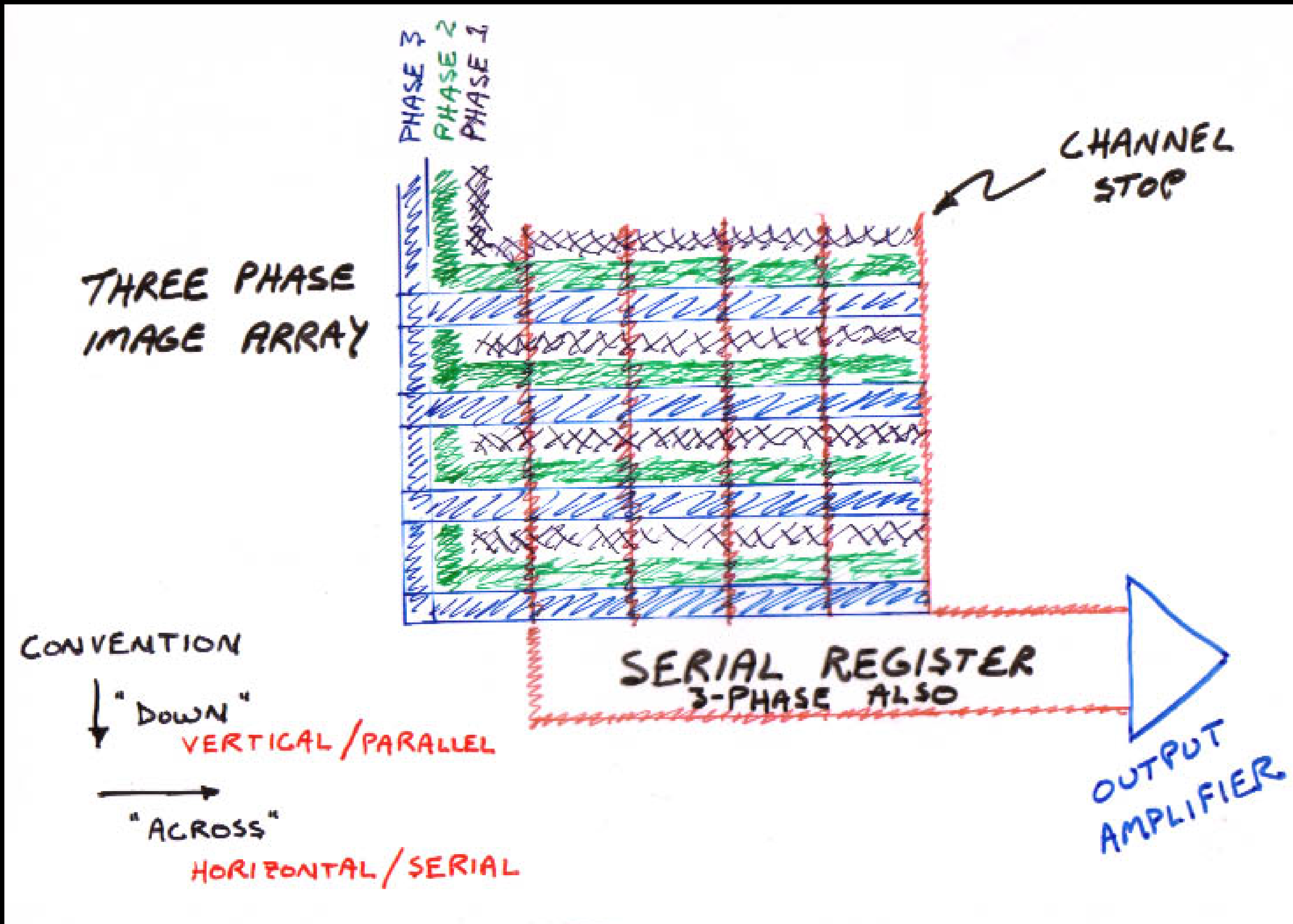

MOSFET Principles

MOSFET = metal oxide semiconductor field effect transistor

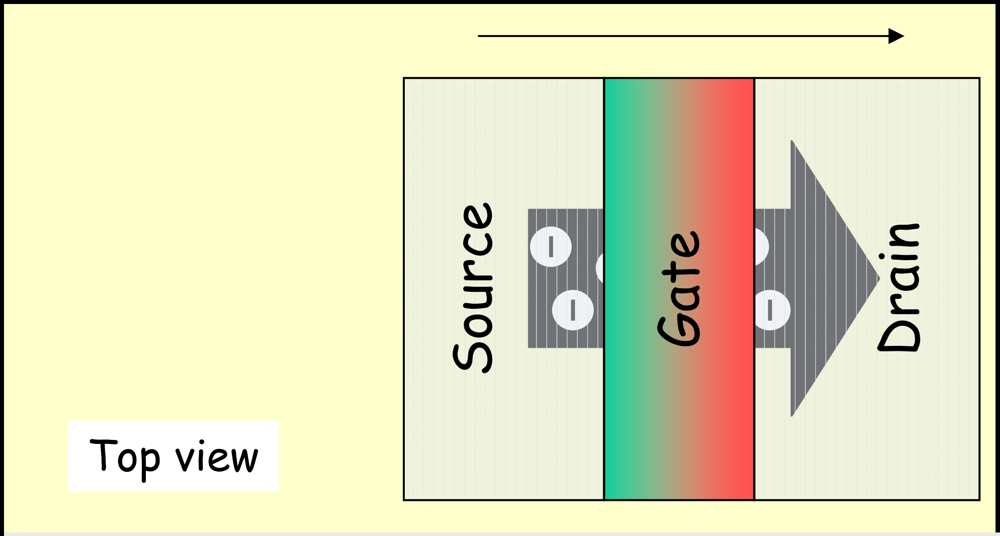

Turn on the MOSFET and current flows from source to drain

Add charge to gate & the current flow changes since the effect of the field of the charge will reduce the current

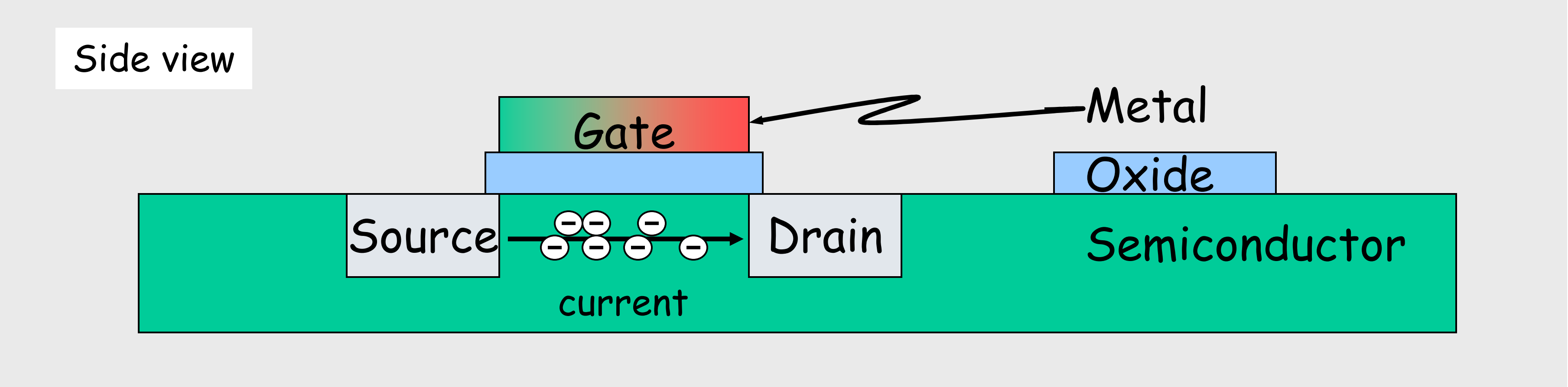

Fluctuations in current flow produce “readout noise”
Fluctuations in reset level on gate produces “reset noise”

MOSFET Amplifier Noise

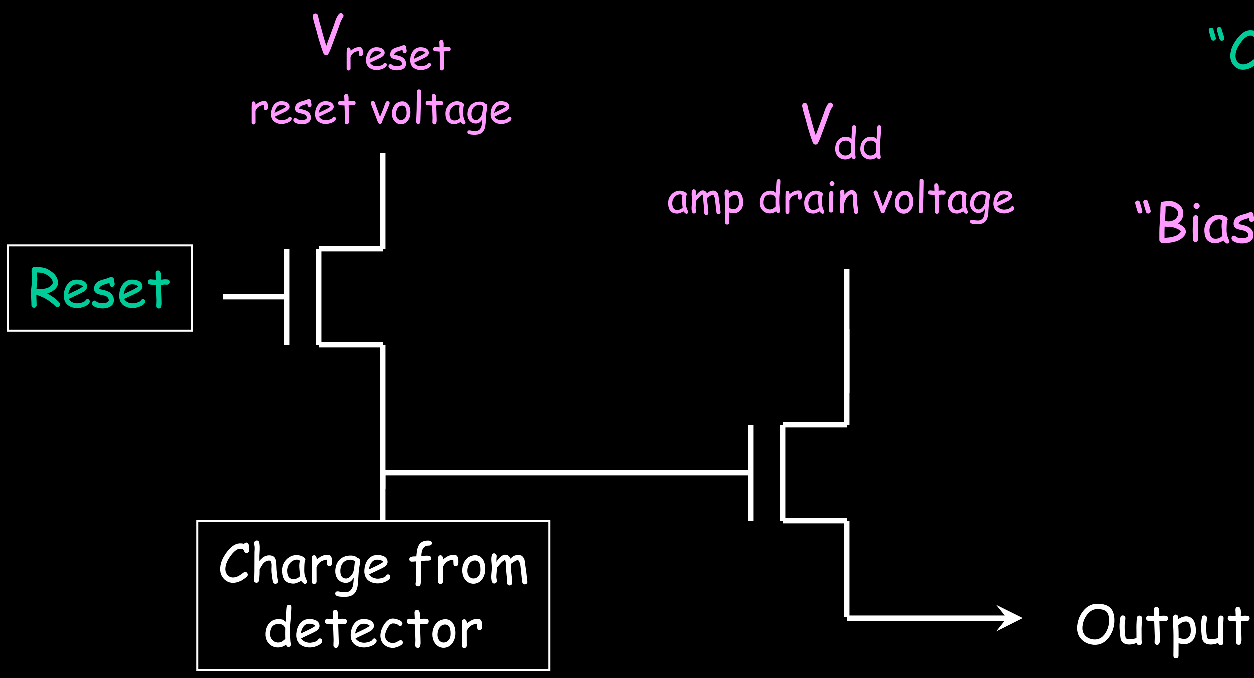

"Clock" (green)

"Bias voltage" (purple)

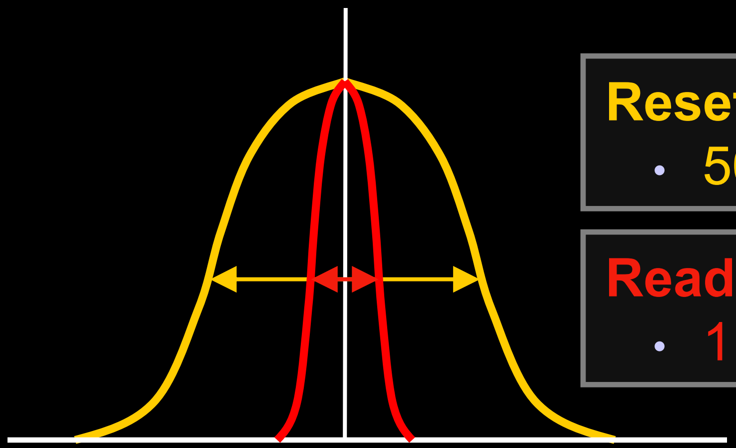

Reset Noise
- 50 to 100 e- rms

Read Noise
- 1.5 to 10 e- rms

Correlated Double Sample (CDS)
- Reset
- Read
- Put charge on gate
- Read

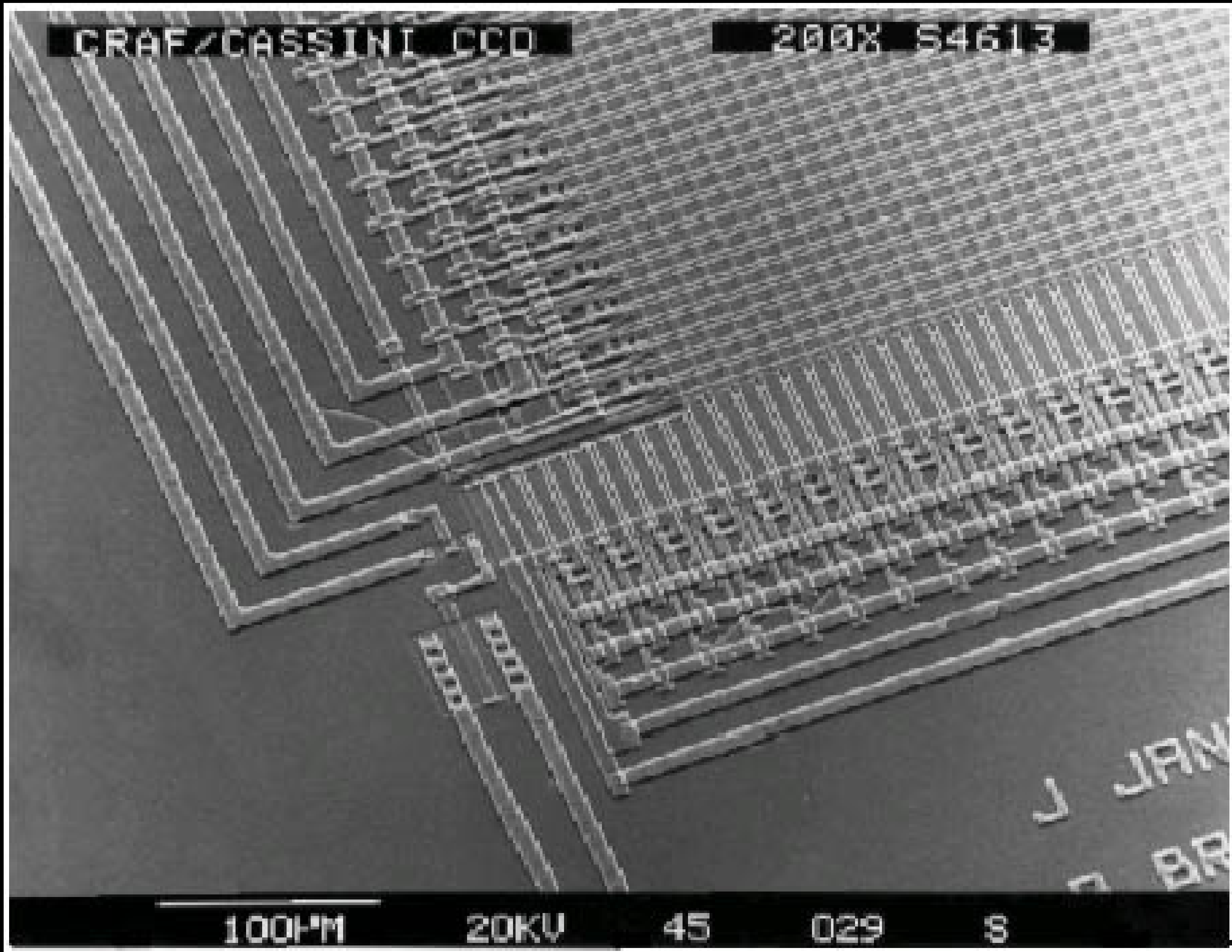
CRAF/CASSINI CCD
200X S4613
100MM
20KV
45
029
S

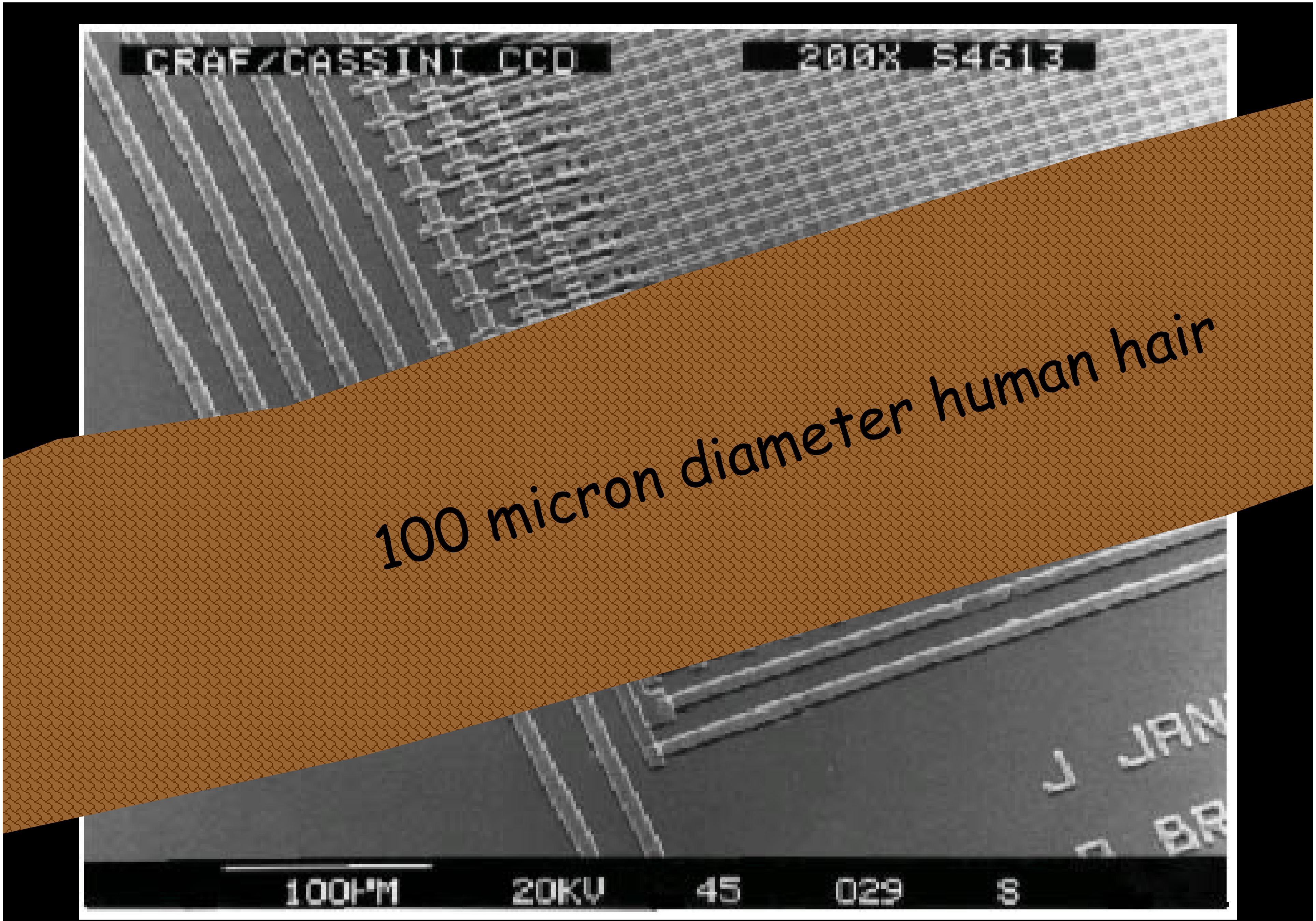
CRAF/CASSINI CCD
200X S4613
100 micron diameter human hair
100µM 20KV 45 029 S

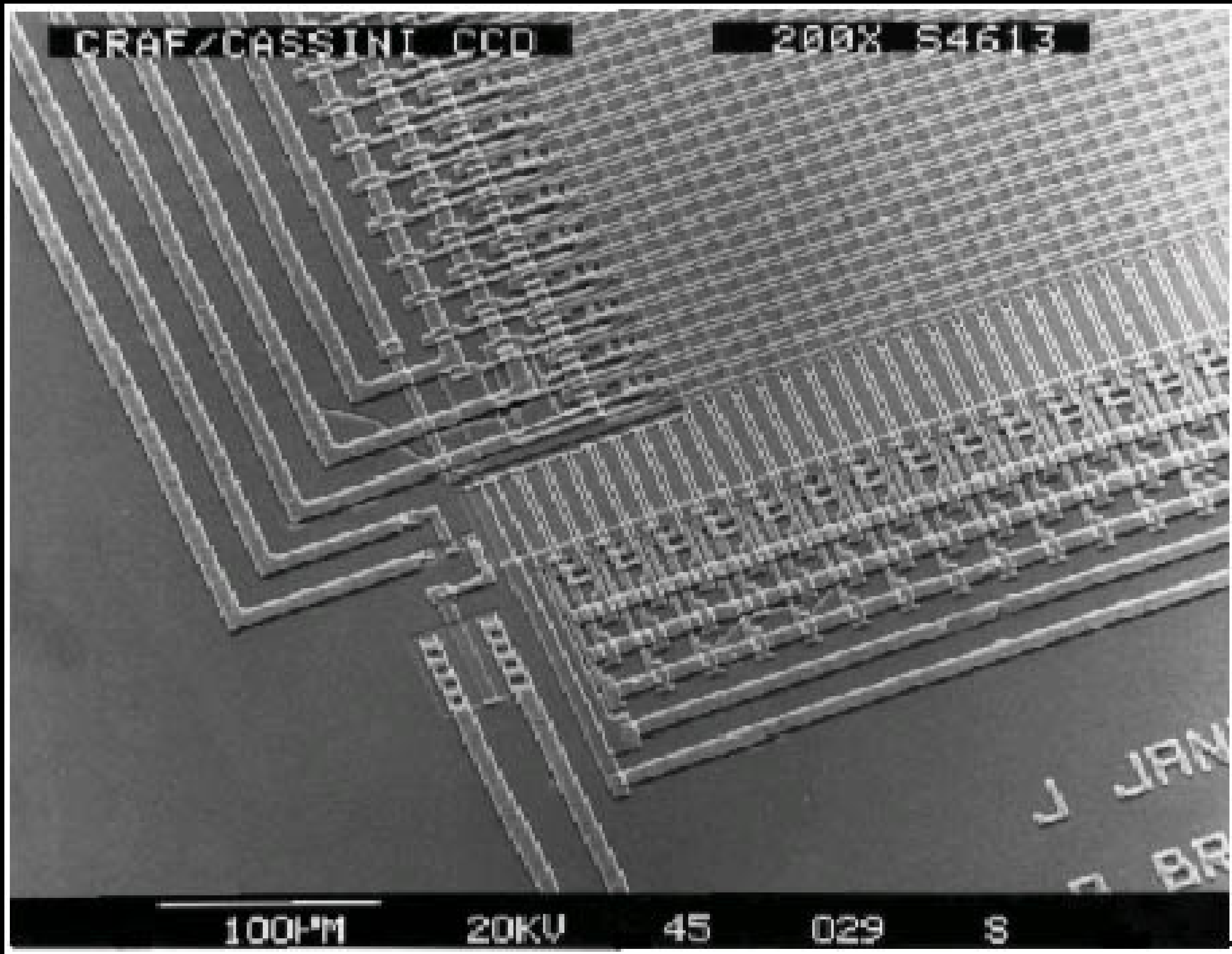
CRAF/CASSINI CCD
200X S4613
100µM
20KV
45
029
S

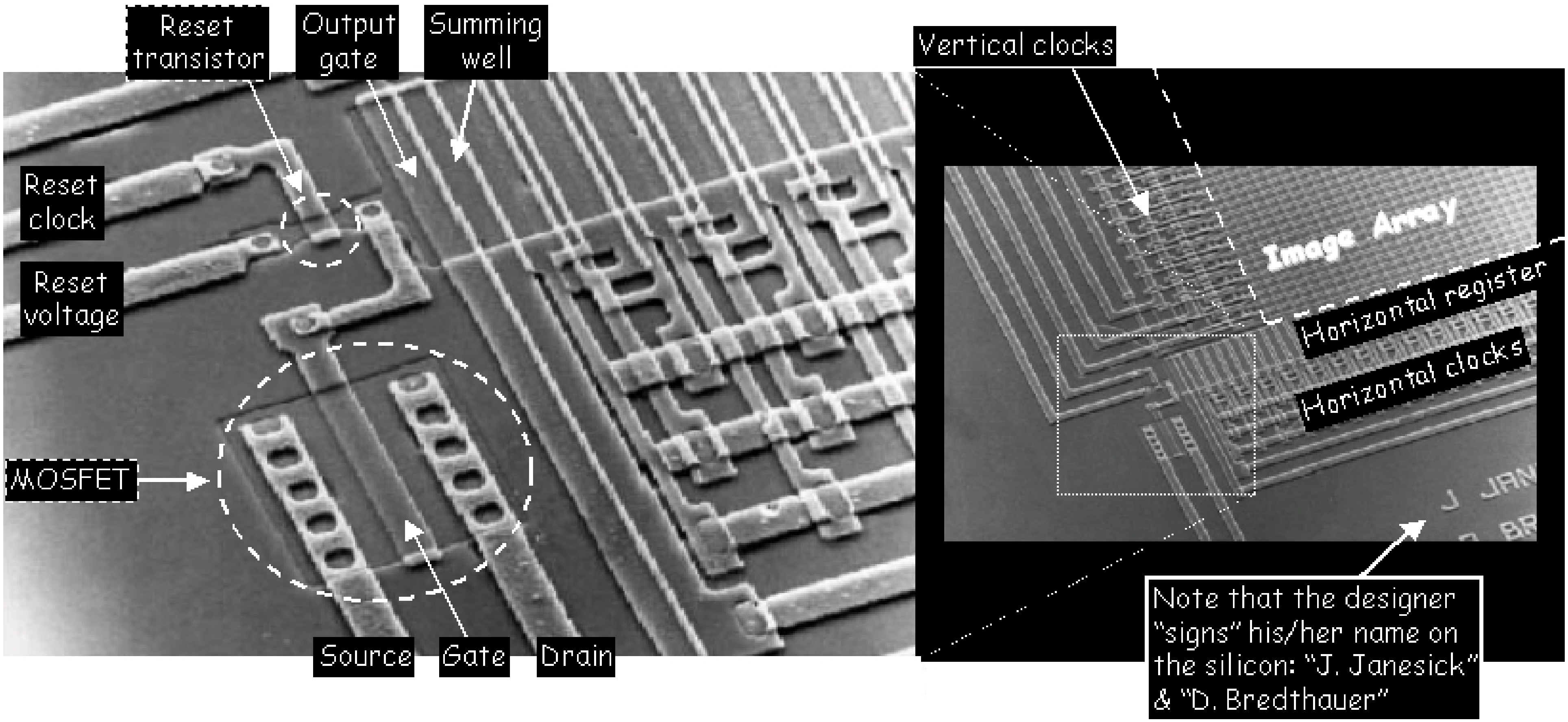
Reset transistor
Output gate
Summing well
Vertical clocks
Reset clock
Reset voltage
Image Array
Horizontal register
Horizontal clocks
MOSFET
J JAN
Source
Gate
Drain
Note that the designer "signs" his/her name on the silicon: "J. Janesick" & "D. Bredthauer"

Typical CCD Readout Noise (single CDS)

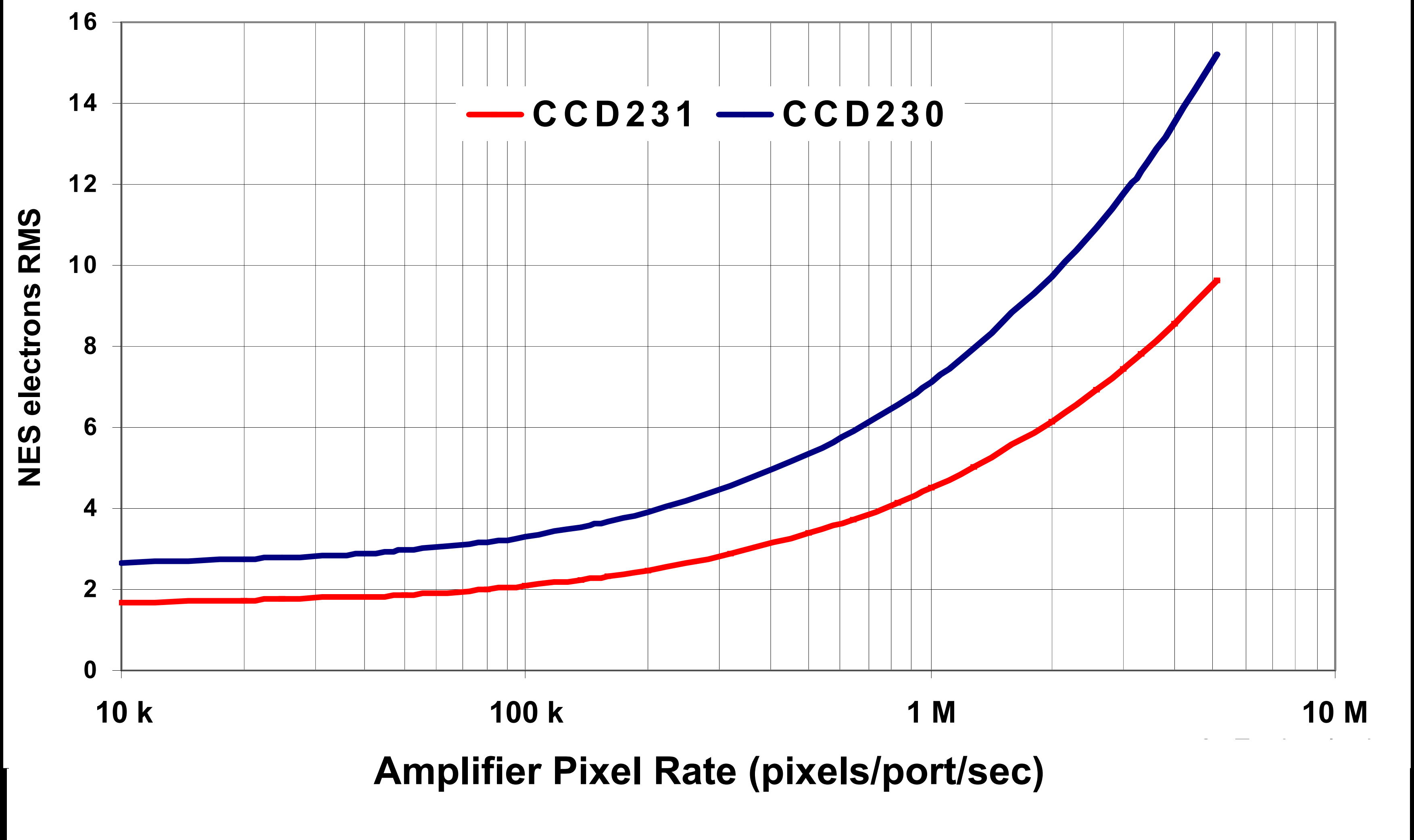

e2v technologies

CCD Noise as function of amplifier & data rate

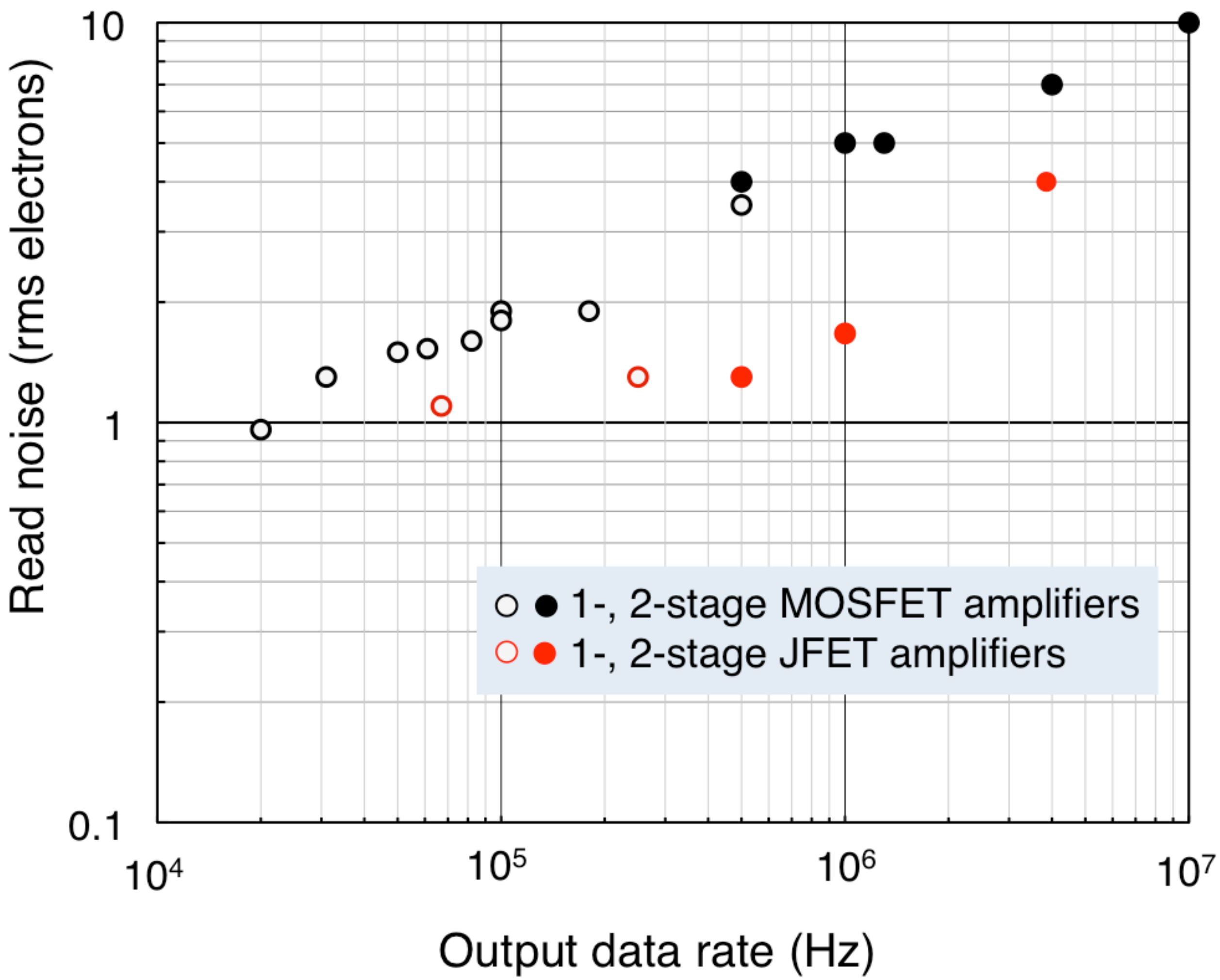

CCD Rain bucket analogy

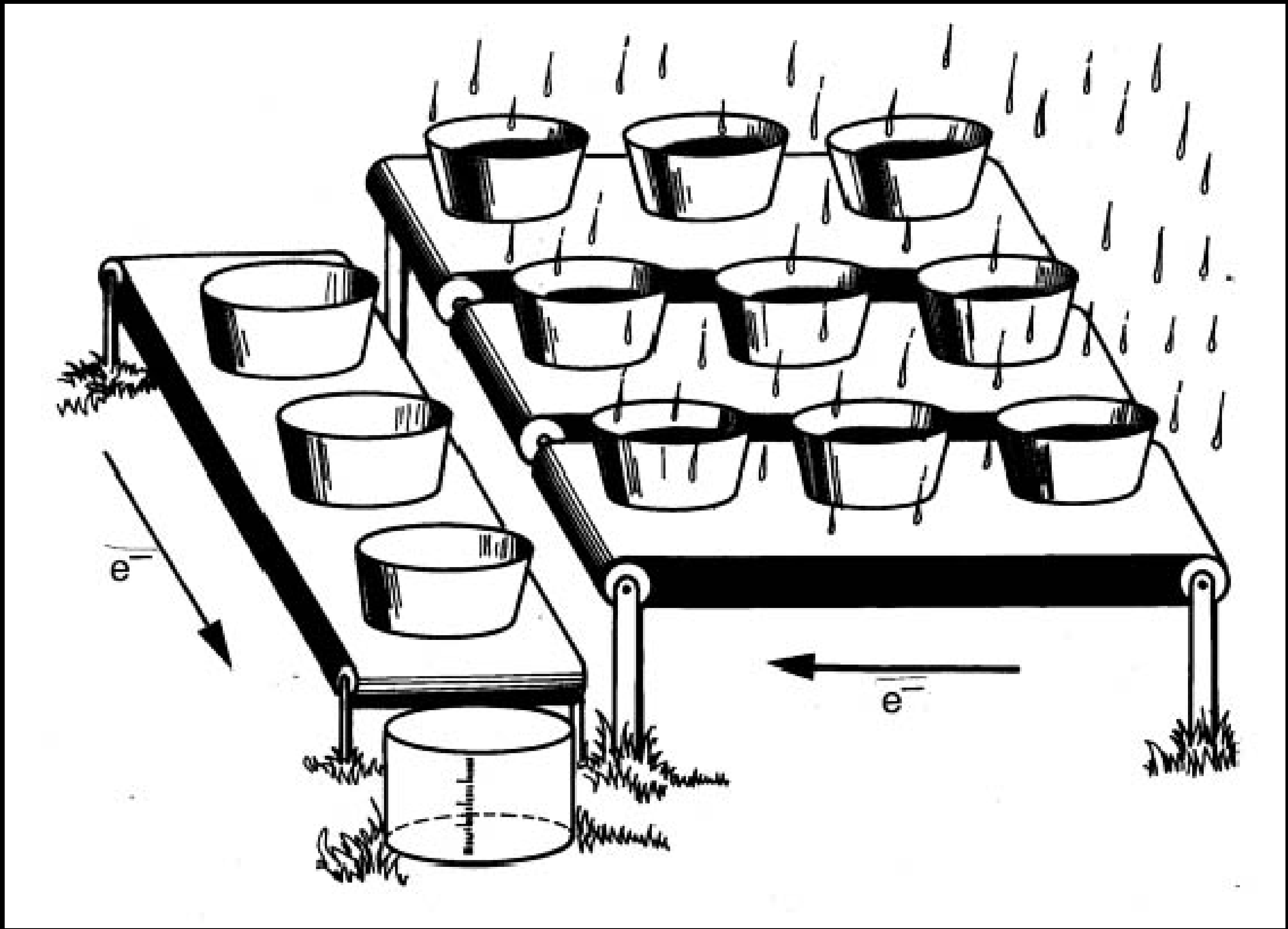

World’s Largest Monolithic CCDs

e2v
8.4 million pixels
2048×4096, 15 µm
18.9 cm2

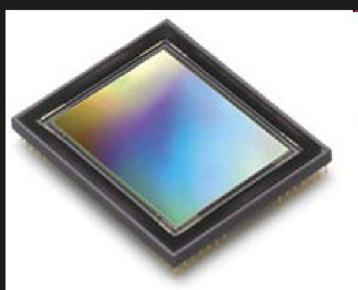

Dalsa
48 million pixels
6000×8000, 6 µm
17.3 cm^2

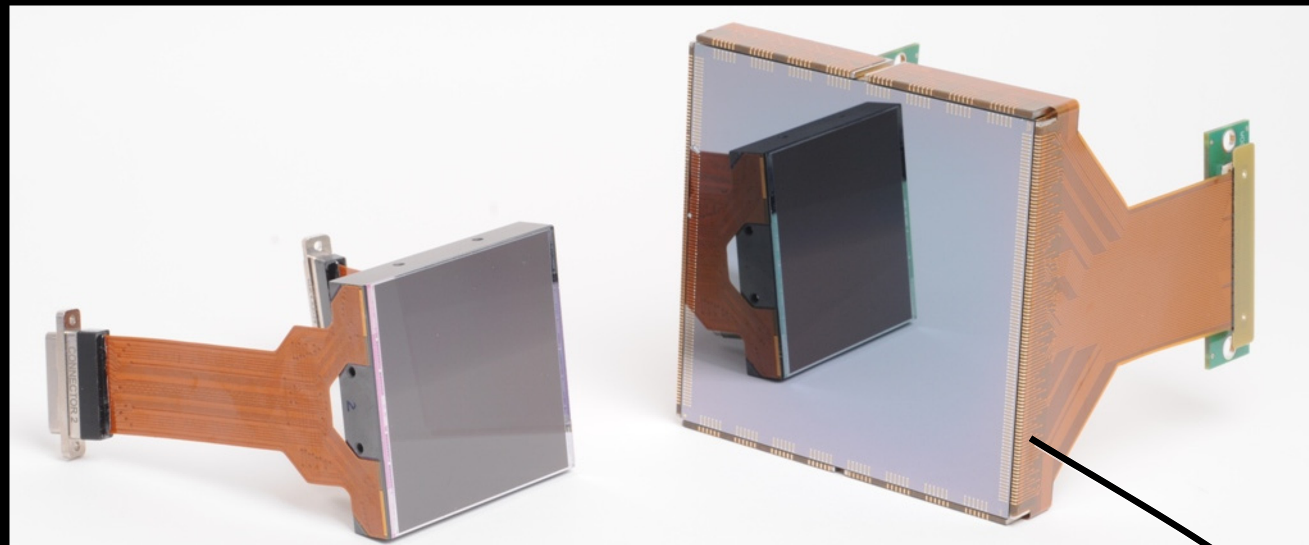

e2v
16.8 million pixels
4096×4096, 15 µm
37.7 cm2

STA
111.5 million pixels
10,240×10,240, 9 µm
90.3 cm2

Philips
66.1 million pixels
7168×9216, 12 µm
95.1 cm2

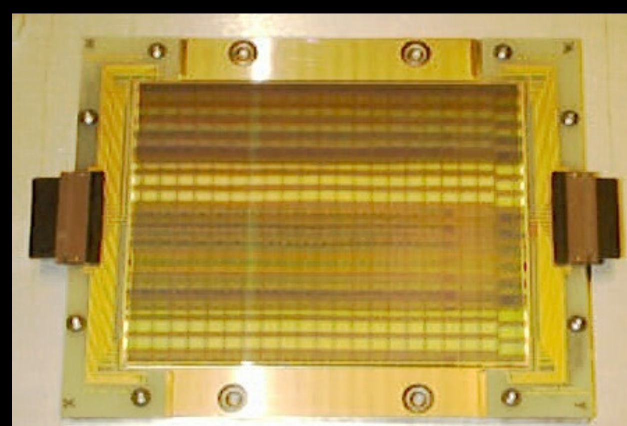

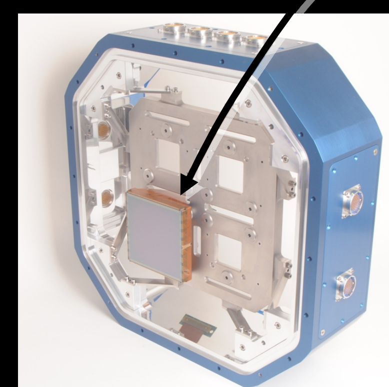

445 Mpixel mosaic

STA1600B 111 Mega pixel imager

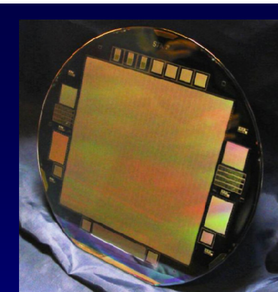

- Full 6-inch wafer imager
- 10,560 × 10,560 pixels
- 9 micron pixel
- 111.5 Megapixels per frame
- 16 dual stage high speed outputs
- Backside thinned available
- Acquisition speeds up to 1 frame/sec

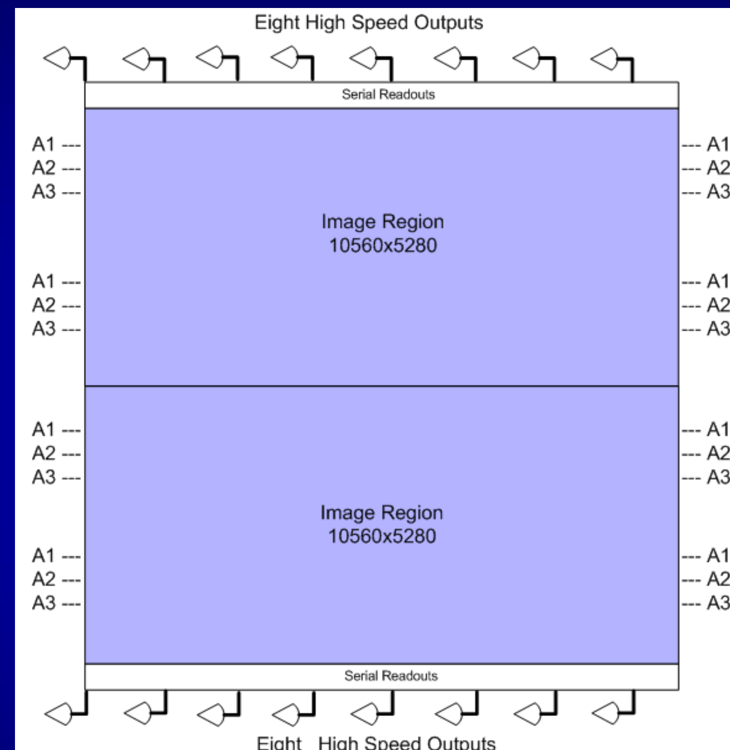

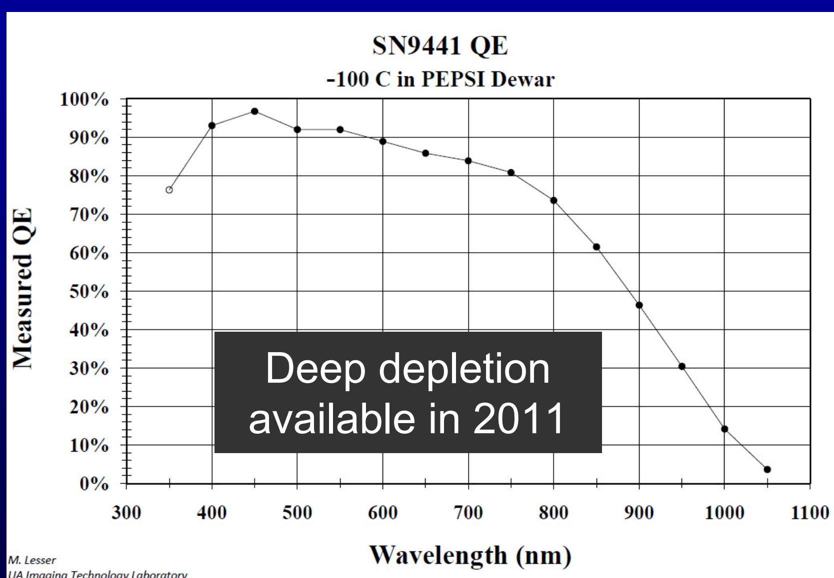

- 7.0-9.0 electrons noise @ 1.0 MHz
- 5.0 electrons @ 100 kHz
- Full well > 80,000 electrons non-MPP

CCD486 6-cm 4k x 4k

Fairchild Imaging

- 4096(H) x 4097(V) full frame CCD
- 15 μm x 15 μm pixels
- 61.44 mm x 61.44 mm image area
- 100% fill factor
- Front or back-illuminated
- Multi-Pinned Phase (MPP) mode
- Readout noise less than 4 e- at 50kHz
- 86 dB dynamic range
- 4 output ports
- 3-phase buried channel architecture
- 800 ke- summing well supports on-chip binning
- Volume production

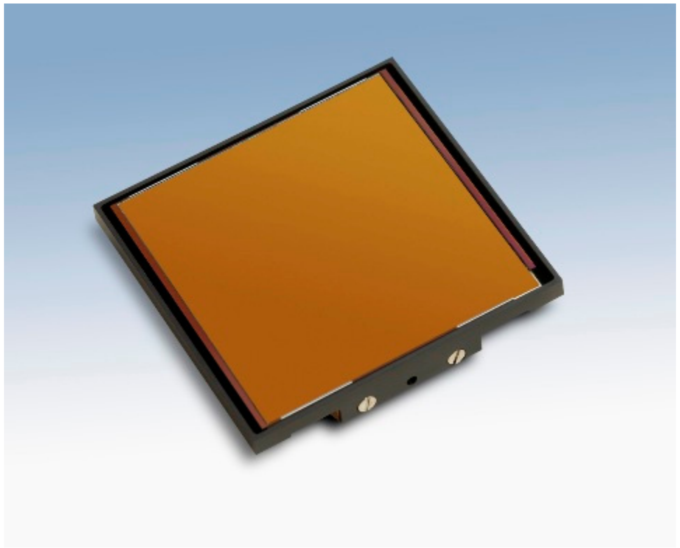

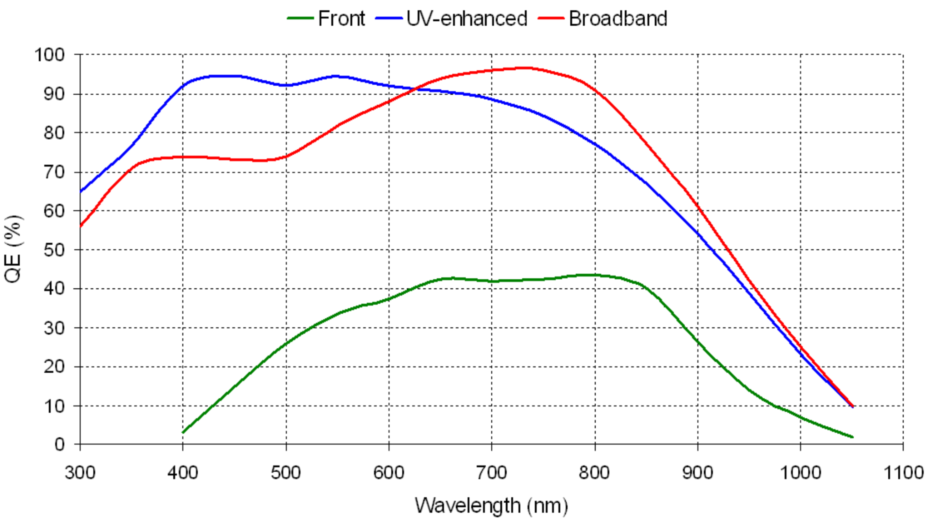

3K×8K Spectrograph CCD

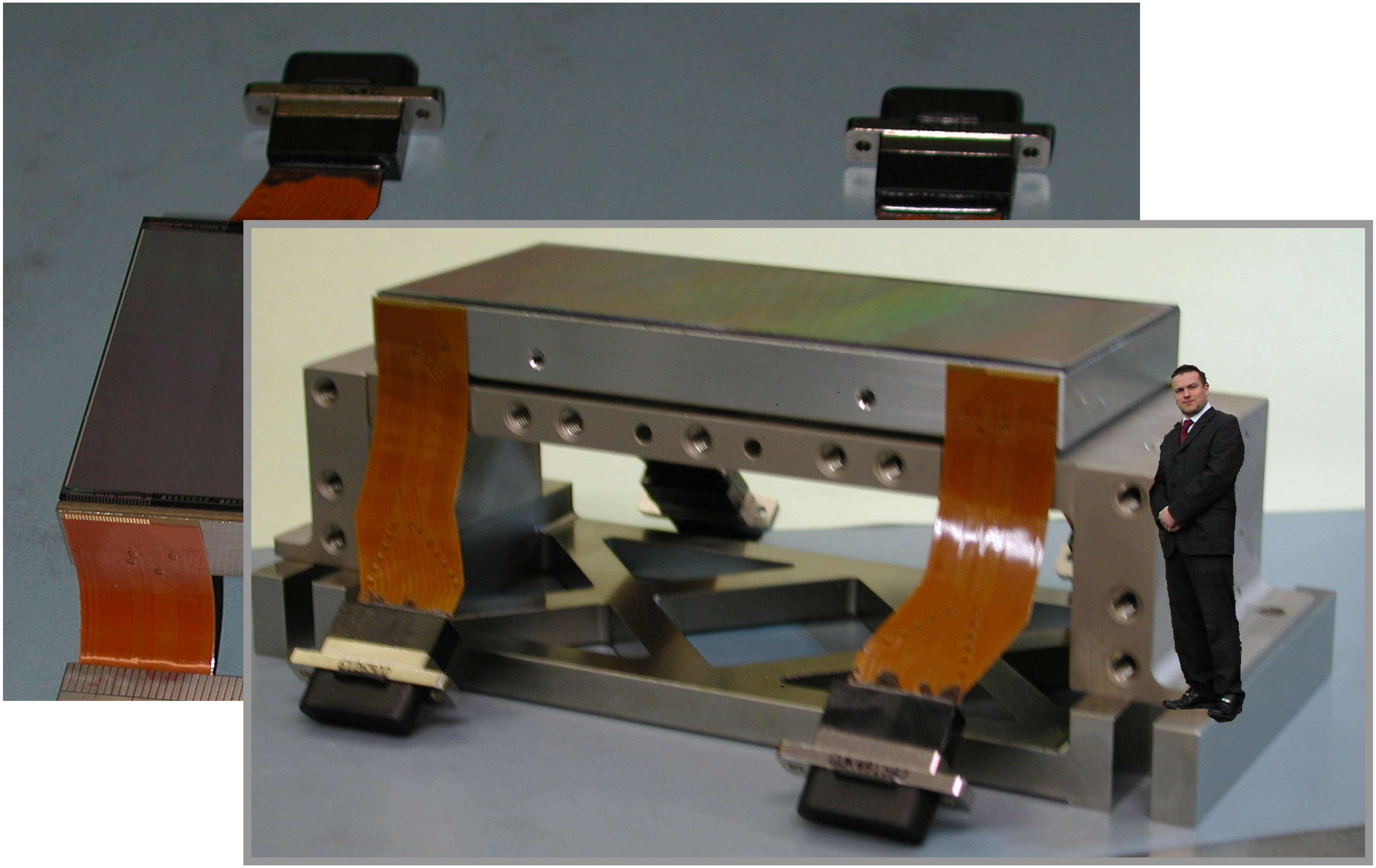

Stability of HARPS due in part to mechanical stability of the CCD cryostat – it doesn't move

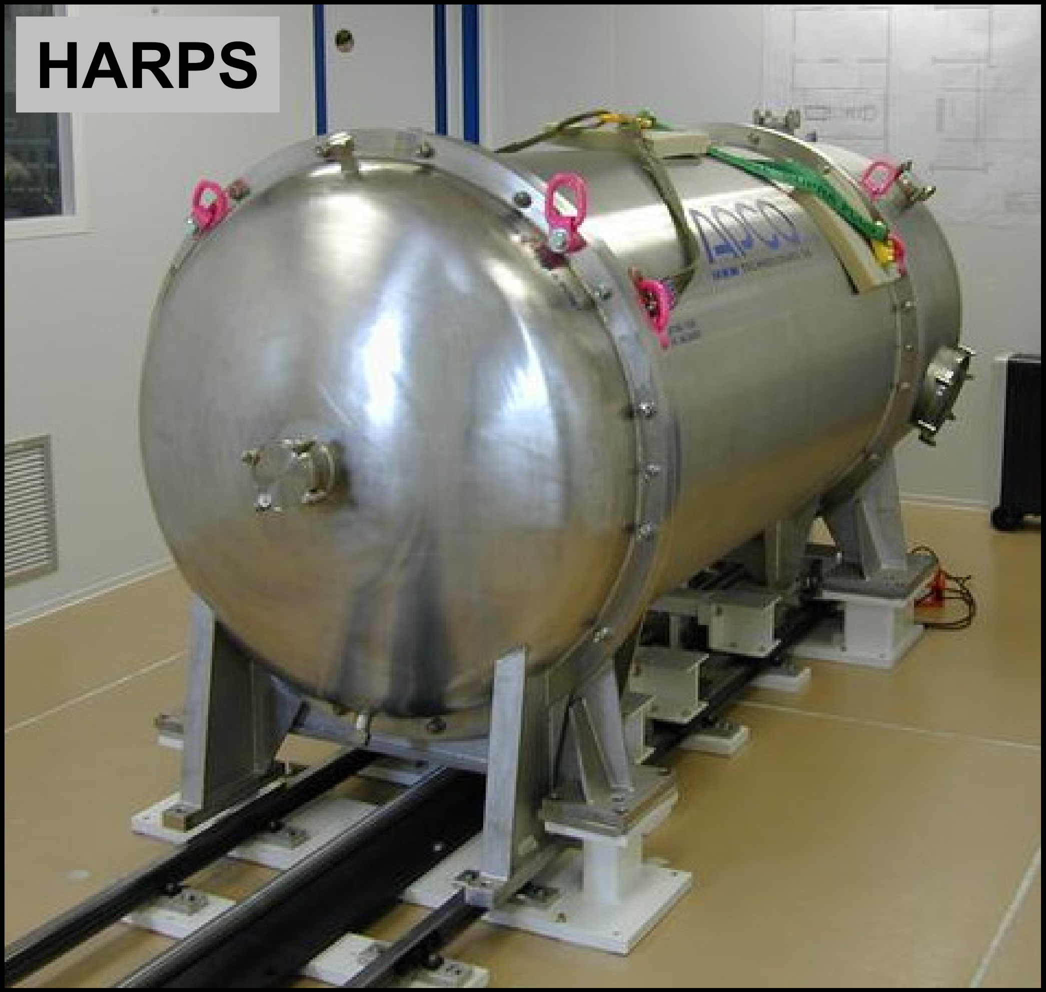

Continuous flow cryostat

HARPS CCD stitch boundary effect

e2v has provided me with new information to state that they now have a new stepper for stitching with 100 nm precision, and this stitch issue should no longer be an effect.

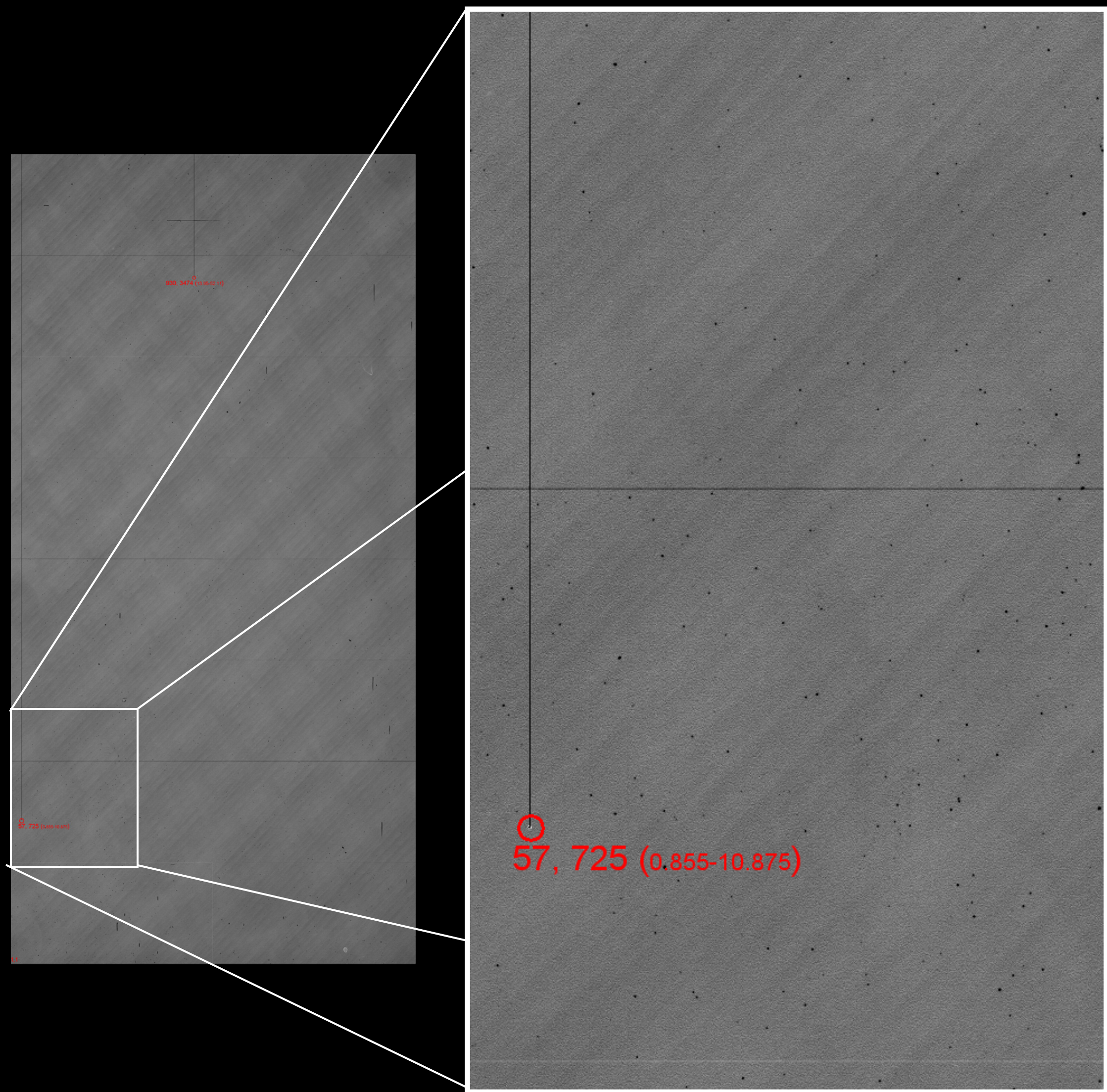

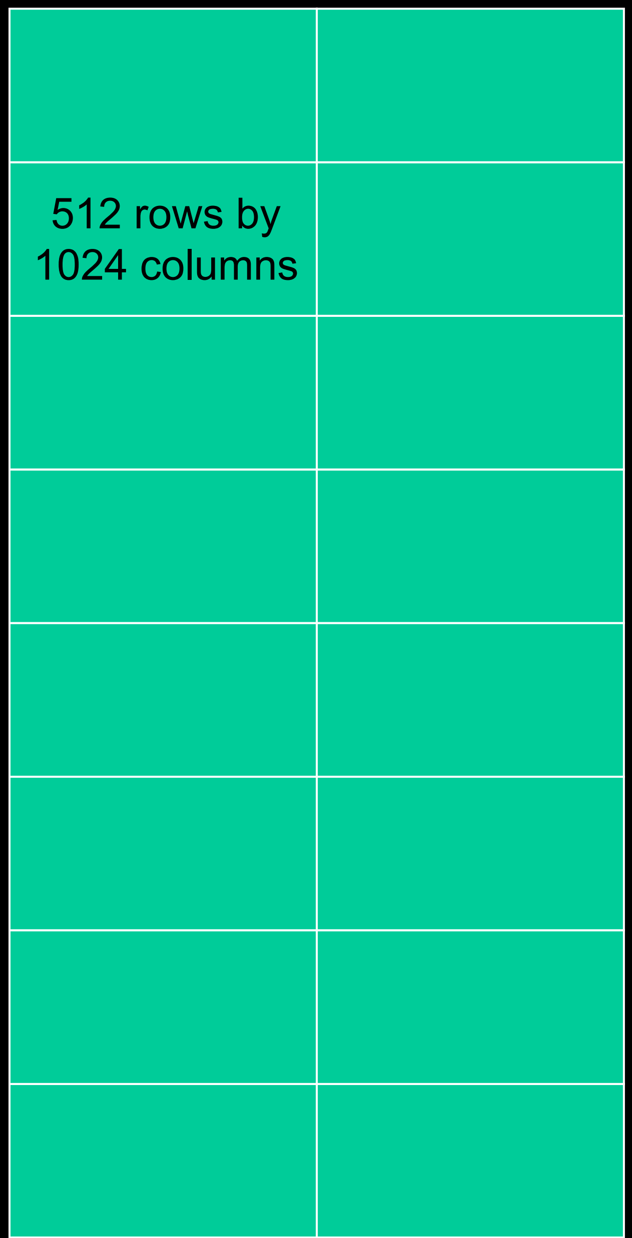

Large-Format, Modular CCD Imagers

- Example: 3K x 3K OTCCD image sensor with 8µm x 8µm pixels
- Pixels with submicron dimensions require high-resolution (248-nm) patterning
  - Lithography field size is smaller than device size
- Design is fractured into functional blocks onto a multi-field reticle and precisely stitched back together on wafer

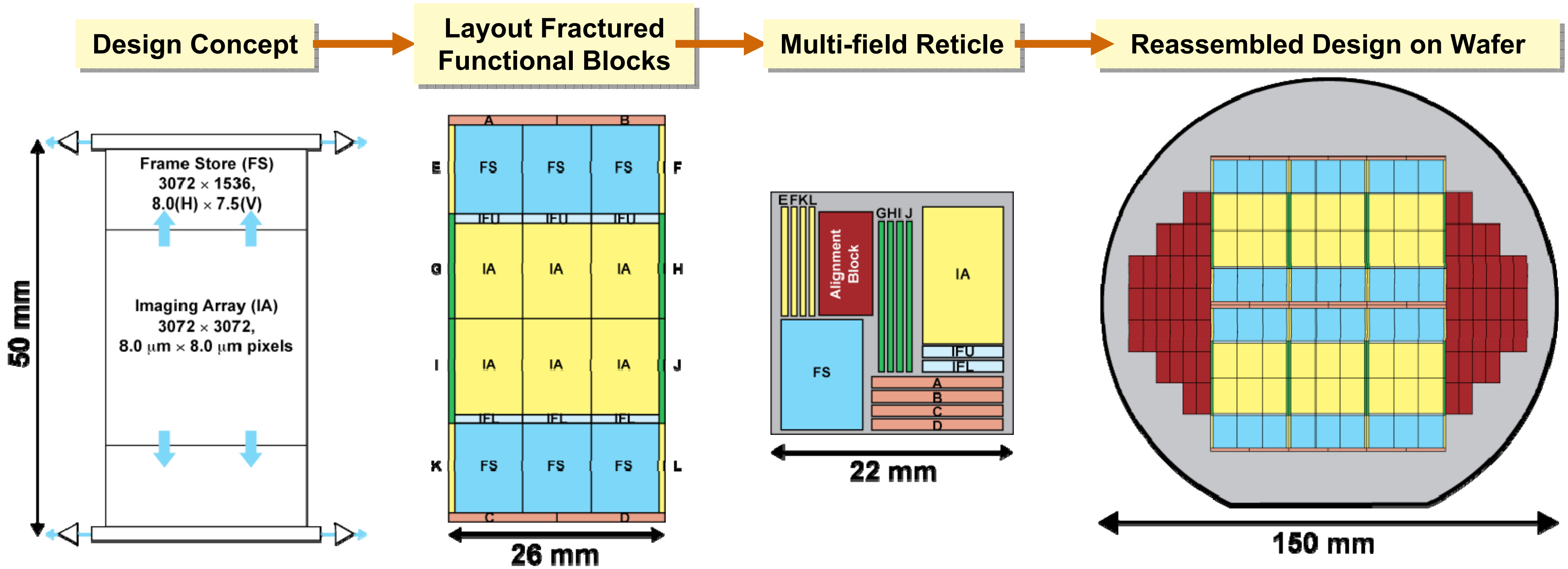

Completed 3K x 3K OTCCD Devices

- Large-area devices (26 mm x 50 mm) fabricated with low-voltage CCD technology
- Stitching methods achieve 35nm (3σ) precision with 8-µm pixel active devices
- Device test results expected in Nov 2010
- Process technology will be migrated to 200-mm substrates

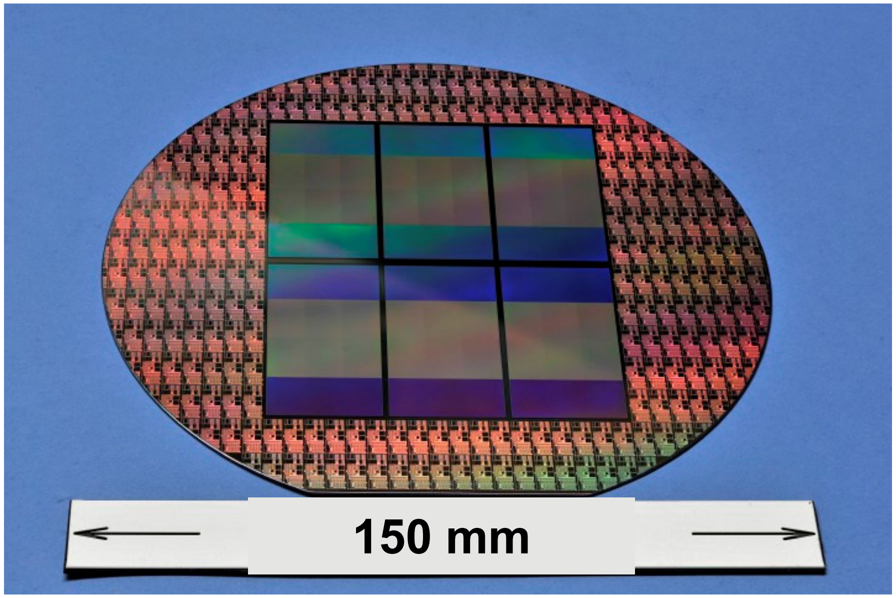

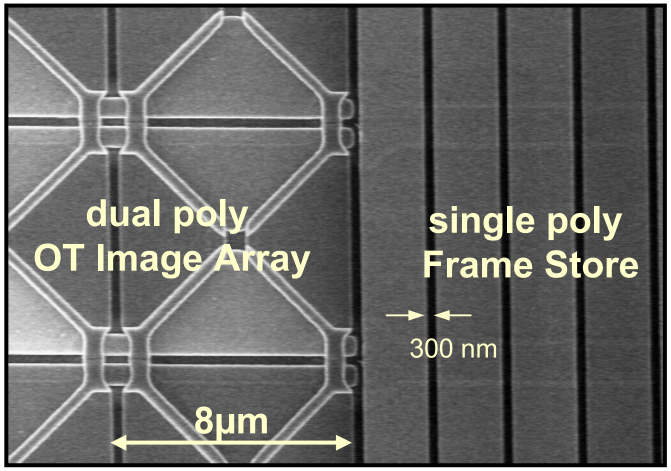

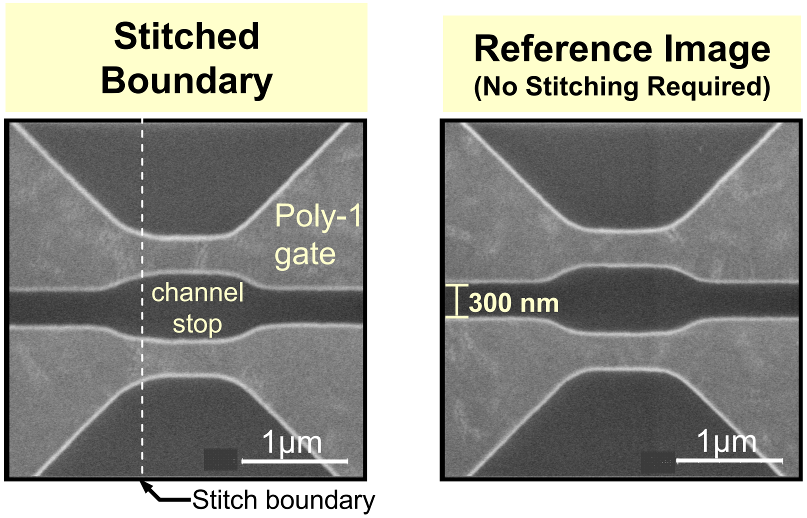

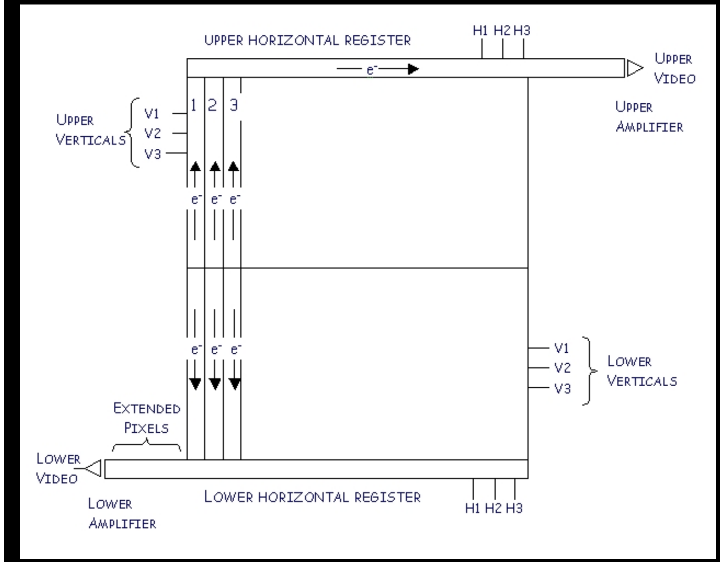

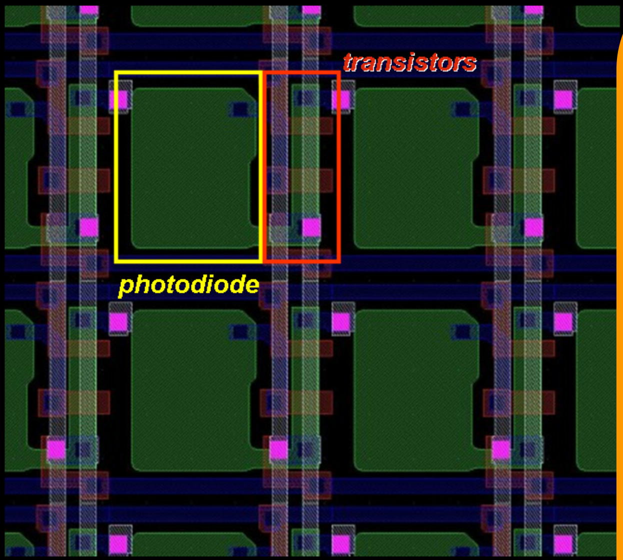

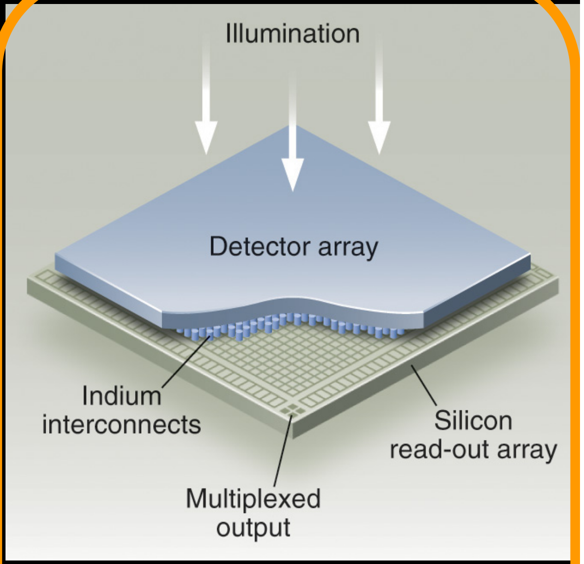

CCD

Monolithic CMOS

Hybrid CMOS

HgCdTe
Visible through IR

Silicon - Visible through near IR

Hybrid Imager Architecture

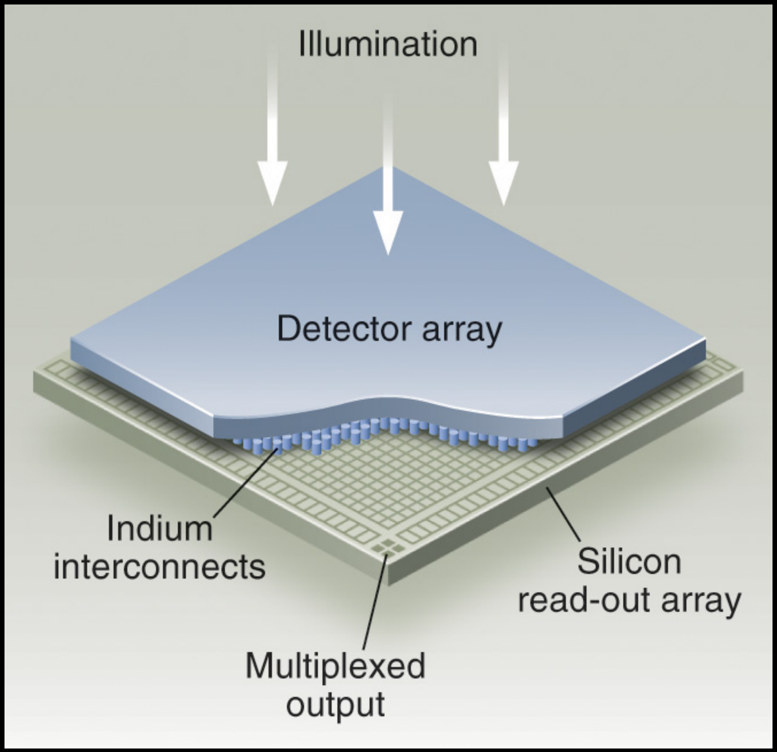

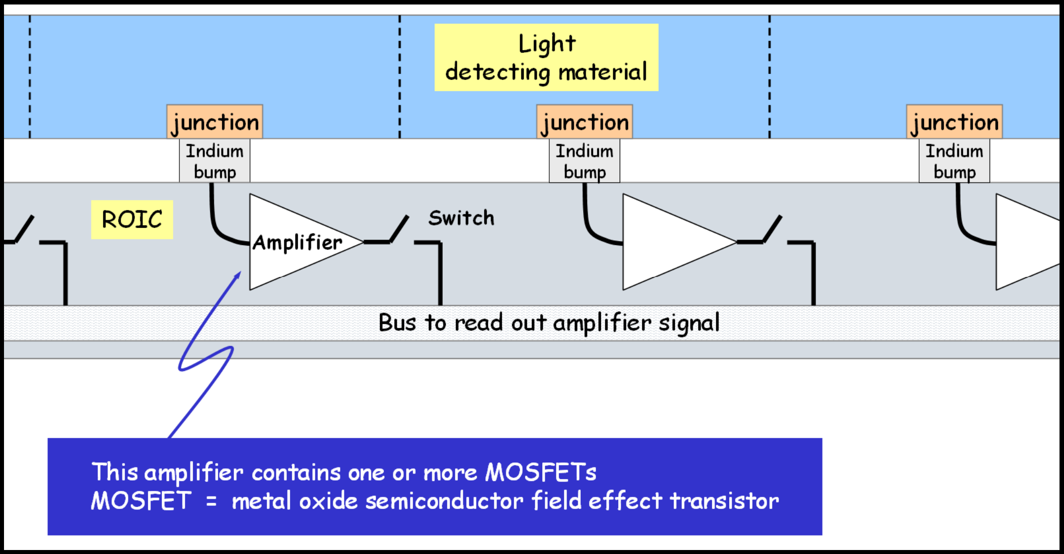

H4RG-10
4096x4096 pixels
10 micron pixel pitch
HyViSI silicon PIN

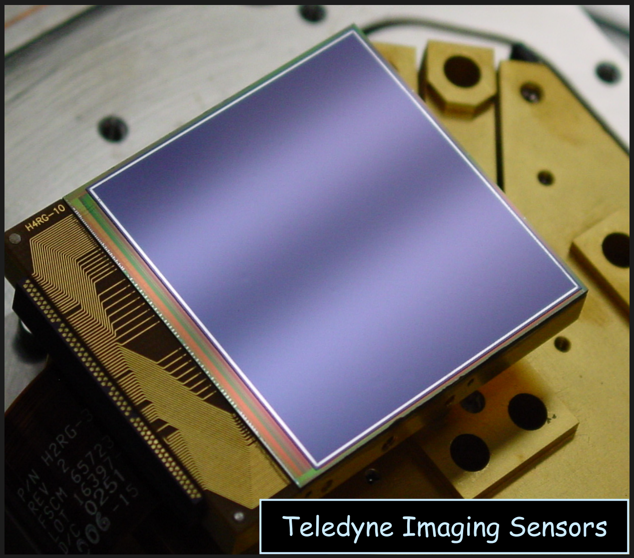

Mature interconnect technique:

- Over 16,000,000 indium bumps per Sensor Chip Assembly (SCA) demonstrated
- >99.9% interconnect yield

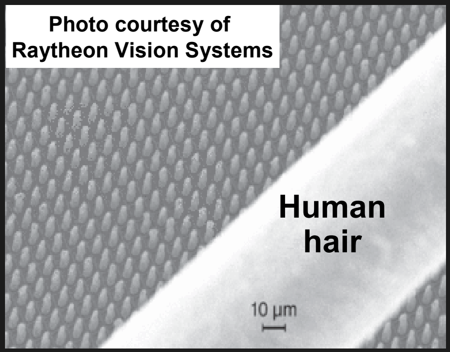

Tunable Wavelength: Valuable property of HgCdTe

$Hg_{1-x}Cd_xTe$ Modify ratio of Mercury and Cadmium to "tune" the bandgap energy

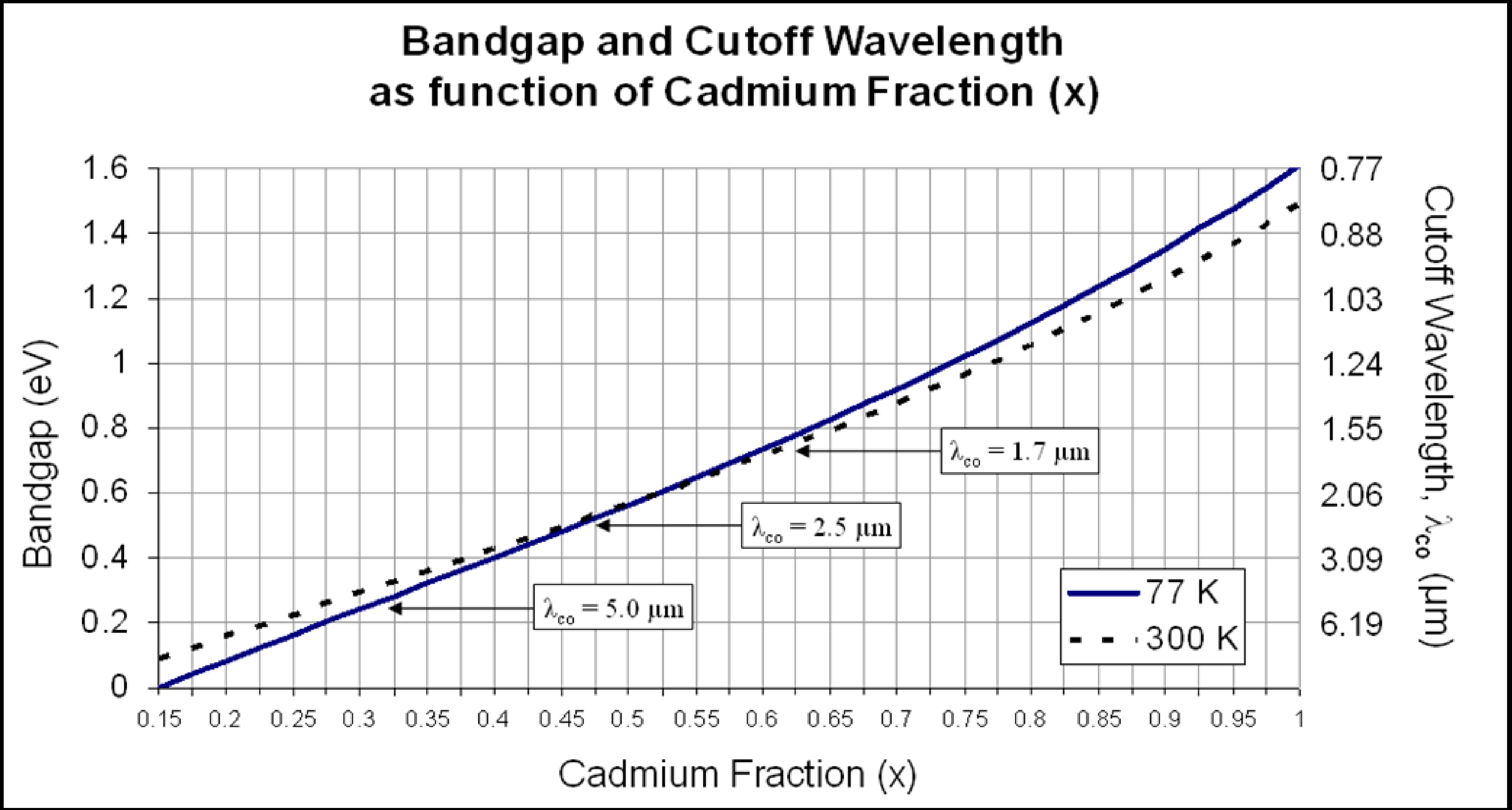

$$E_g = -0.302 + 1.93x - 0.81x^2 + 0.832x^3 + 5.35\times10^{-4}T(1-2x)$$

G. L. Hansen, J. L. Schmidt, T. N. Casselman, J. Appl. Phys. 53(10), 1982, p. 7099

Absorption Depth of HgCdTe

Rule of Thumb

Thickness of HgCdTe layer needs to be about equal to the cutoff wavelength

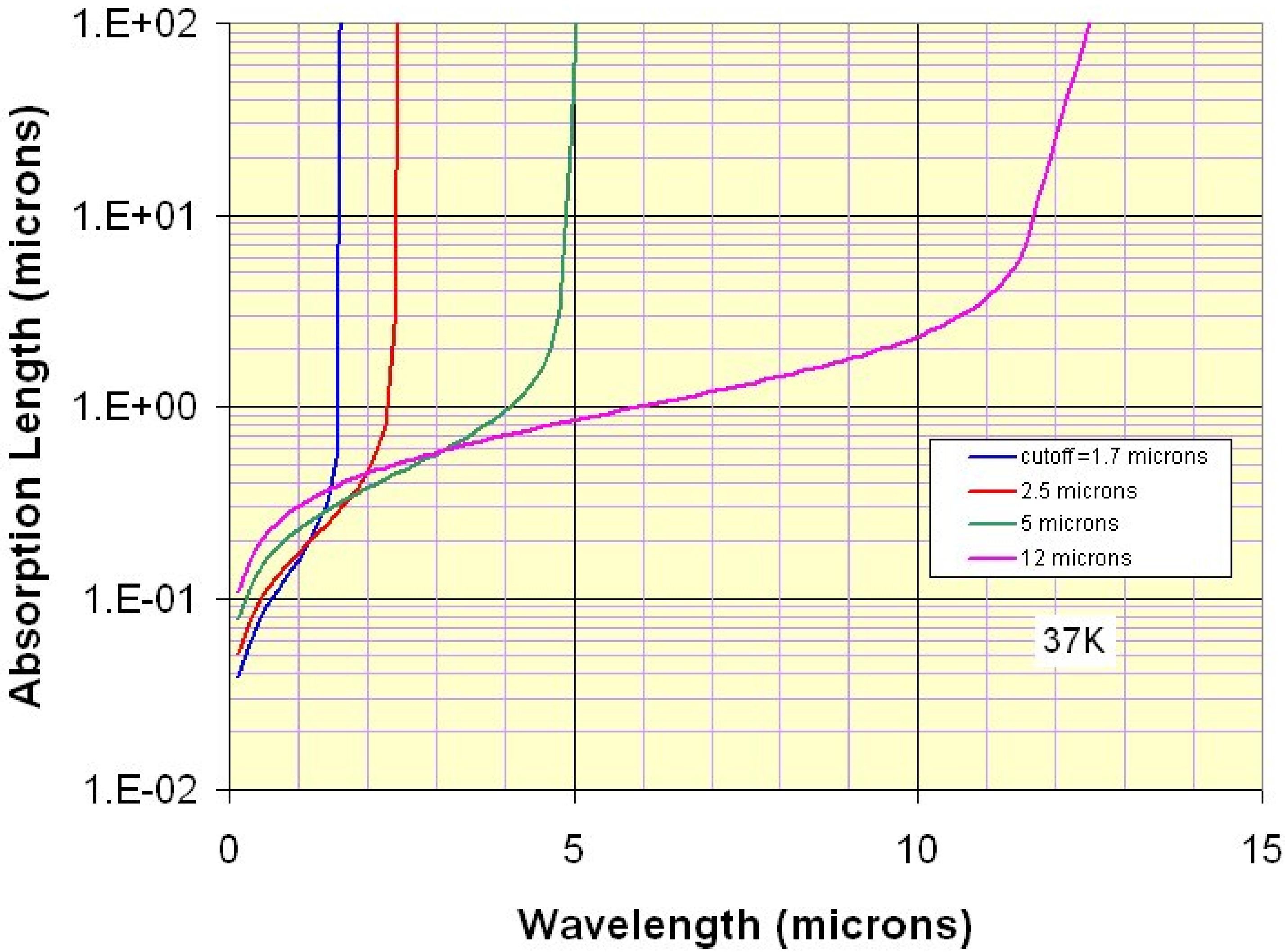

MBE growth of HgCdTe

1. Molecular Beam Epitaxy (MBE)
   - Enables very accurate deposition ⇒ "bandgap engineering"
   - Teledyne has 4 MBE machines for detector growth

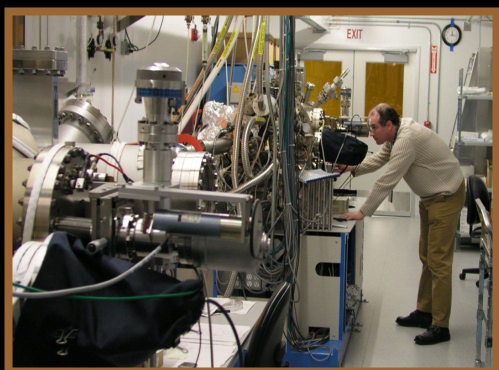

RIBER 10-in MBE 49 System

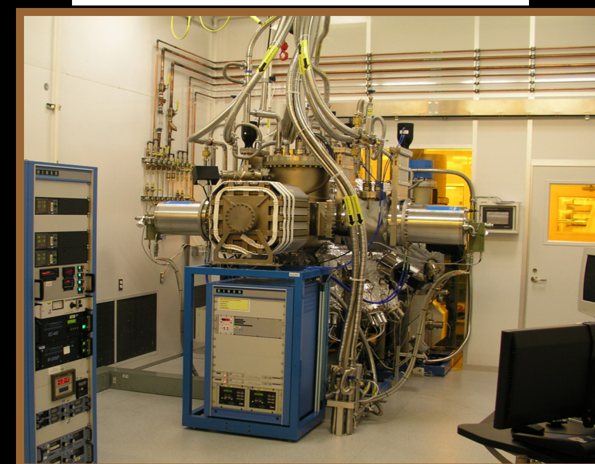

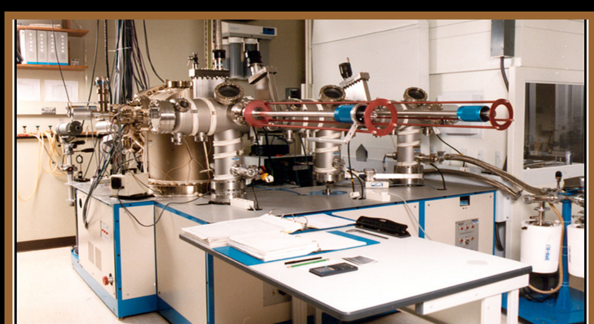

RIBER 3-in MBE Systems

3 inch diameter platen allows growth on one 6x6 cm substrate

More than 7500 MCT wafers grown to date

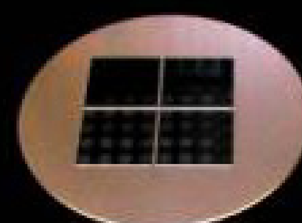

10 inch diameter platen allows simultaneous growth on four 6x6 cm substrates

HgCdTe IR FPA Manufacturing Process

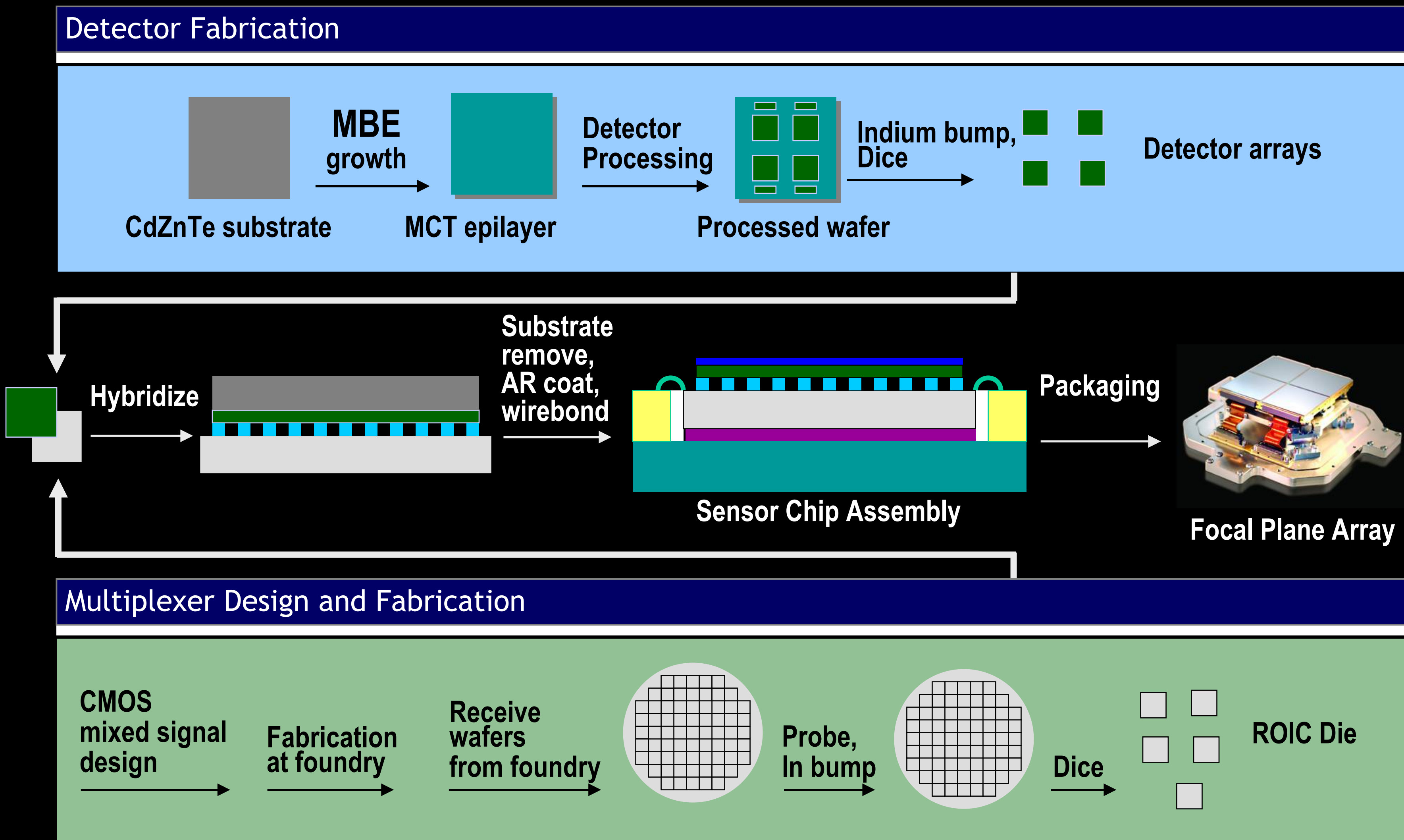

HgCdTe hybrid FPA cross-section
(substrate removed)

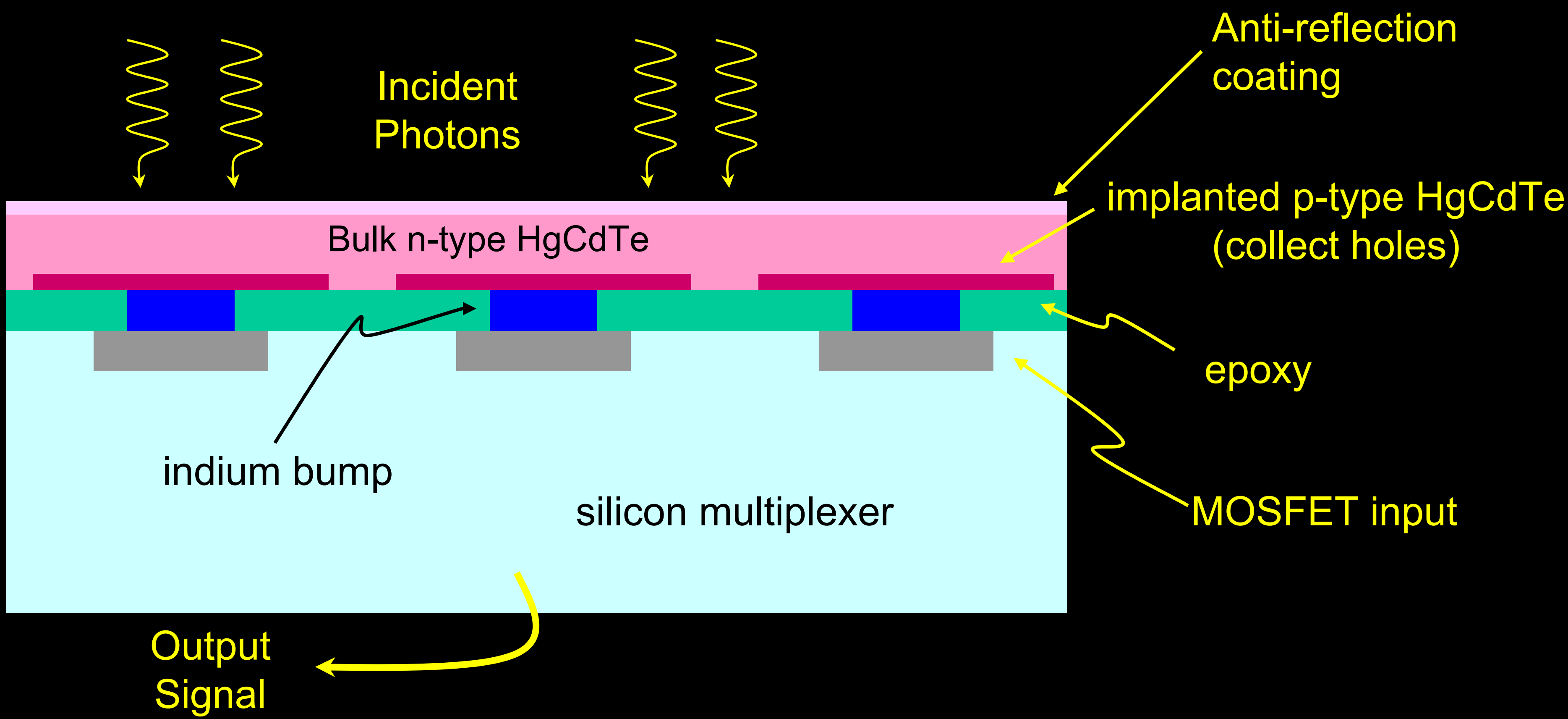

- Field in detector layer pushes charge to p-n junction
- Thin detector minimizes charge diffusion

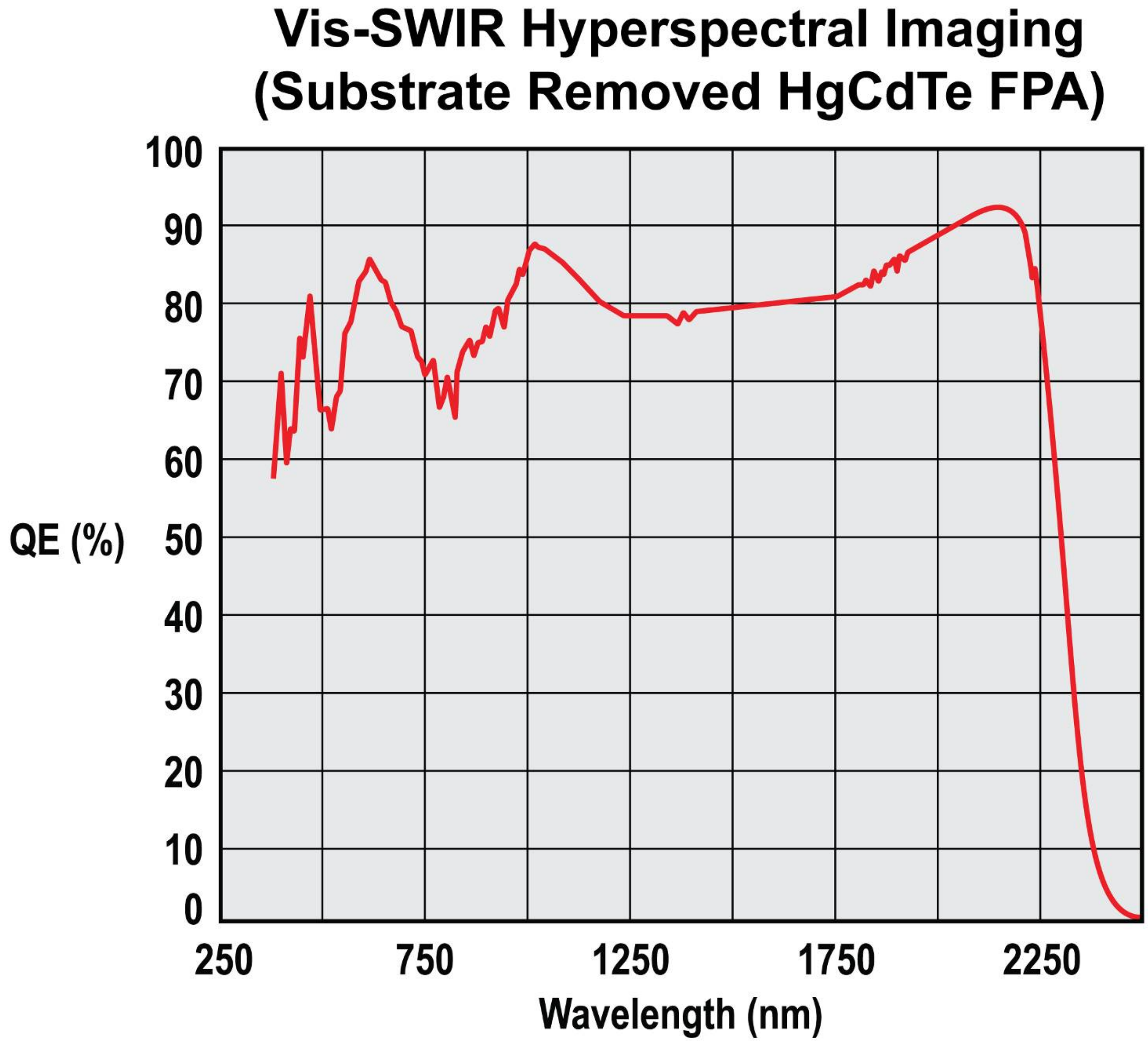

Public Domain Information - OSR Public Release Authority (08-S-0965).

HgCdTe Quantum Efficiency
Measured by the European Southern Observatory

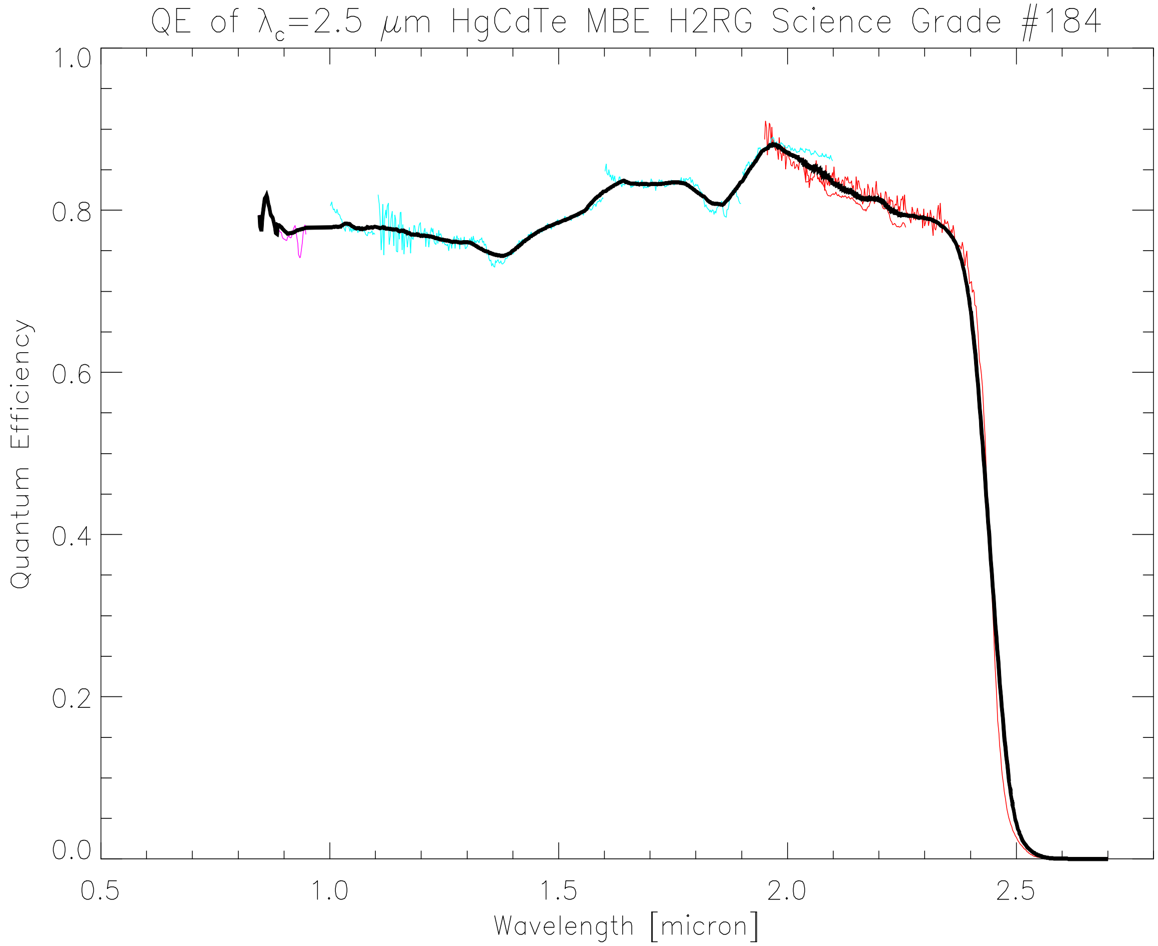

Data: Courtesy of ESO, KMOS project

Moon Mineralogy Mapper Discovers Water on the Moon

Moon water findings are a game-changer

Discovery calls into question 40 years of assumptions about lunar surface

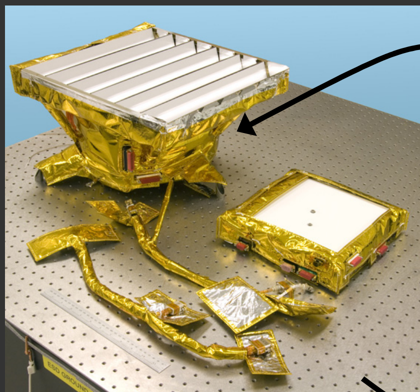

Instrument at JPL before shipment to India

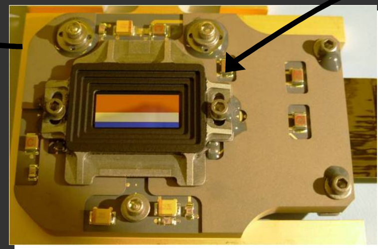

Focal Plane Assembly

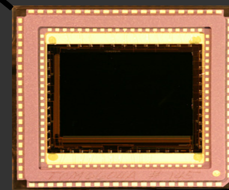

Sensor Chip Assembly

By Andrea Thompson
SPACE
updated 12:38 p.m. PT, Thurs., Sept . 24, 2009

The discovery of widespread but small amounts water on the surface of the moon, announced Wednesday, stands as one of the most surprising findings in planetary science.

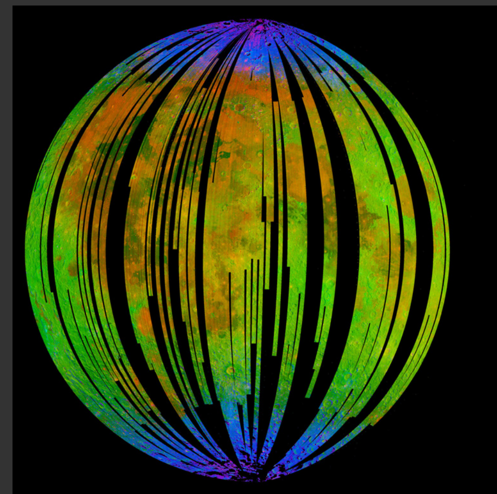

Teledyne Infrared FPA

- 640 x 480 pixels (27 µm pitch)
- Substrate-removed HgCdTe (0.4 to 3.0 µm)
- 650,000 e- full well, <100 e- noise
- 100 Hz frame rate (integrate while read)
- < 70 mW power dissipation
- Package includes order sorting filter
- Total FPA mass: 58 grams

Completion of Chandrayaan-1 spacecraft integration
Moon Mineralogy Mapper is white square at end of arrow

Chandrayaan-1 in the Polar Satellite Launch Vehicle

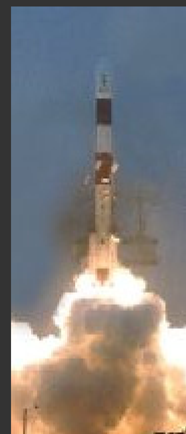

Launch from Satish Dhawan Space Centre

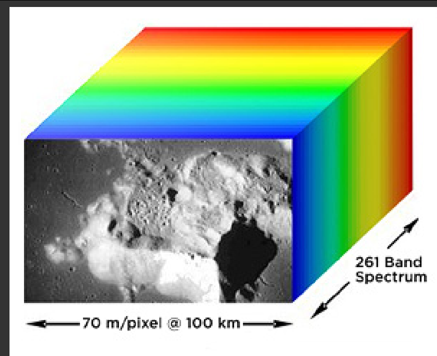

Moon Mineralogy Mapper resolves visible and infrared to 10 nm spectral resolution, 70 m spatial resolution 100 km altitude lunar orbit

Dark Current of HgCdTe Detectors

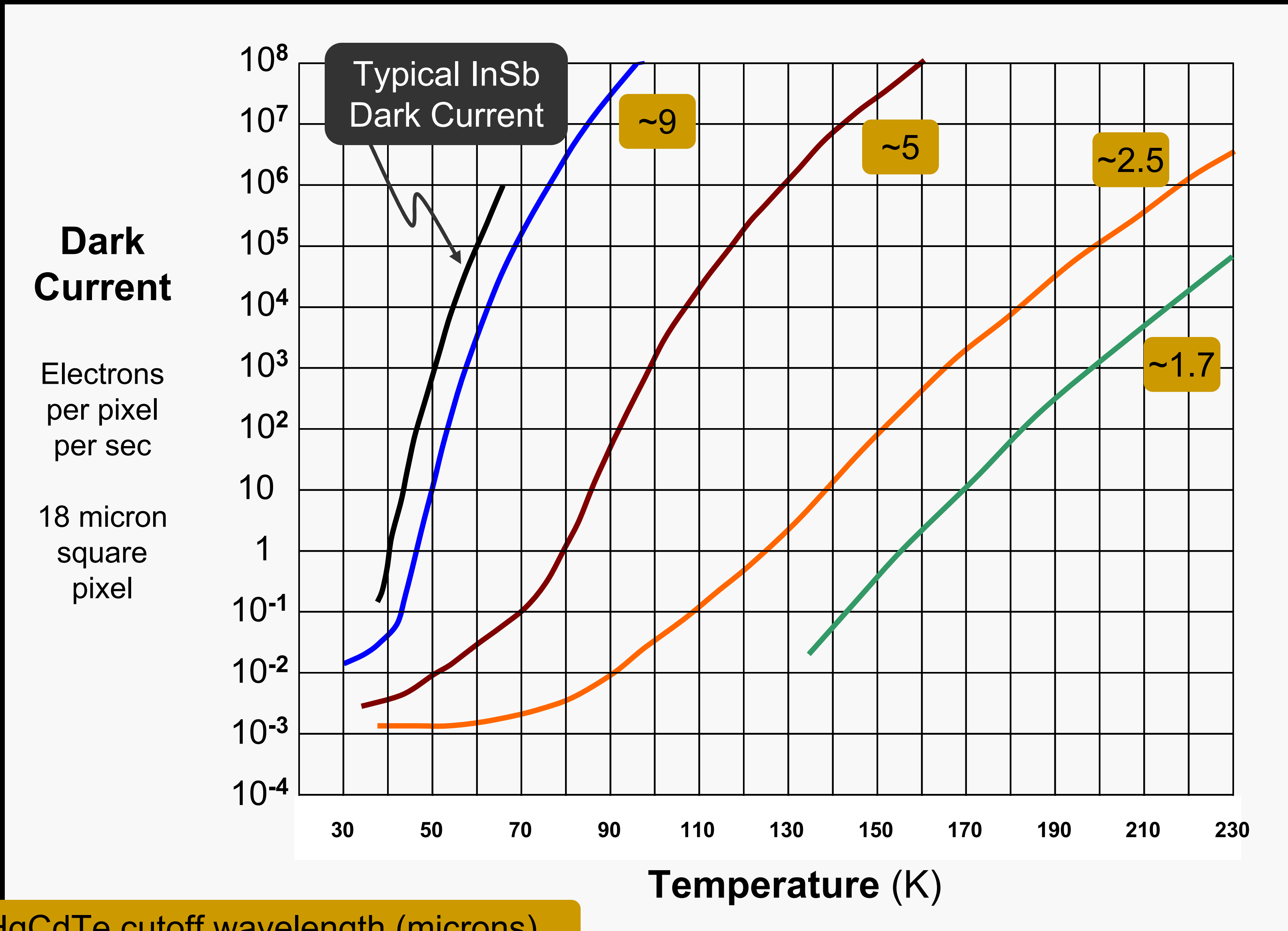

HgCdTe cutoff wavelength (microns)

Teledyne Imaging Sensors

6 steps of optical / IR photon detection

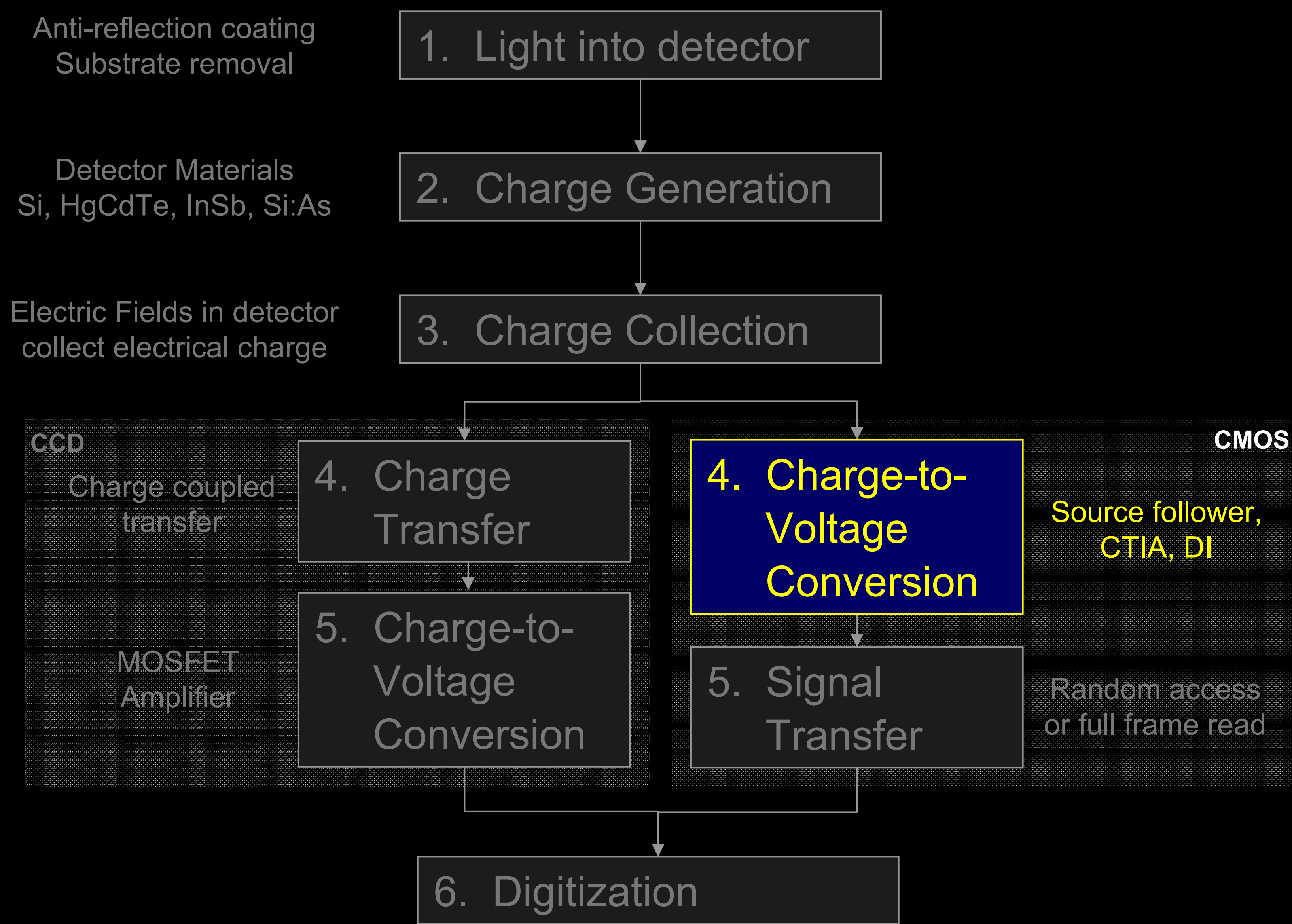

IR multiplexer pixel architecture

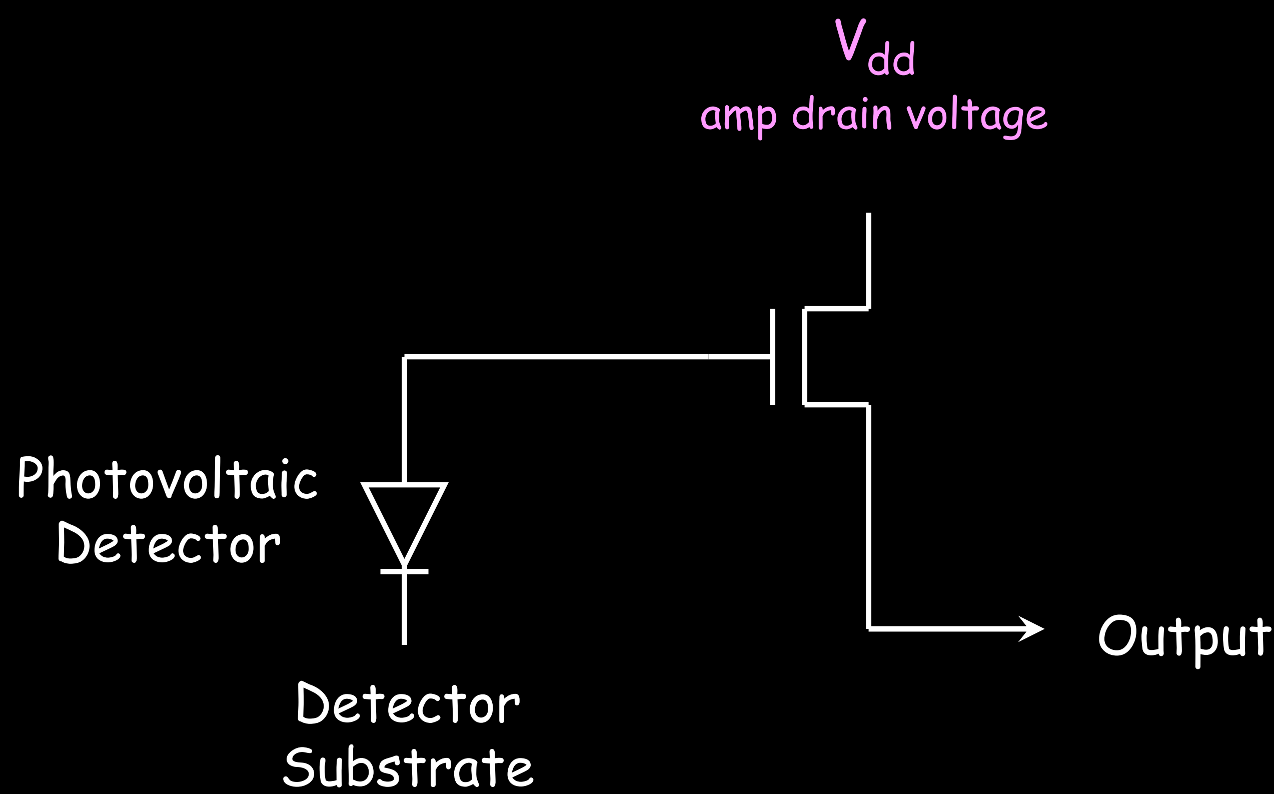

IR multiplexer pixel architecture

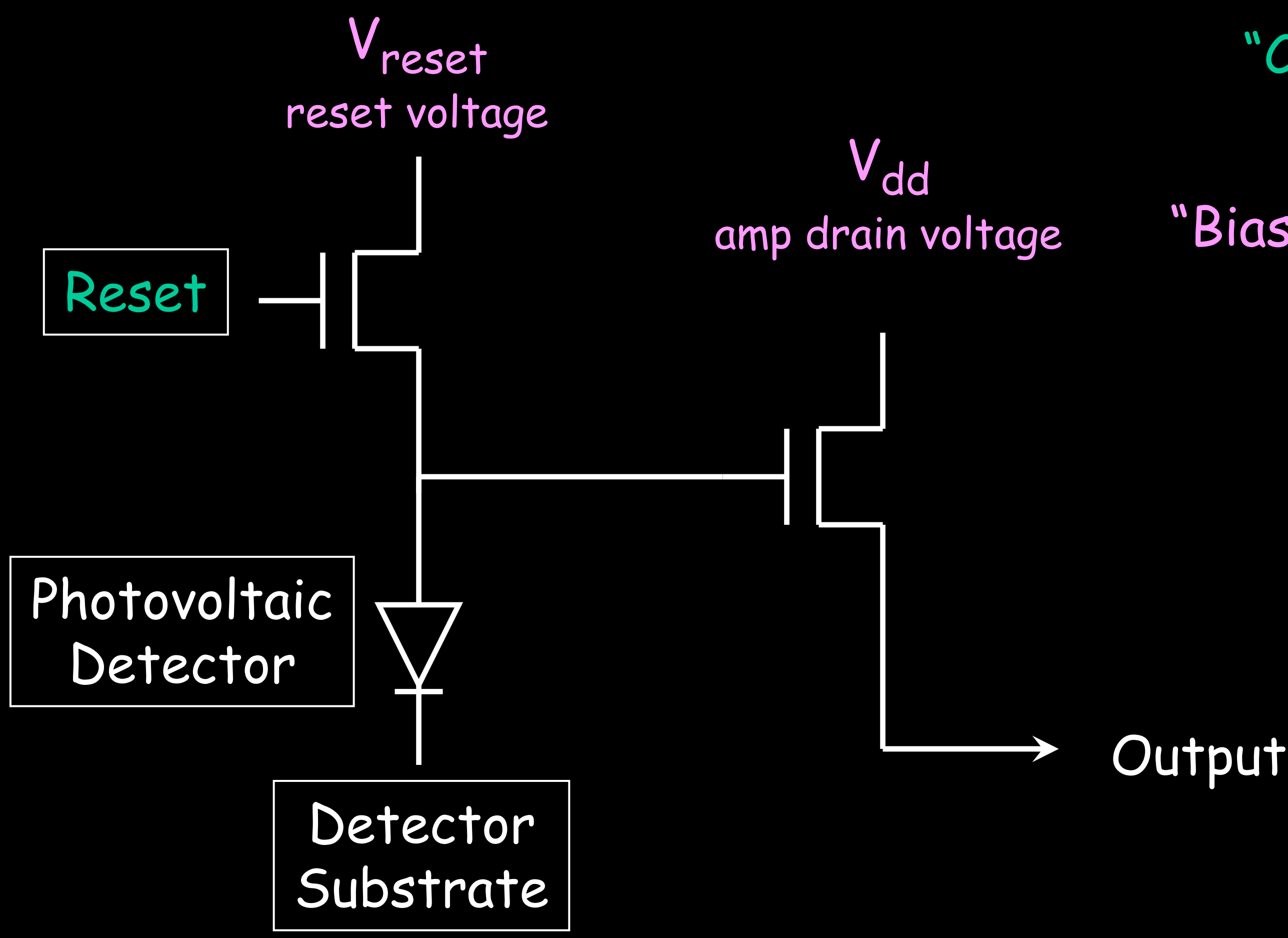

"Clock" (green)

"Bias voltage" (purple)

IR multiplexer pixel architecture

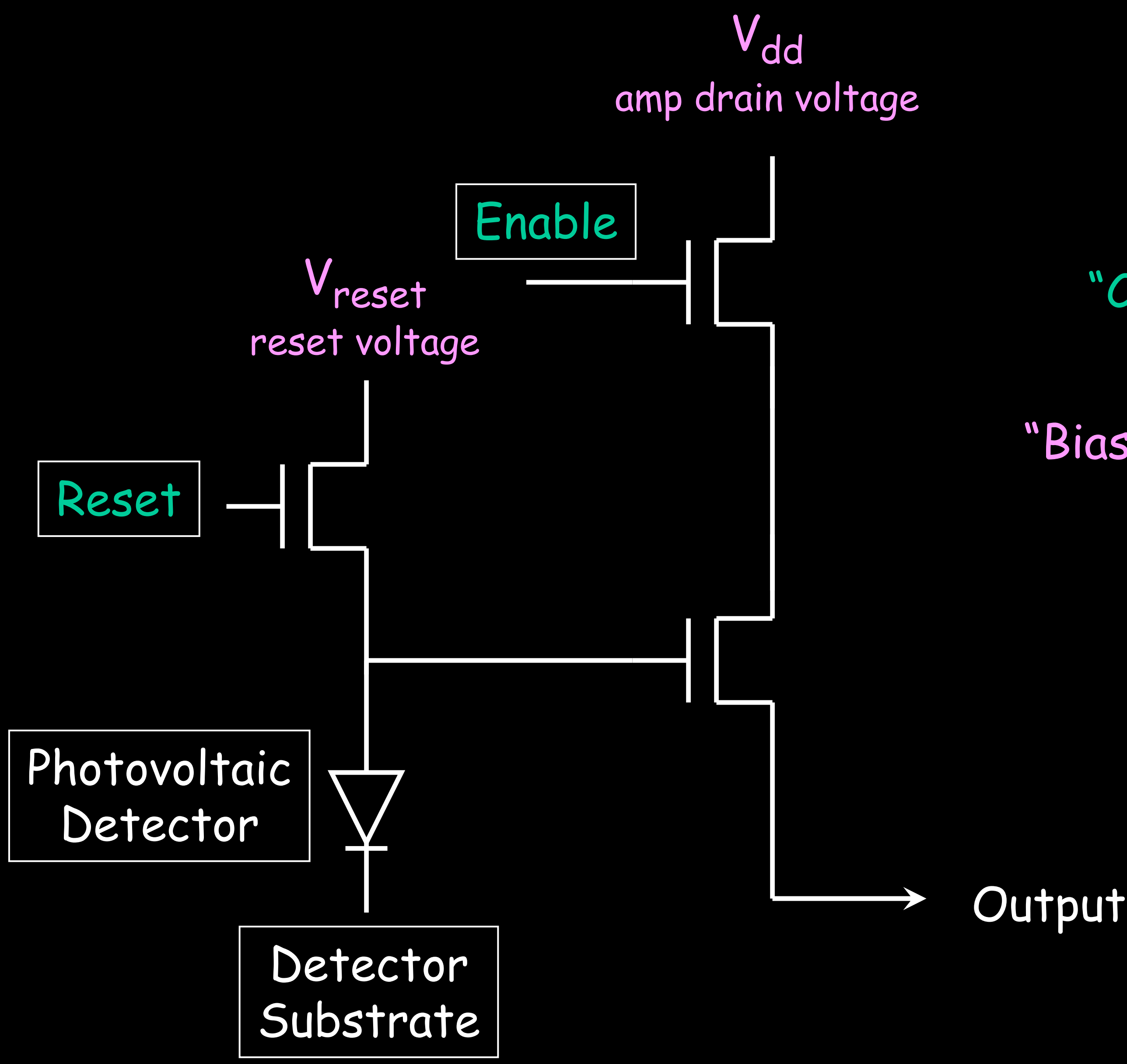

"Clock" (green)

"Bias voltage" (purple)

3T Pixel

MOSFET Amplifier Noise

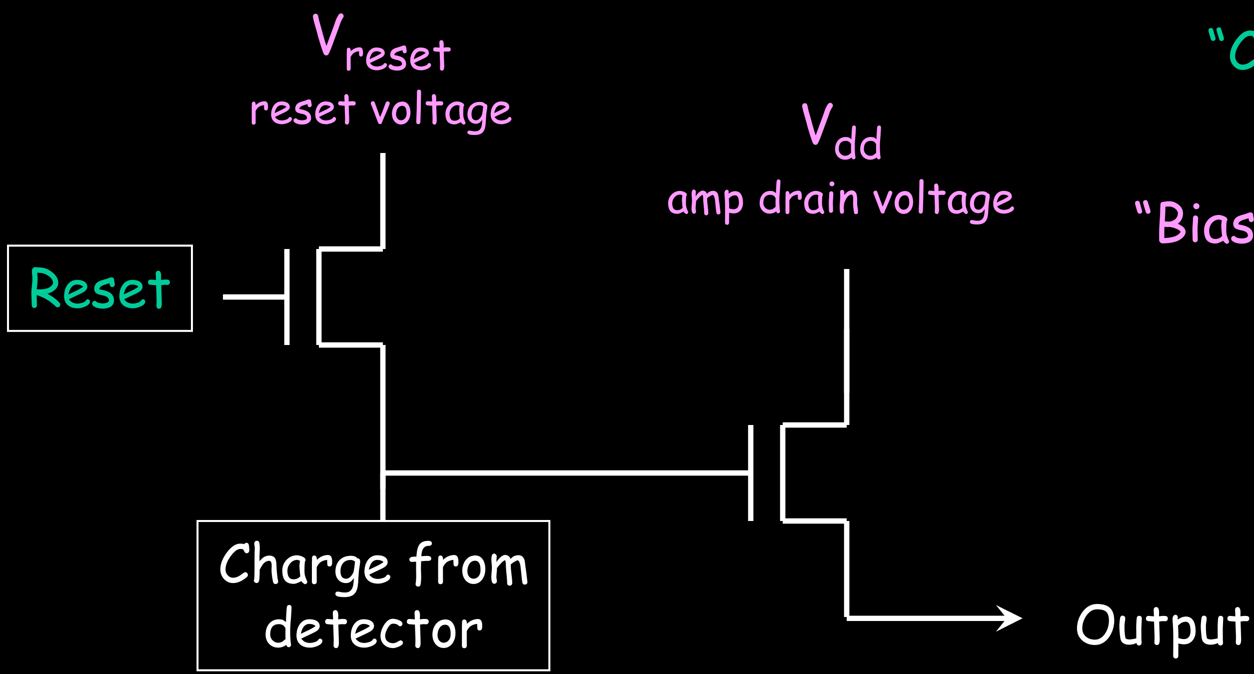

"Clock" (green)

"Bias voltage" (purple)

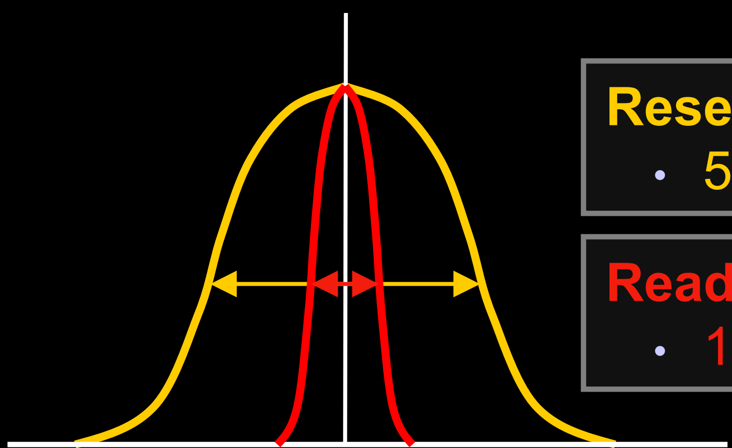

Reset Noise
- 50 to 100 e- rms

Read Noise
- 1.5 to 10 e- rms

Correlated Double Sample (CDS)
- Reset
- Read
- Put charge on gate
- Read

Example of Noise vs Number of Fowler Samples

Non-destructive readout enables reduction of noise from multiple samples

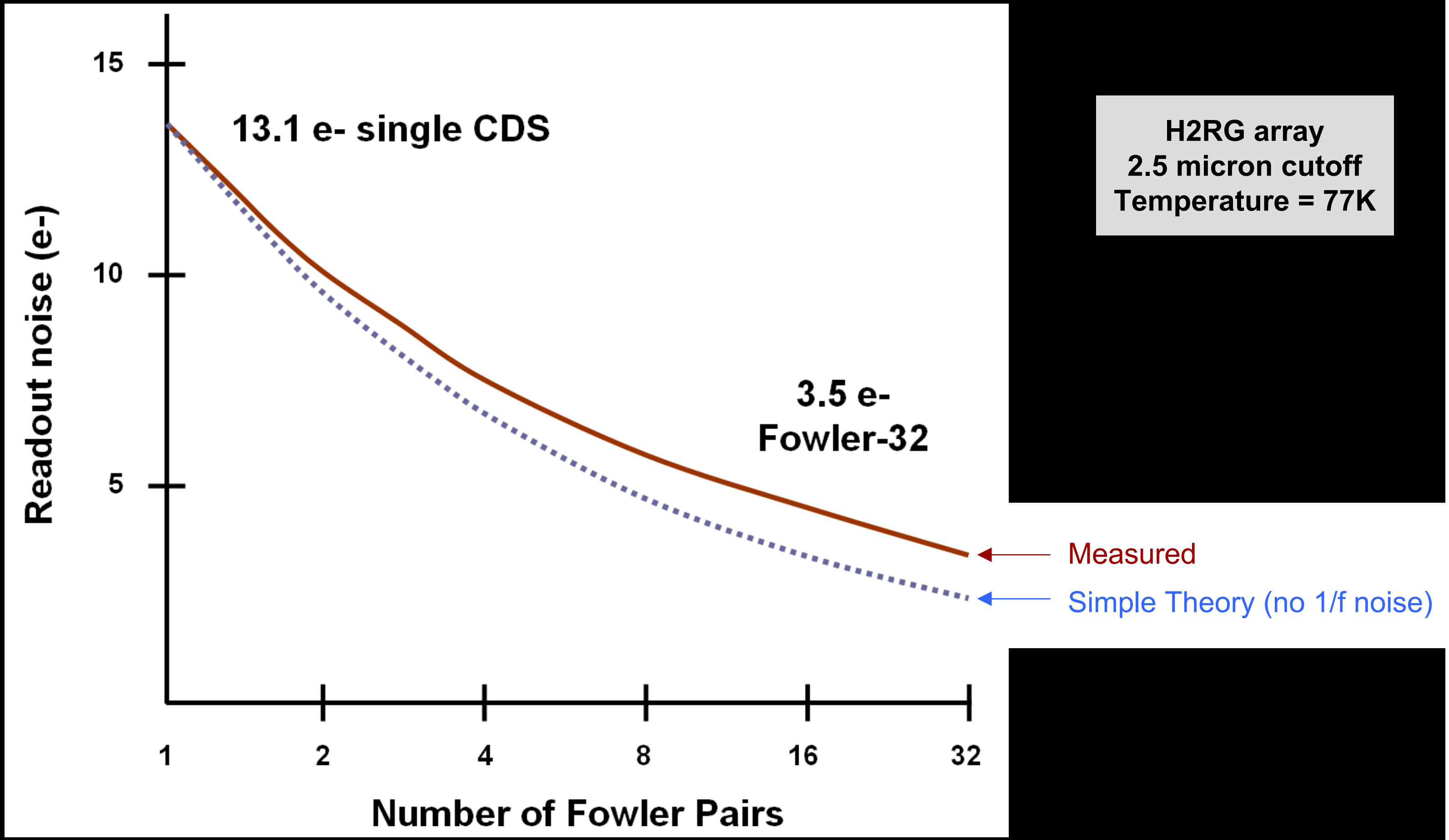

H2RG array
2.5 micron cutoff
Temperature = 77K

Architecture of simplest analog CMOS sensor

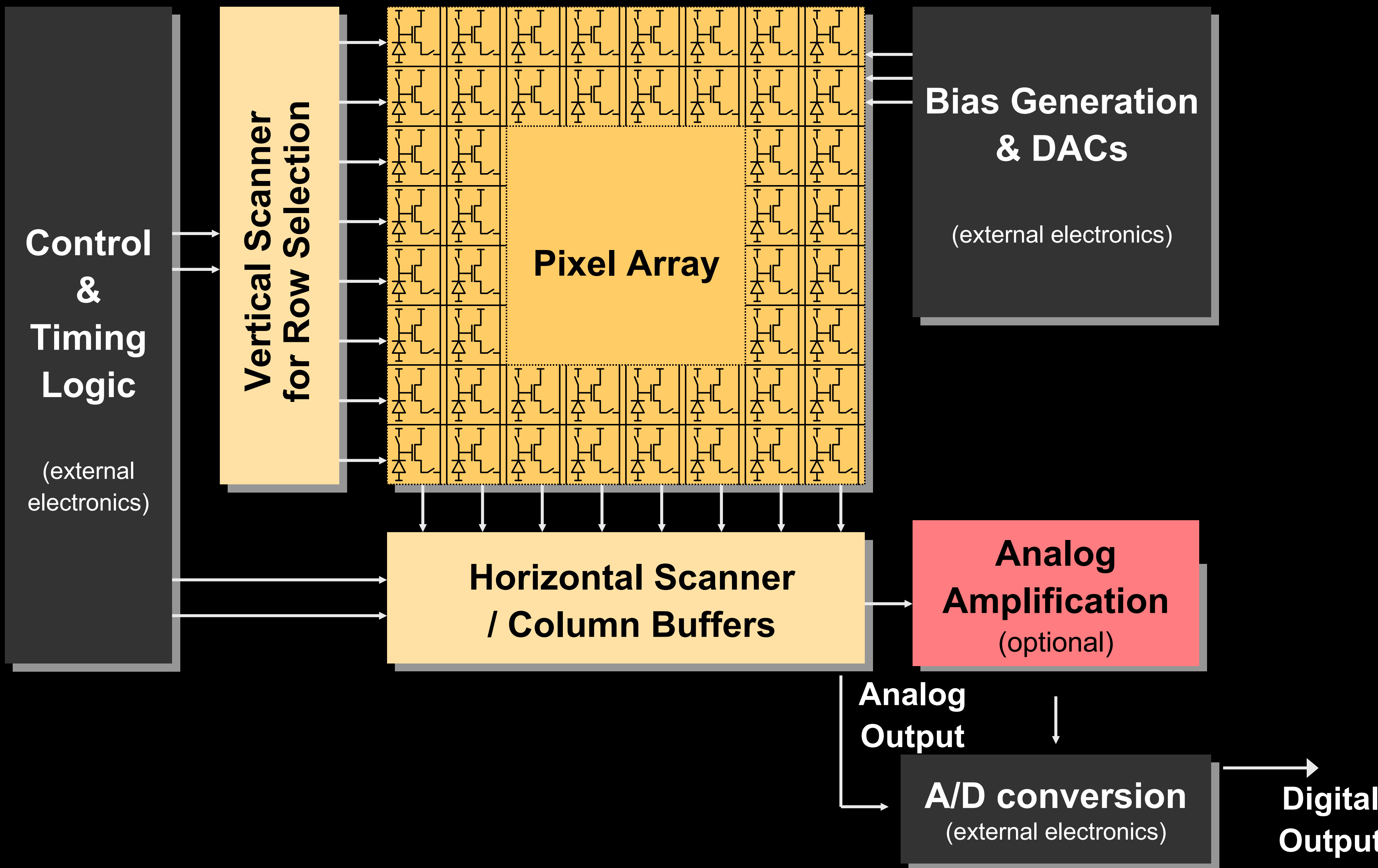

HxRG Family of Hybrid Imaging Sensors

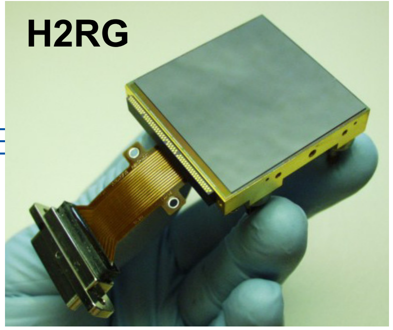

H: HAWAII: HgCdTe **A**stronomical **W**ide **A**rea **I**nfrared **I**mager

x: Number of 1024 (or 1K) pixel blocks in x and y-dimensions

R: **R**eference pixels

G: **G**uide window capability

➔ Substrate-removed HgCdTe for simultaneous visible & infrared observation

➔ Hybrid Visible Silicon Imager; Si-PIN (HyViSI)

Name	Format (# of Pixel)	Pixel Pitch (μm)	# of Outputs	NASA - TRL	Institutions, Observatories, and Programs Using HxRG Arrays
H1RG	1024×1024	18	1, 2, 16	9	Wide-field Infrared Survey Explorer (WISE) Orbiting Carbon Observatory (OCO) Development Programs in Astronomy & Earth Science
H2RG	2048×2048	18	1, 4, 32	6	James Webb Space Telescope (JWST) - NIRCam, NIRSpec, FGS Joint Dark Energy Mission (JDEM) Astronomy institutions and observatories: Calar Alto, Caltech, CFHT, ESO, ESTEC, Gemini, GSFC, IRTF, ISRO, IUCAA, JHU-APL, Keck, LBNL, LMU, MIT, MPIA, MPS, OCIW, Penn State, RIT, SALT, SAO, Subaru, TATA, U. Arizona, UCLA, UC Berkeley, U. Hawaii, U. Rochester, U. Toronto, U. Wisconsin Space surveillance applications
H4RG-10	4096×4096	10	1, 4, 16, 32, 64	6	Joint Milli-Arcsecond Pathfinder Survey (J-MAPS) Development Programs in Astronomy
H4RG-15	4096×4096	15	1, 4, 16, 32, 64	3	In Development, first on sky telescope test in 2011

HxRG Readout Integrated Circuit (ROIC) Architecture

H1RG

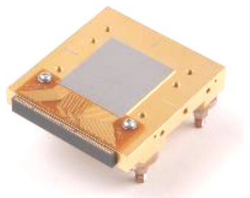

H2RG

H4RG-10

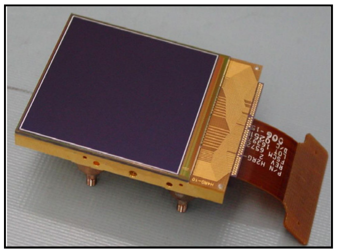

H4RG-15

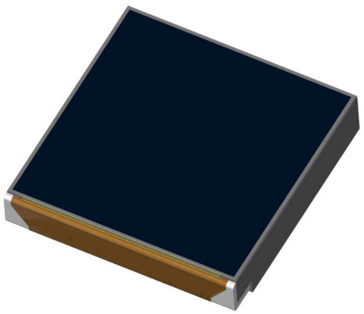

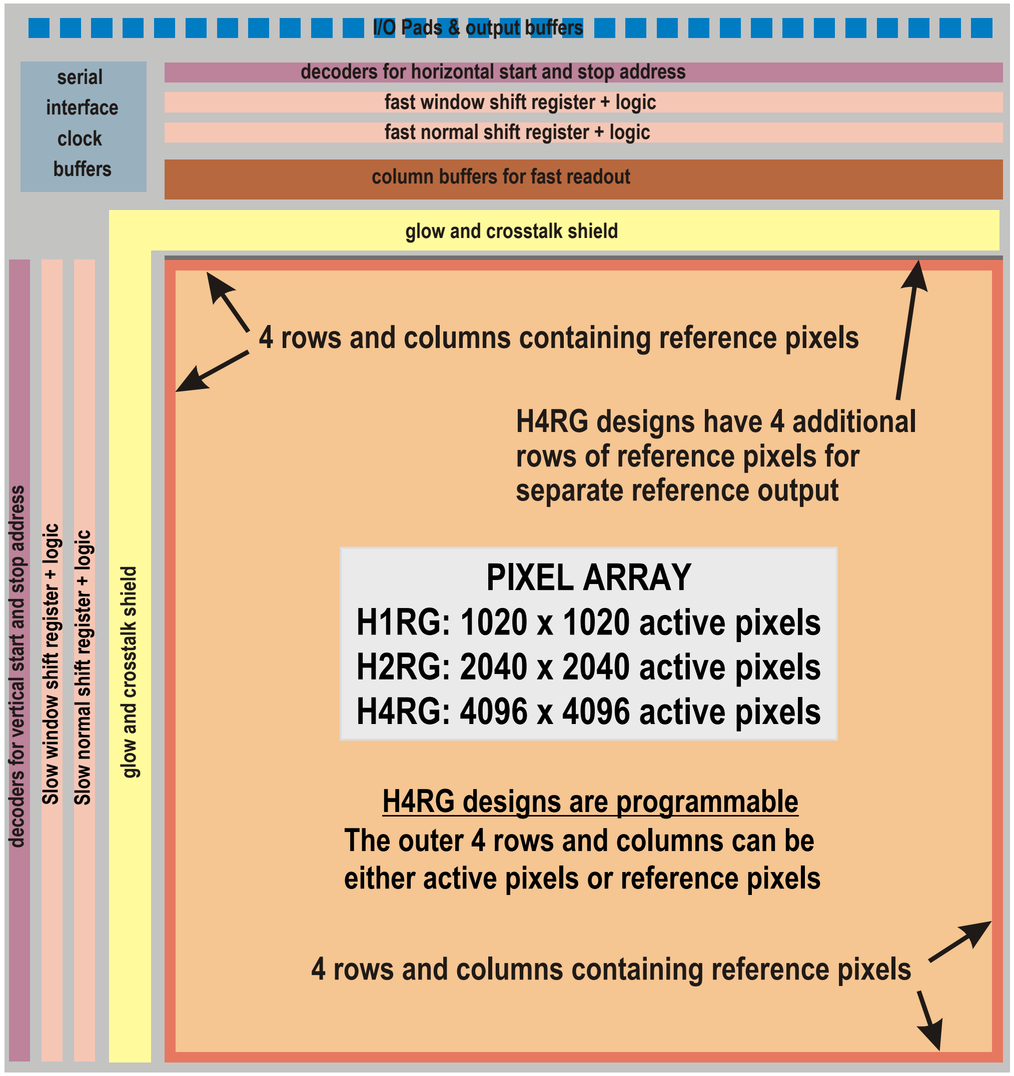

H4RG-15 adds programmable column deselect and serial register read-back

TELEDYNE IMAGING SENSORS
A Teledyne Technologies Company

H2RG Performance Confirmed by ESO

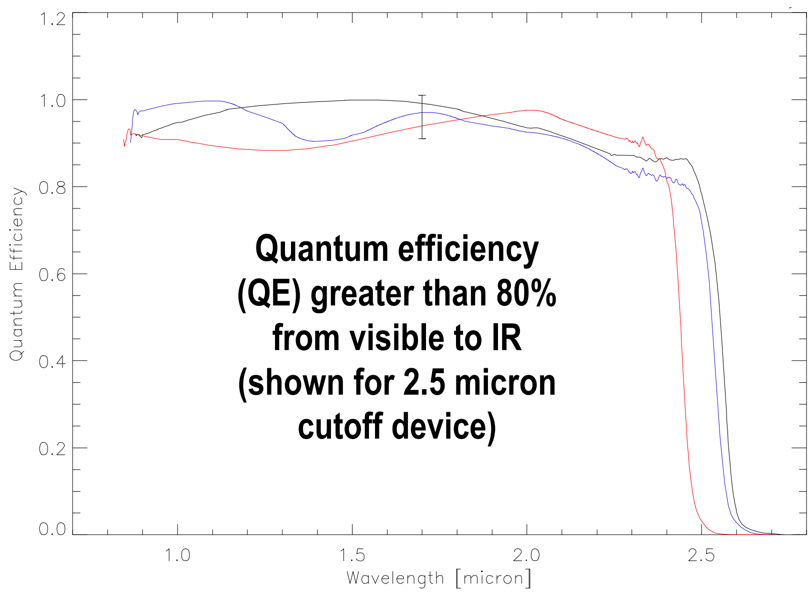

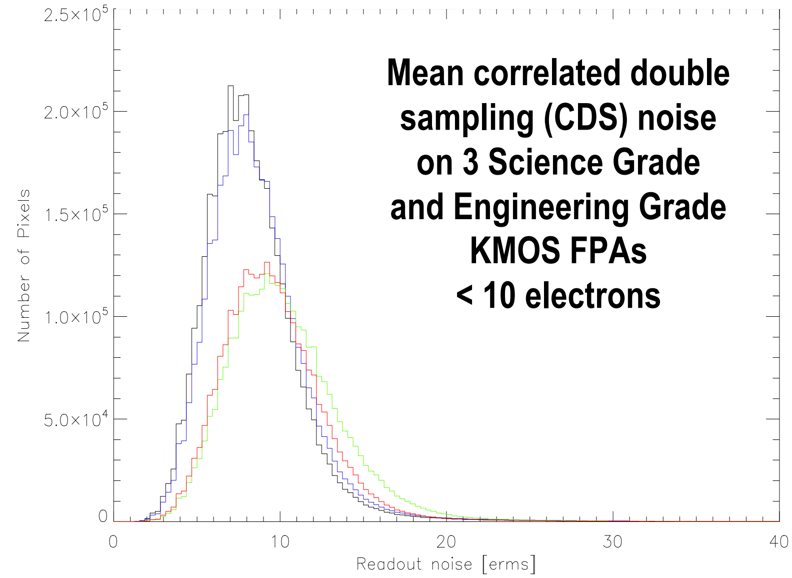

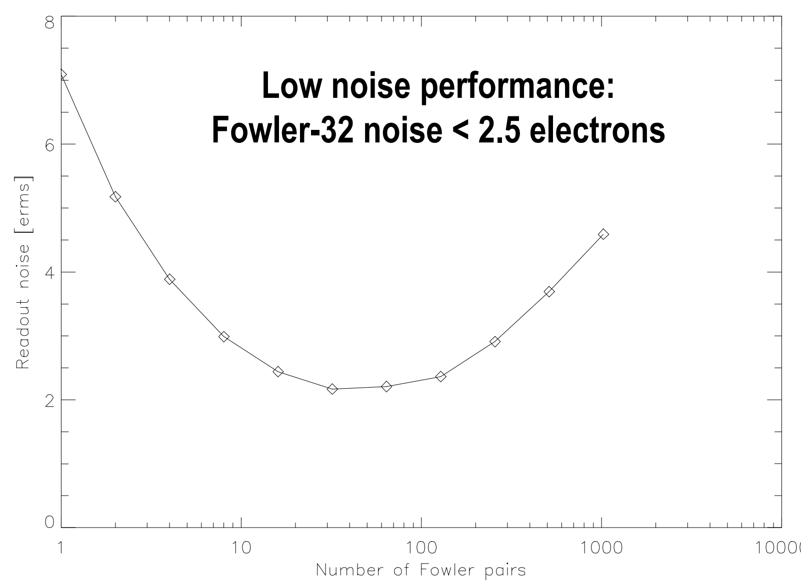

KMOS

Data: Courtesy of ESO, KMOS project

H2RG Standard Cutoff wavelengths

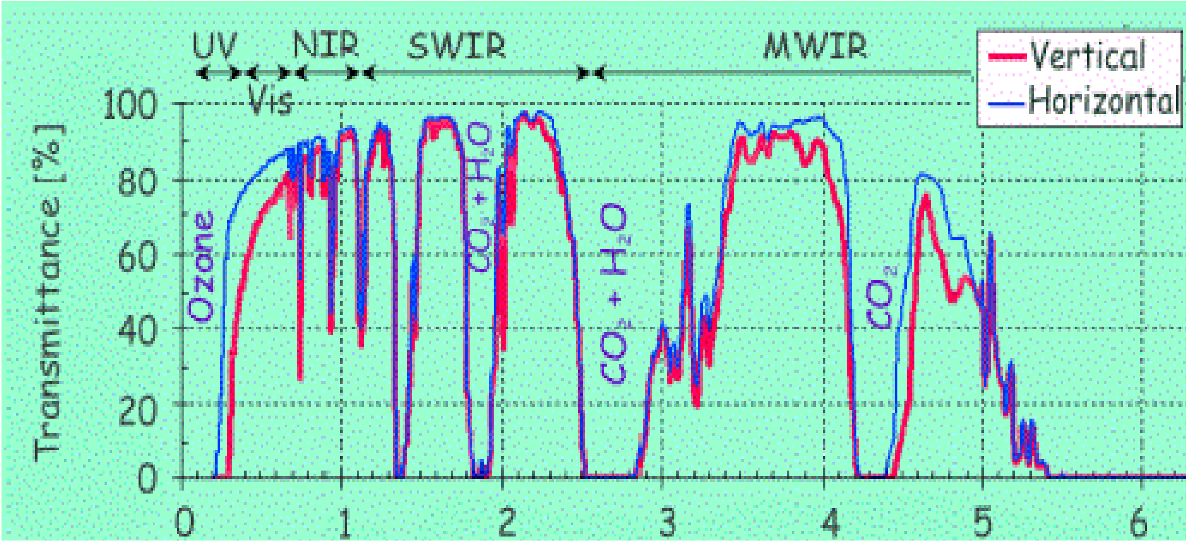

- **The cutoff wavelength can be tuned to the scientific application**
- **To achieve economy of scale, Teledyne produces the H2RG with 3 cutoff wavelengths:**
  - **1.75 microns**
  - **2.5 microns**
  - **5.3 microns**

TELEDYNE
IMAGING SENSORS
A Teledyne Technologies Company

Large Visible Astronomy Focal Plane Array: H4RG-10

H4RG-10: 4096 x 4096, 10 μm Pixel Pitch FPA

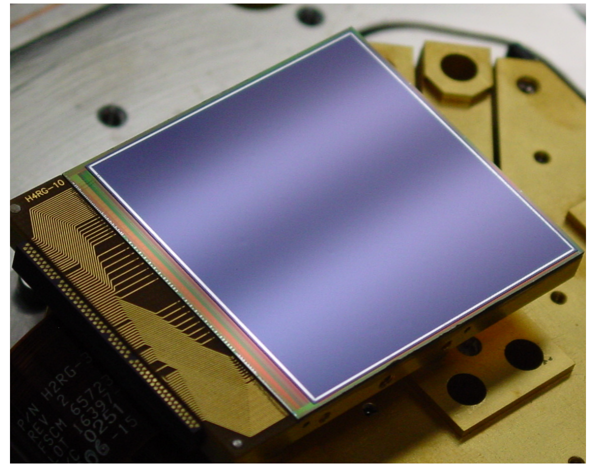

H4RG-10 HyViSI Prototype Focal Plane Array

- H4RG-10 Hybrid Visible Silicon Imager (HyViSI™) focal plane array is baseline precision astrometry space mission Joint Miliarcsecond Pathfinder Survey (J-MAPS) by the US Naval Observatory (USNO)
  - ❑ First use of CMOS for astrometry in space
  - ❑ 2×2 H4RG-10 mosaic – 67 Megapixel Imager

- Focal planes delivered in 2008 and 2009 provide required performance at 193 K

- 2009 / 10 focus on operability improvement
  - ❑ Operability > 99.9%

- Flight arrays will be delivered to the U.S. Naval Research Laboratory (NRL) in 2011

Large Infrared Focal Plane Development: H4RG-15

- 4096×4096, 15 µm pixel pitch array
- Significantly reduce price / pixel and maintain established H2RG performance
- Four-side buttable (three-side close buttable) for large mosaics
- H4RG-15 adds:
  - ❑ **Programmable column deselect and other advanced features for manufacturability**
  - ❑ **Serial register read back**

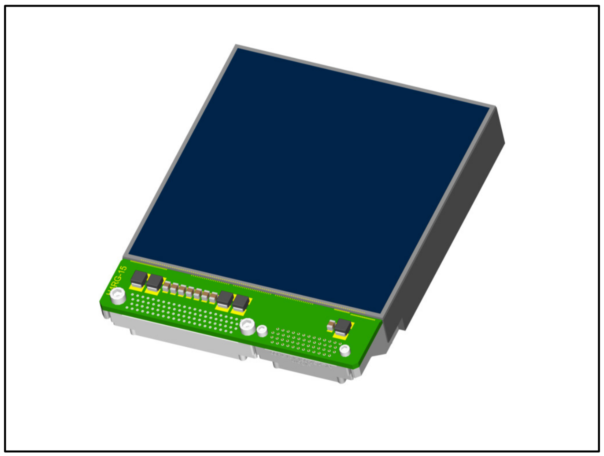

- $6.2M grant received from the U.S. National Science Foundation (NSF)
- Project kicked off December 2009
- H4RG-15 readout circuit taped out 25 June 2010
- First prototype arrays are planned to ship to University of Hawaii in summer of 2011 for on-sky testing

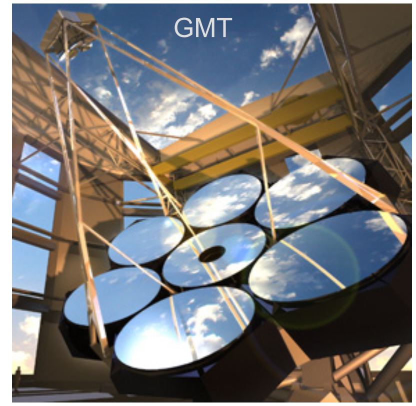

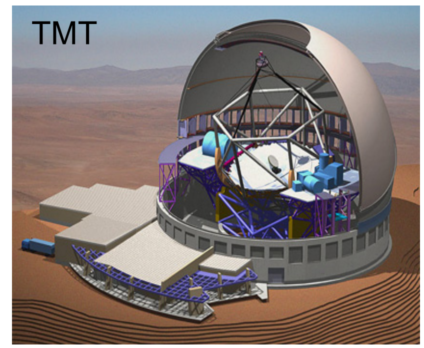

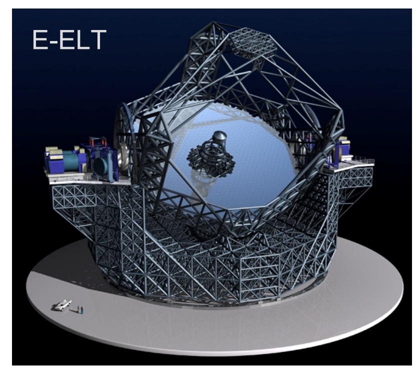

University of Hawaii Institute for Astronomy

TELEDYNE IMAGING SENSORS
A Teledyne Technologies Company

GL SCIENTIFIC

The SIDECAR ASIC
Complete Electronics on a Chip

Replace this

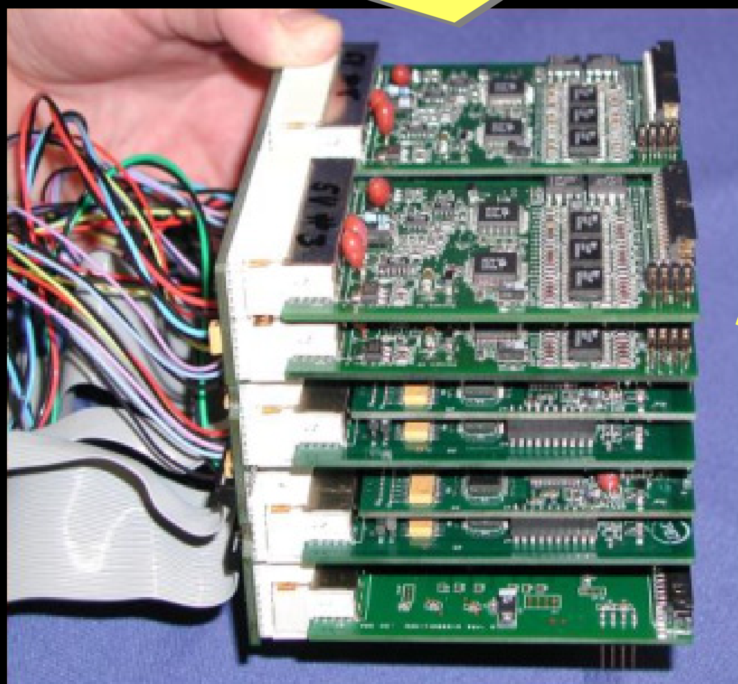

with this!

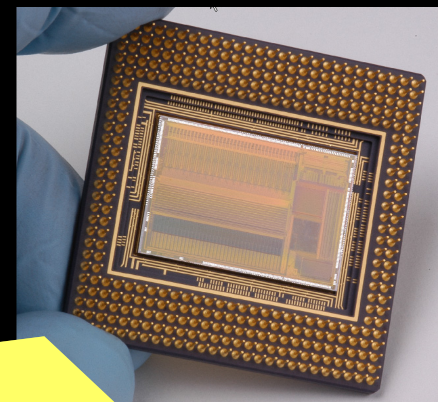

1% volume
1% power
less hassle

SIDECAR: System for Image Digitization, Enhancement, Control And Retrieval

Teledyne Imaging Sensors

SIDECAR ASIC Functionality

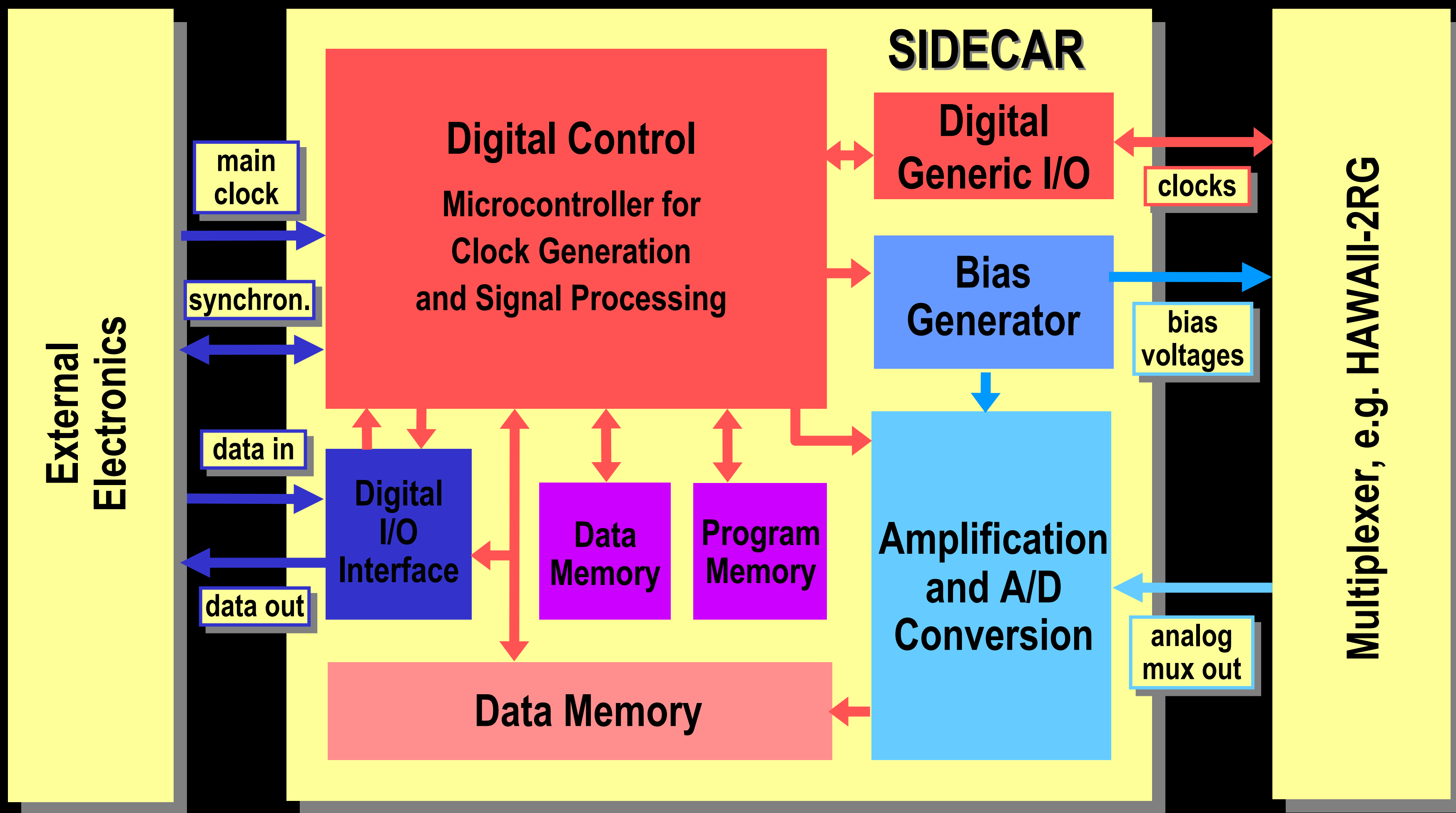

Teledyne Imaging Sensors

SIDECAR ASIC Floorplan

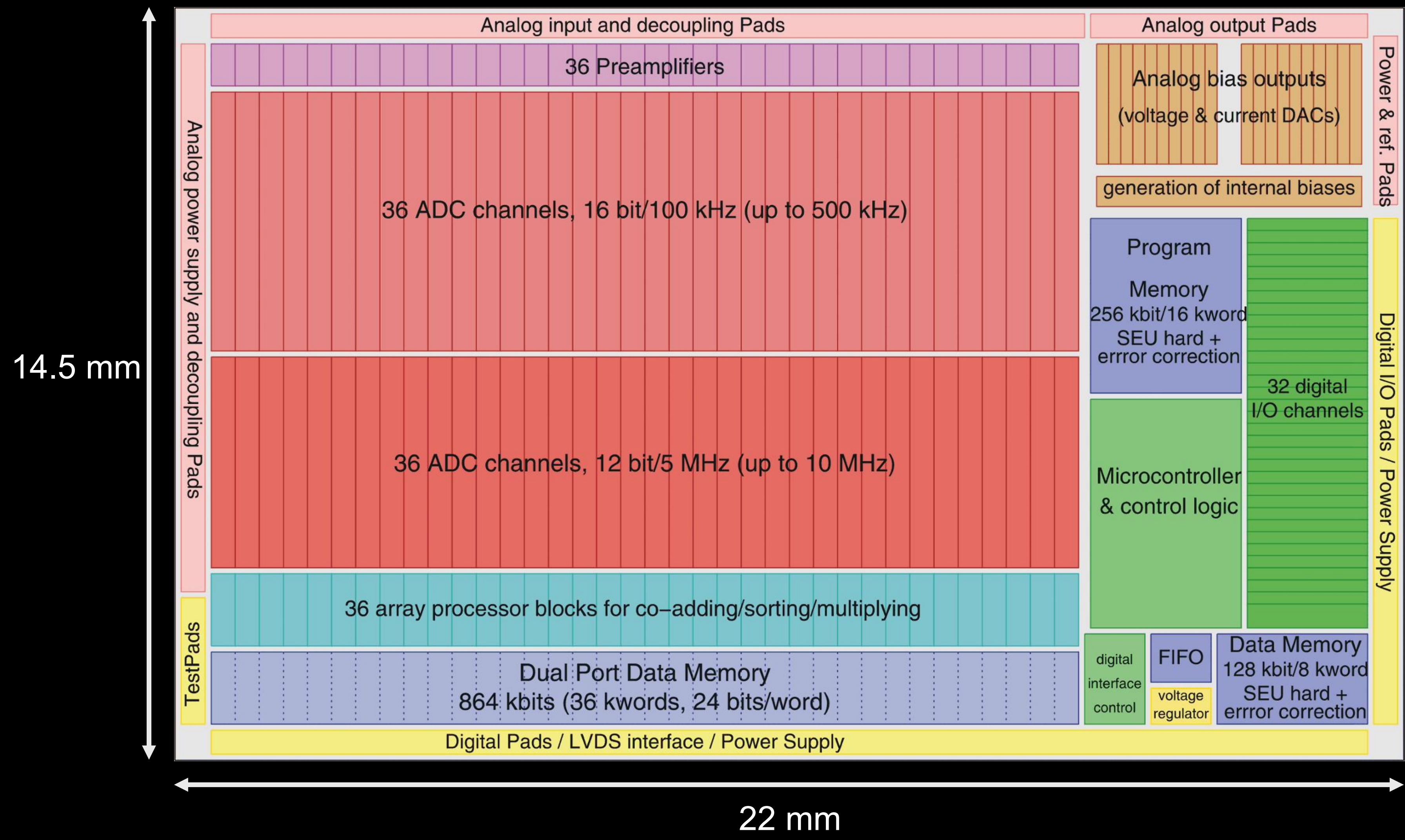

Teledyne Imaging Sensors

SIDECAR ASIC Flight Package for JWST

- Ceramic board with ASIC die and decoupling caps
- Invar box with top and bottom lid
- Two 37-pin MDM connectors
  - FPE-to-ASIC connection
  - ASIC-to-SCA connection
- Qualified to NASA Technology Readiness Level 6 (TRL-6)
- <15 mW power when reading out of four ports in parallel, with 16 bit digitization at 100 kHz per port.

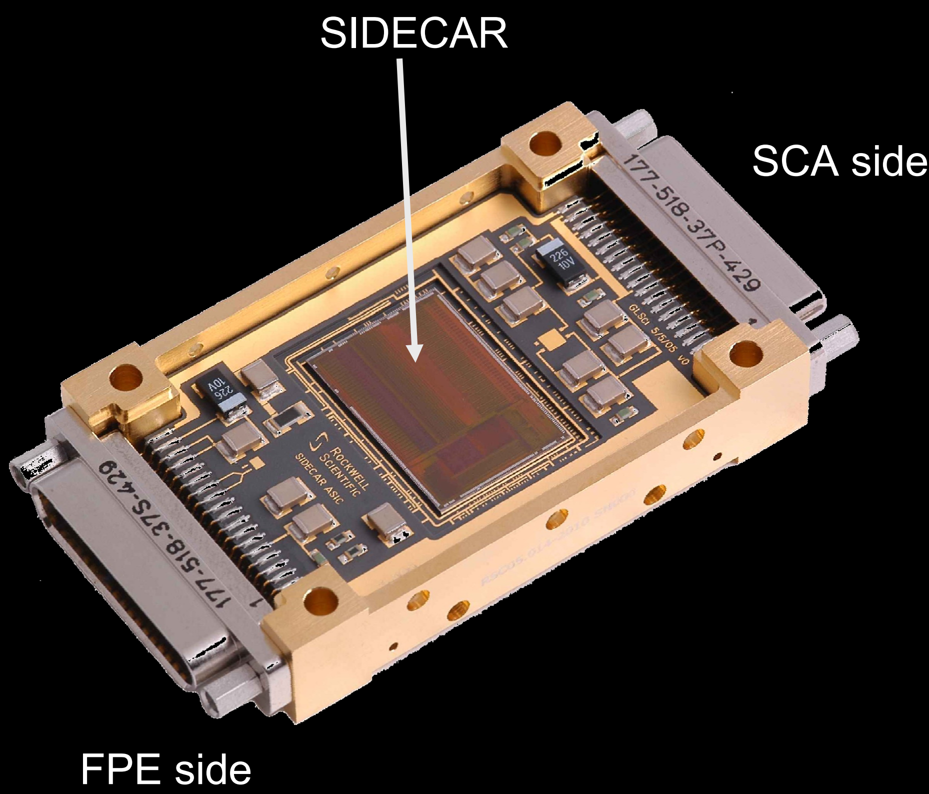

James Webb Space Telescope

15 H2RG 2K×2K infrared arrays on board (63 million pixels)

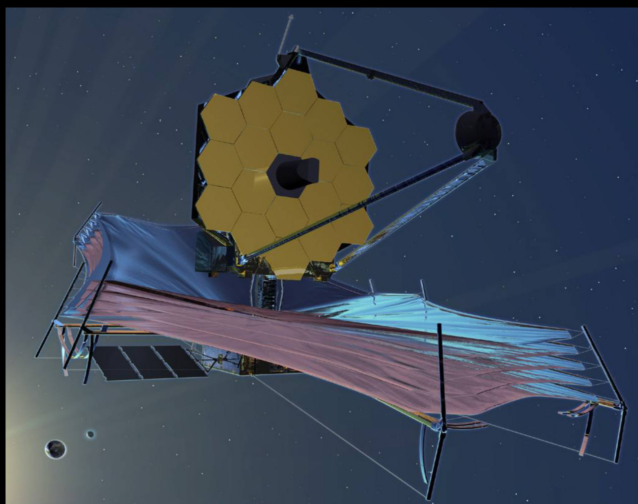

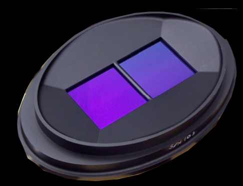

NIRSpec
(Near Infrared Spectrograph)
<6 e- noise for 1000 sec exposure

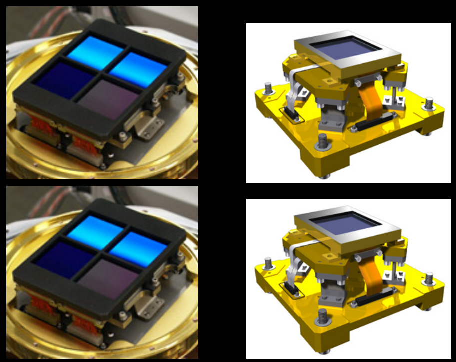

NIRCam
(Near Infrared Camera)

FGS
(Fine Guidance Sensors)

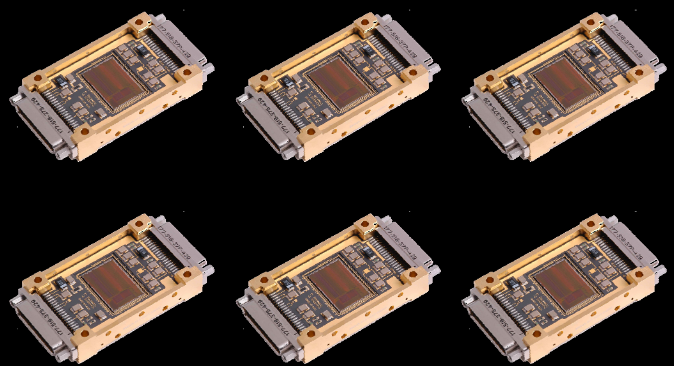

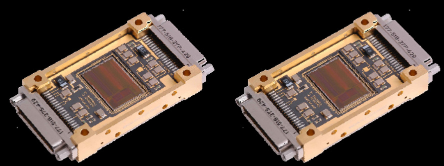

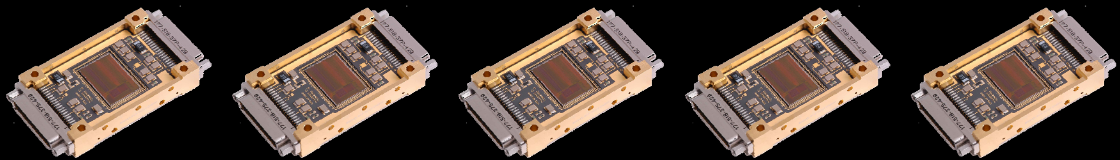

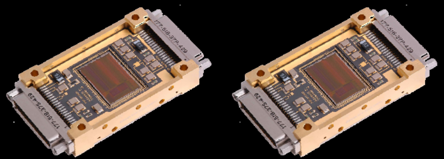

Hubble Servicing Mission 4

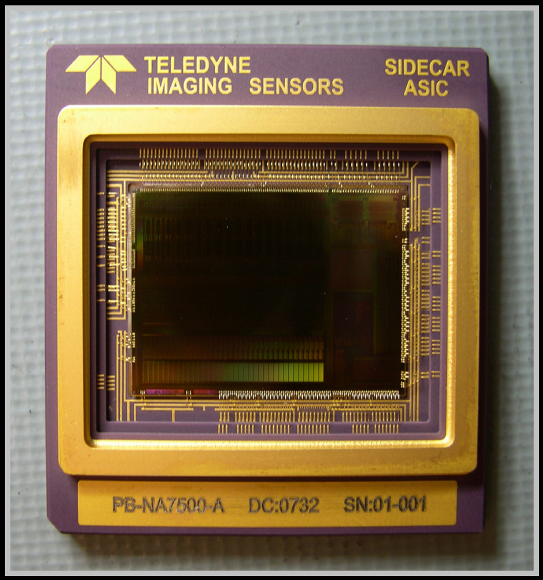

Repair of the
Advanced Camera for Surveys
(ACS)
Teledyne SIDECAR ASIC

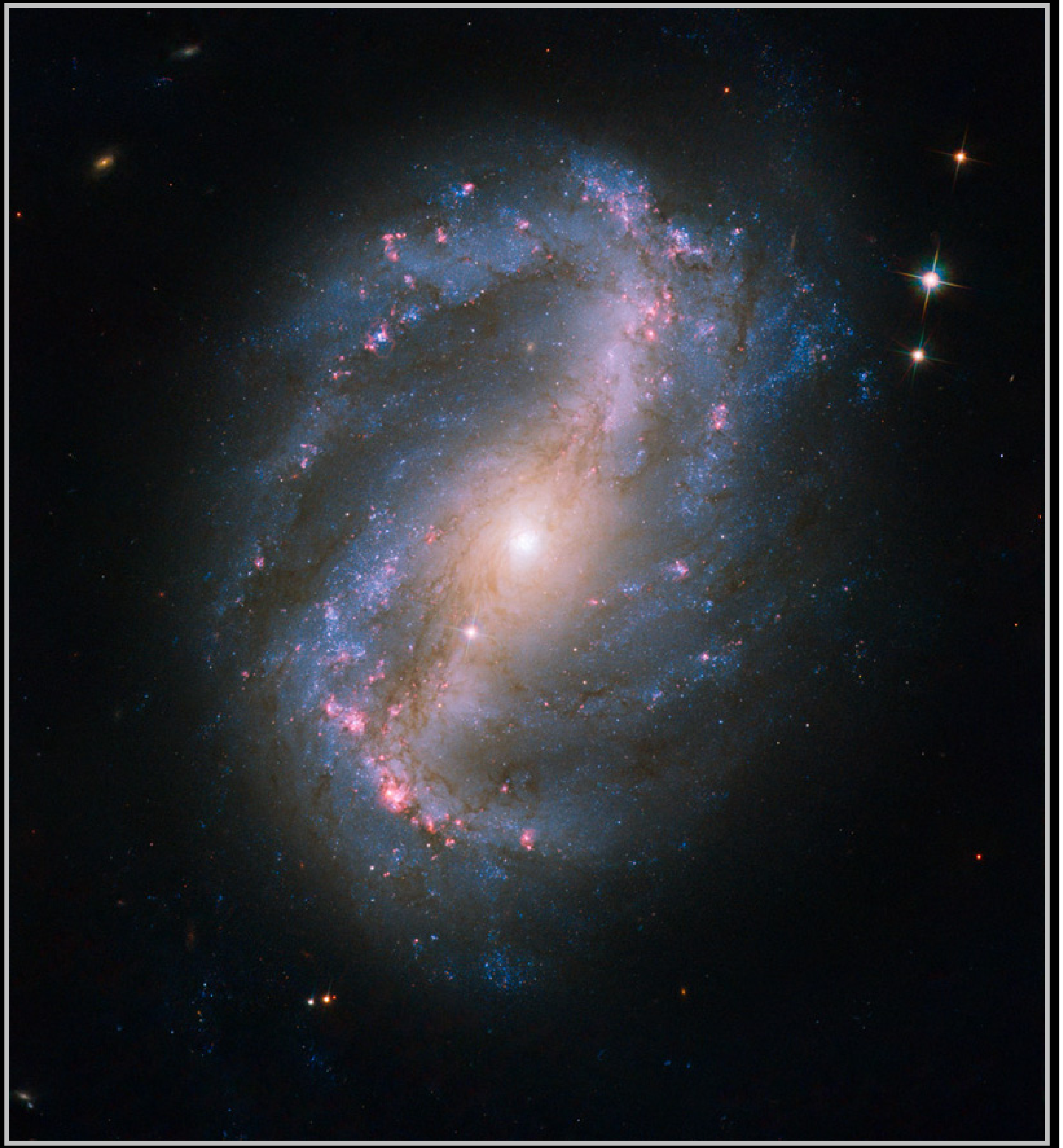

HxRG – SIDECAR ASIC Package Development

One modular approach for all applications:

- Silicon Carbide (SiC) carrier for visible and substrate removed IR focal planes
- Rigid-flex cable with wirebond pads and with passives for flight or ground-based application

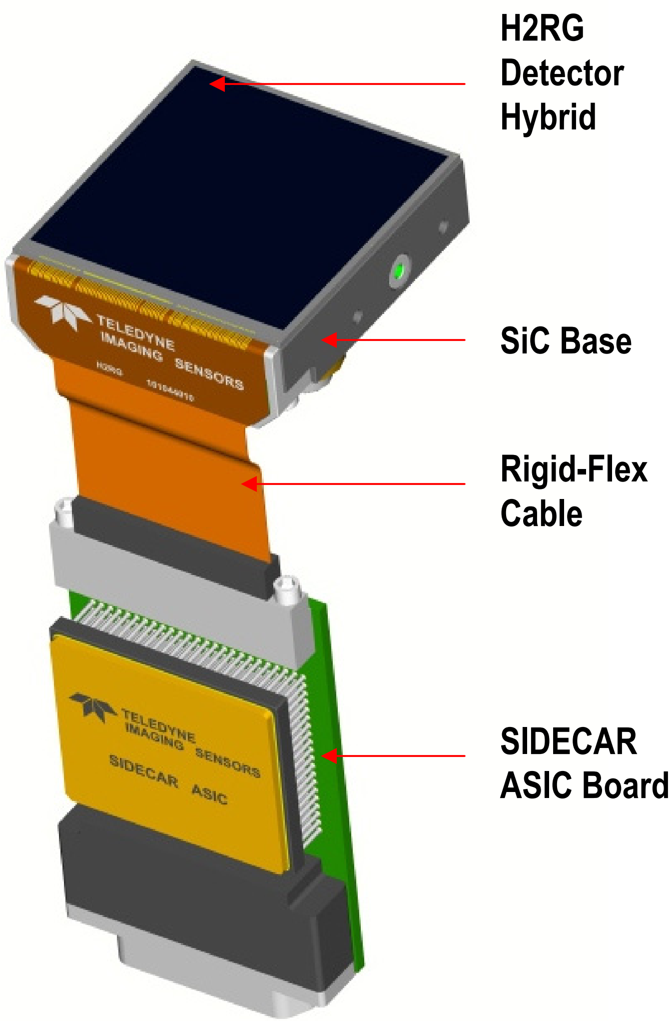

Image Data of H2RG + HgCdTe Detector

- Typical 2.5µm cutoff detector
- Images taken under weak flat field illumination (non-uniform)
- All images shown at the same scaling factor

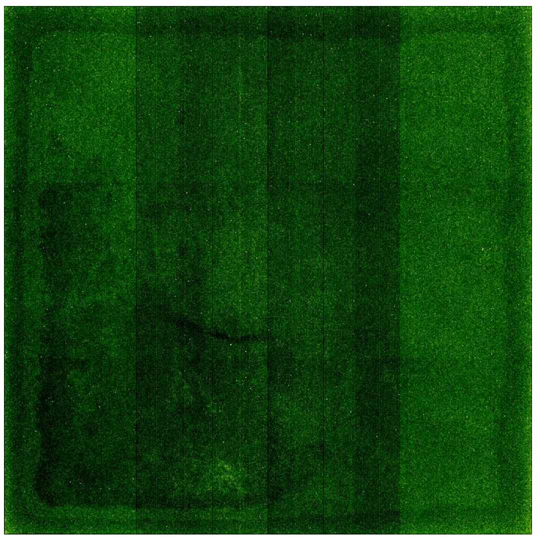

Raw frame

(1st read after reset)

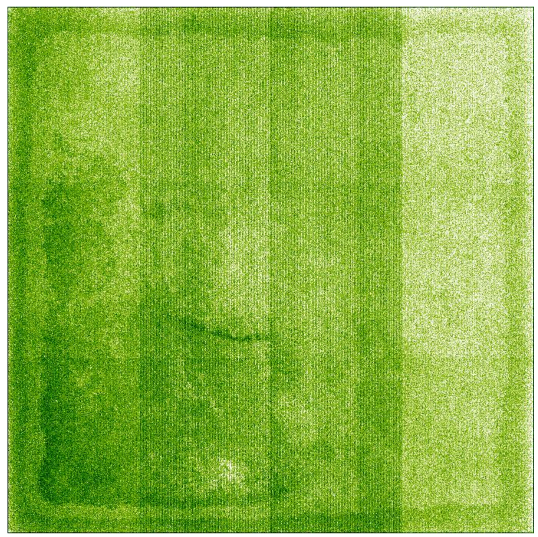

Raw frame

(2nd read after reset)

Correlated Double Sample

(2nd – 1st read)

Removes all offset artifacts

Non-Ideal Sensor Attributes

Inter-Pixel Capacitance

Persistence (latent image)

Interpixel Capacitance (IPC)

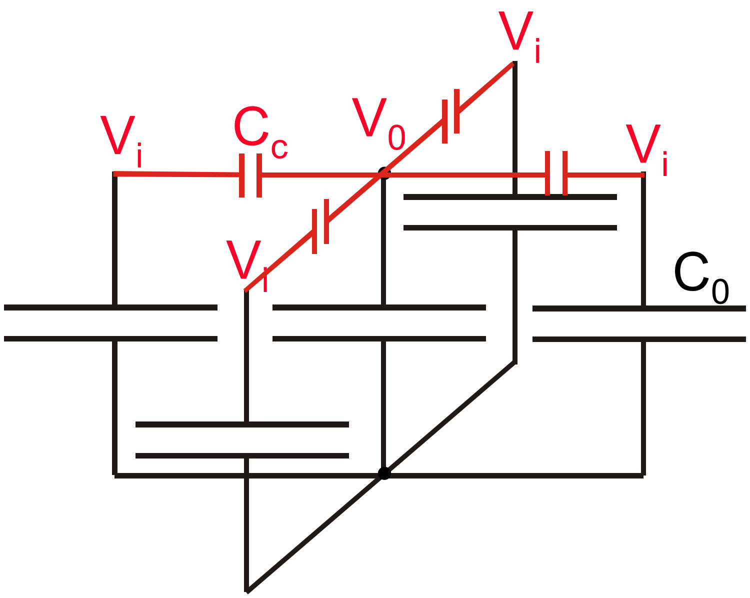

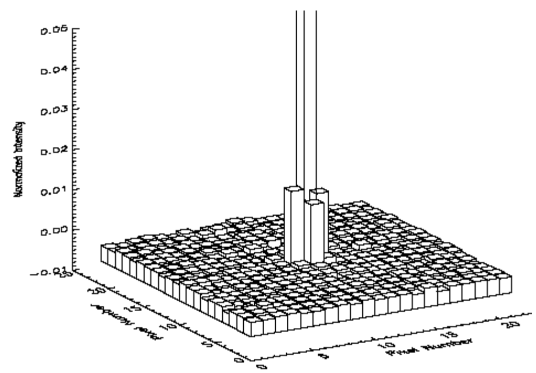

Chart 85

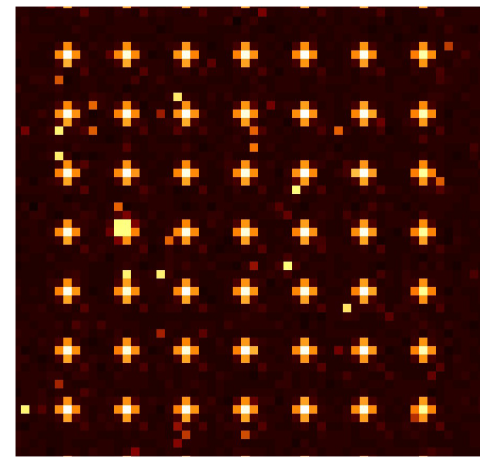

Single Pixel Resets

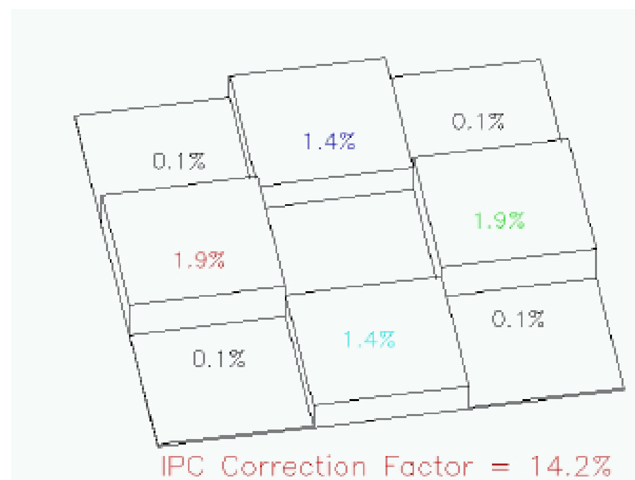

- C_0 node capacity of pixel
- Coupling capacitance C_c ($x = C_c/C_0$)
- Apparent capacitance for shot noise: $C=C_0\ (5x+1)/(x+1)$
- $V_0+4V_i = V$
- Photometry conserved
- For uniform illumination no signal charge stored on C_c
- C_c reduces noise, but also sharpness and contrast

Residual Image (CDS Latency)

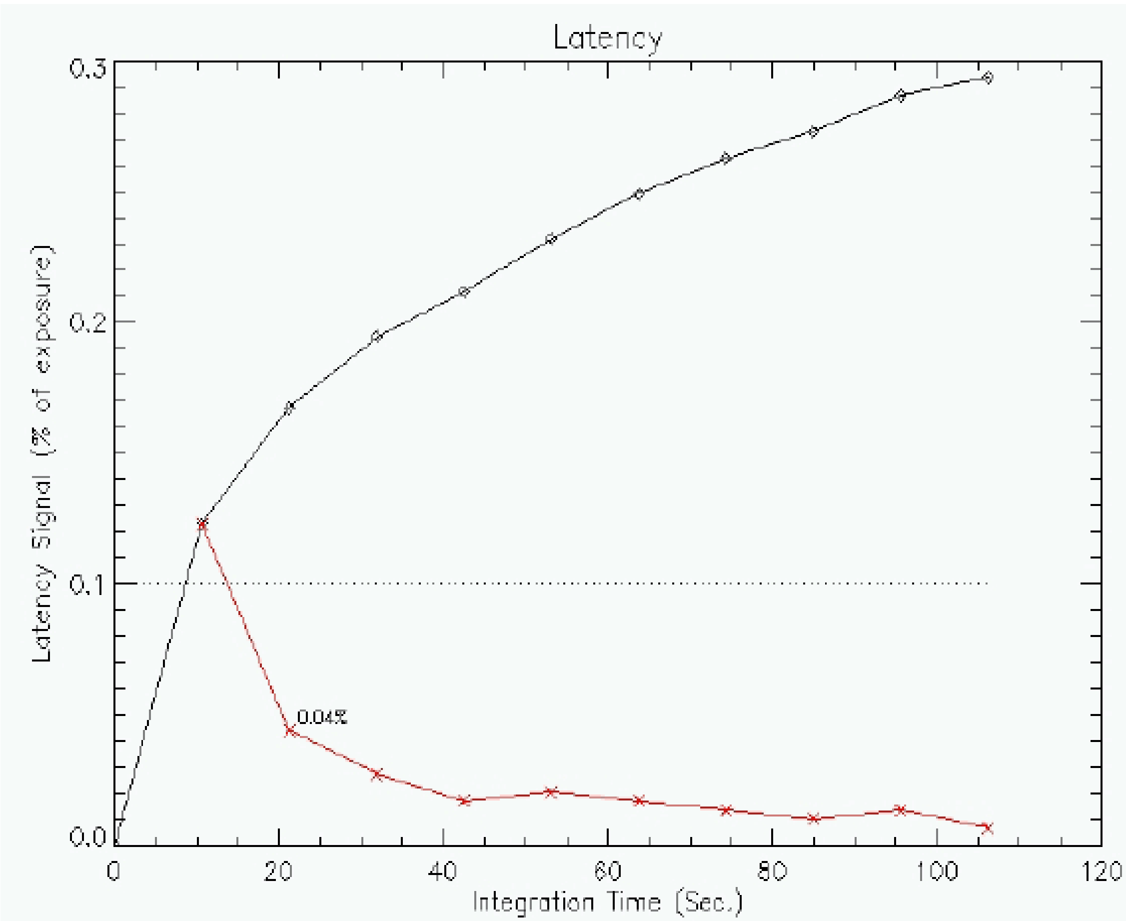

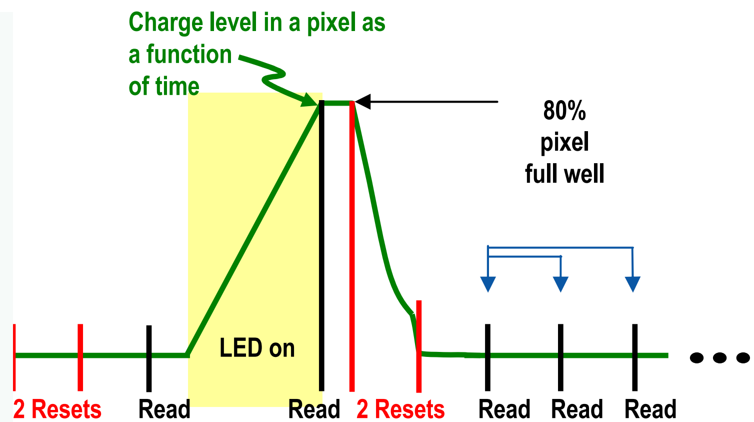

The latent image is the CDS signal measured on the second frame (i.e., the difference of the first latent frame from the second latent frame) after performing 2 resets following the removal of the illumination source. Integration time for each post-exposure frame is equal to the integration time used to provide the ~80% full well signal frame.

Cumulative and differential signal as percent of illumination signal vs. time is shown.

Example Test Measurements

Interconnect
Operable Pixels
Quantum Efficiency
Single Correlated Double Sample (CDS) Readout Noise
Readout Noise after multiple sampling
Dark current
Well depth

Interconnect at Room Temperature – nearly perfect

Chart 88

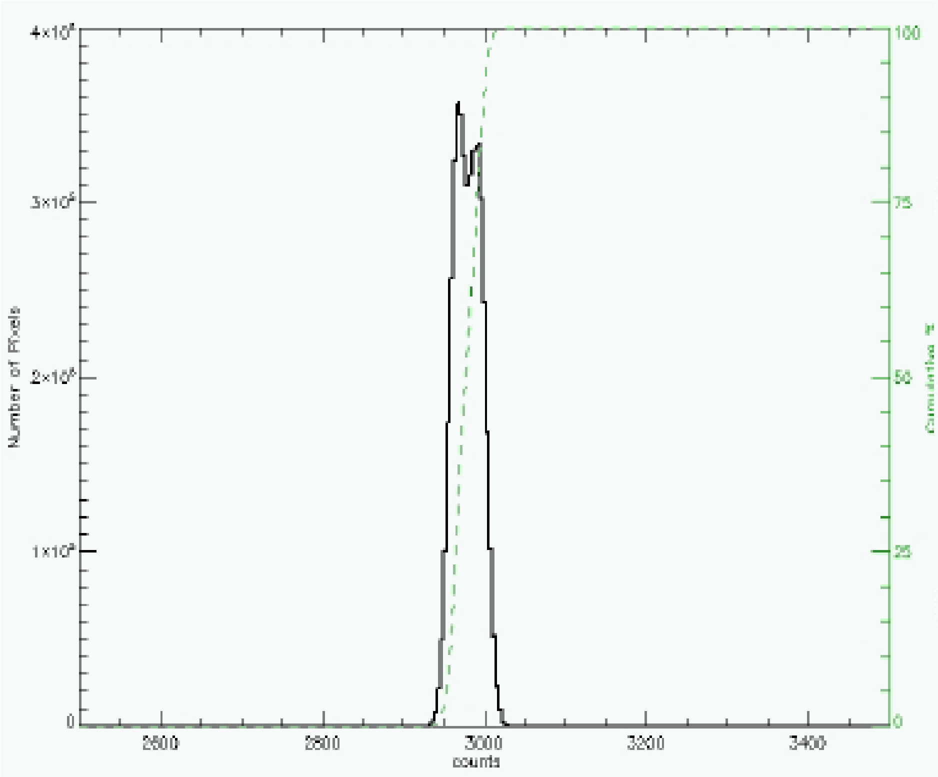

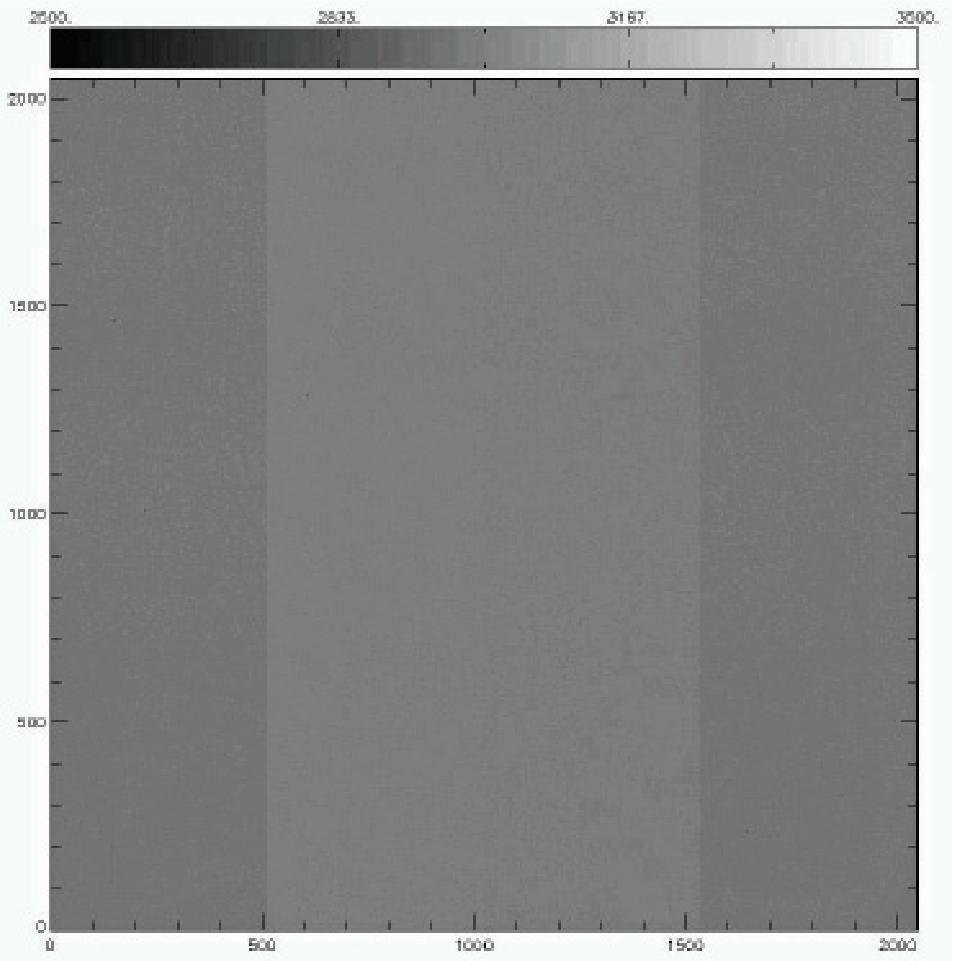

Operable Pixels

- To be operable, a pixel must pass all 3 criteria: quantum efficiency, dark current and single CDS readout noise
- Difference between the mean value and 90% operability level:
  - 3-4% for quantum efficiency
  - ~0.01 e-/pix/sec for dark current
  - 4-5 e- for readout noise

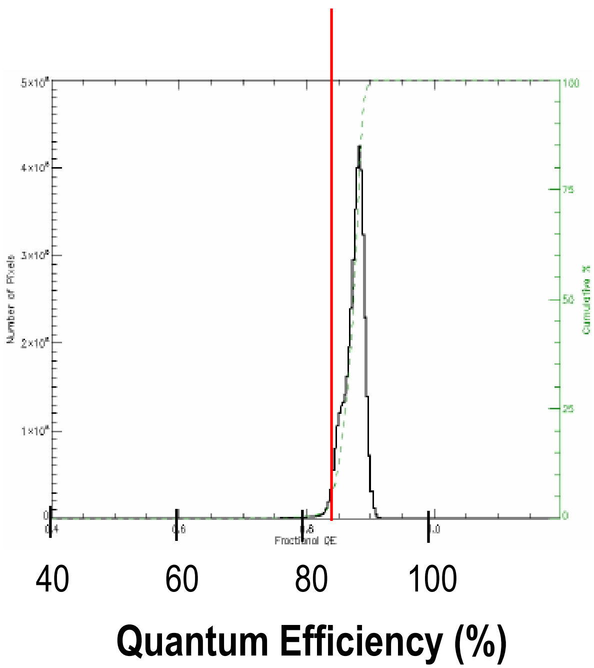

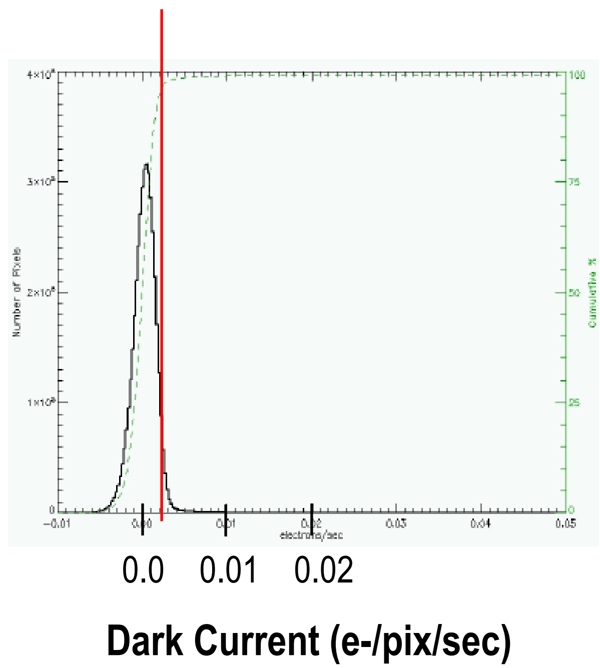

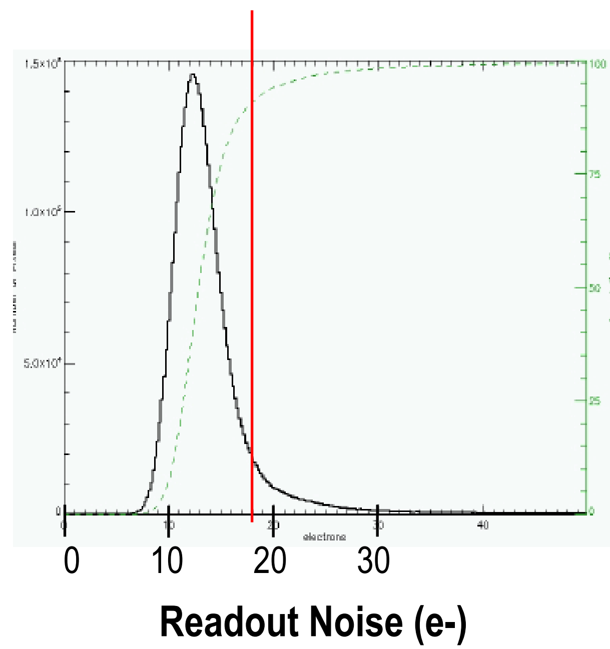

Quantum Efficiency

Chart 90

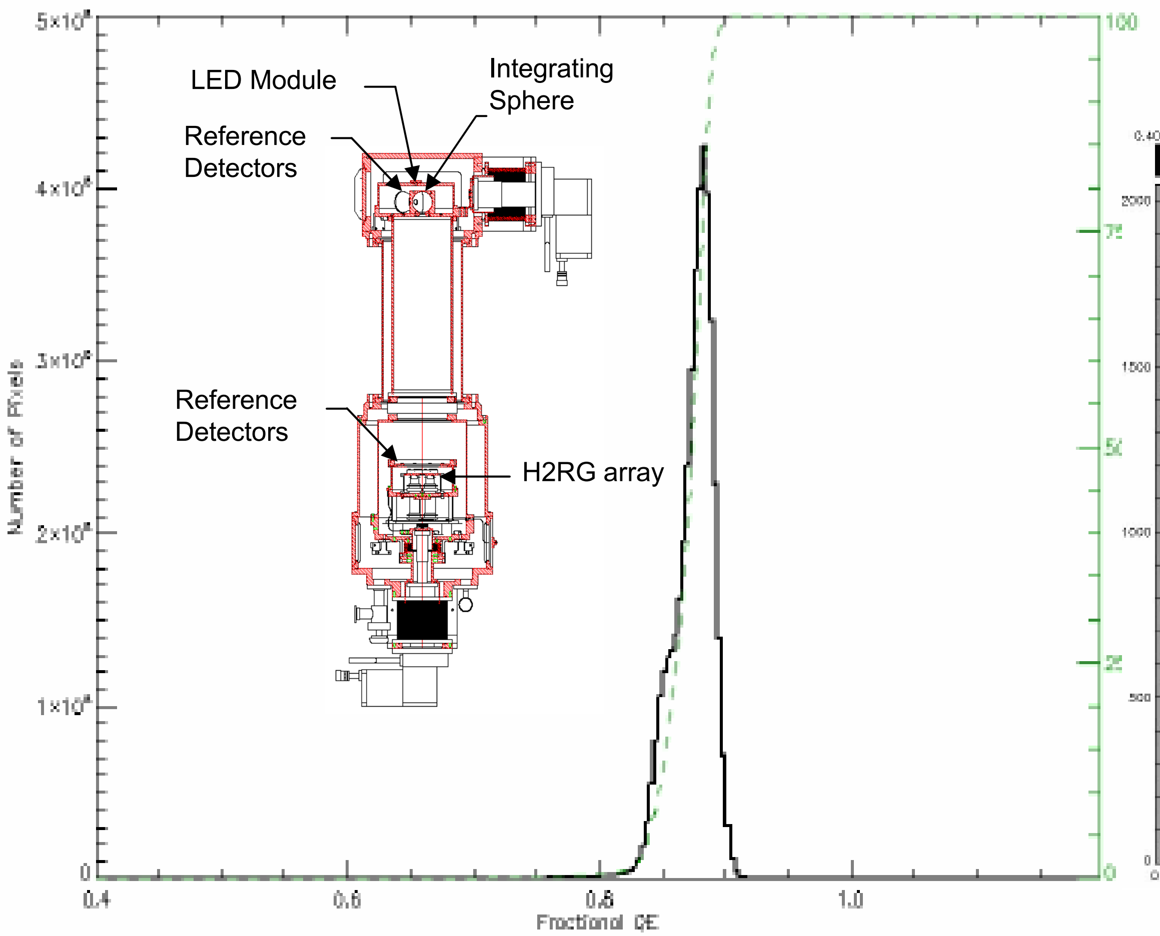

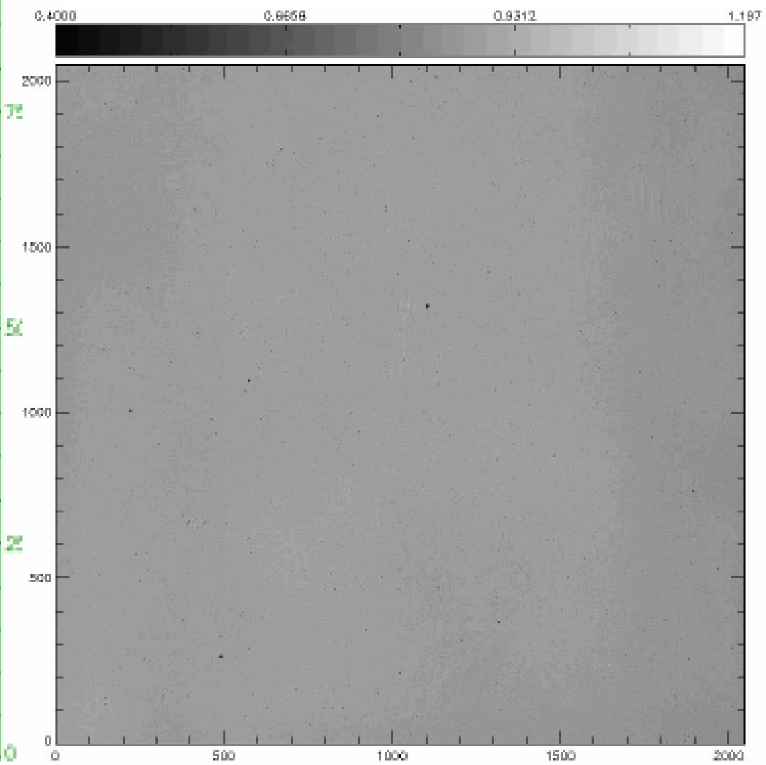

Single Correlated Double Sample (CDS) Read Noise

CDS from two subsequent frames, i.e. 10.6 sec.

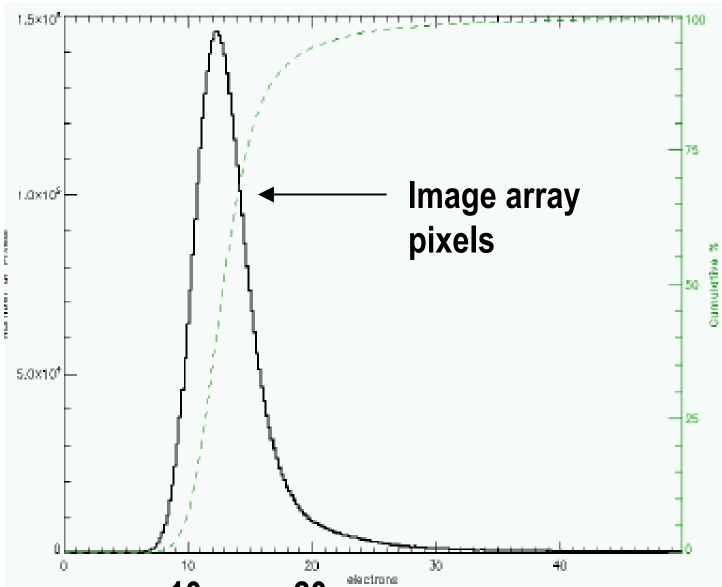

10 20

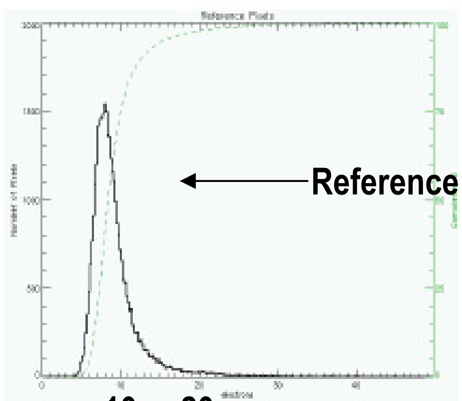

10 20

electrons noise

Display artifact caused by PDF conversion

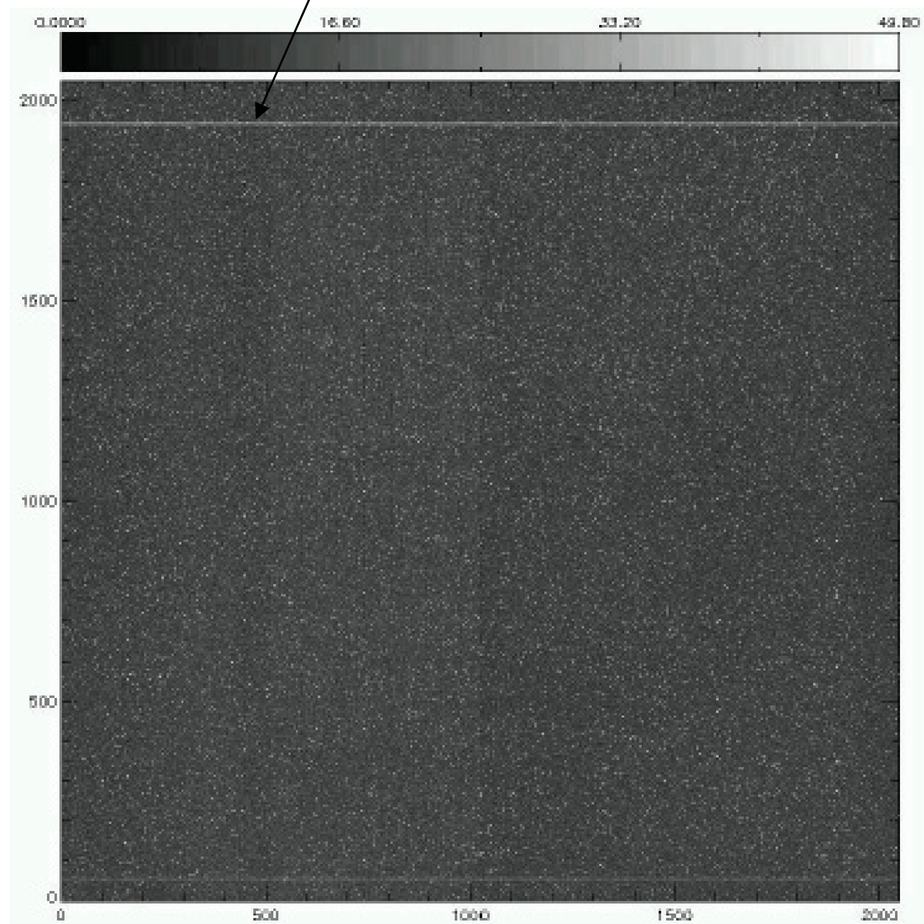

Readout Noise after multiple sampling

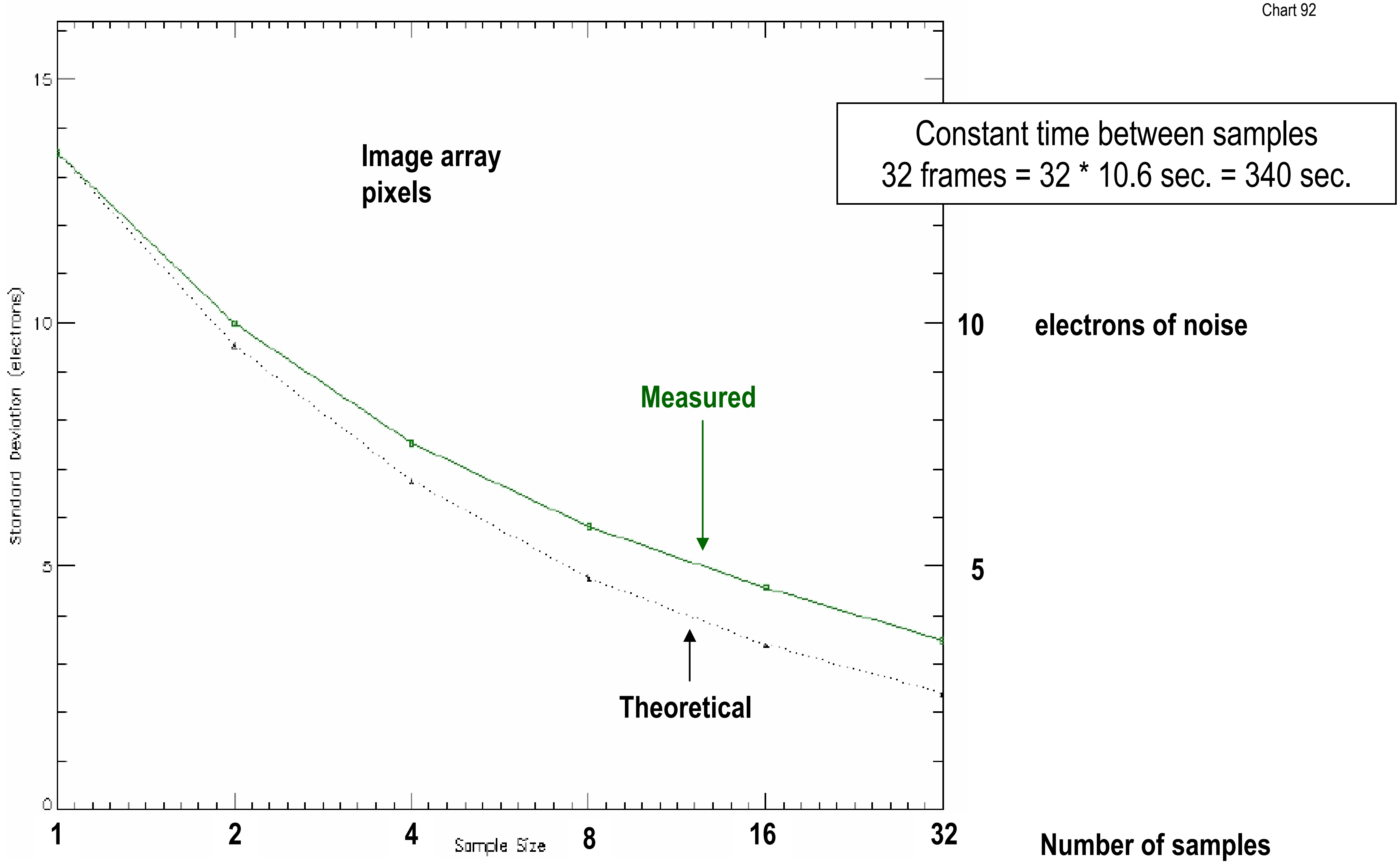

Dark Current

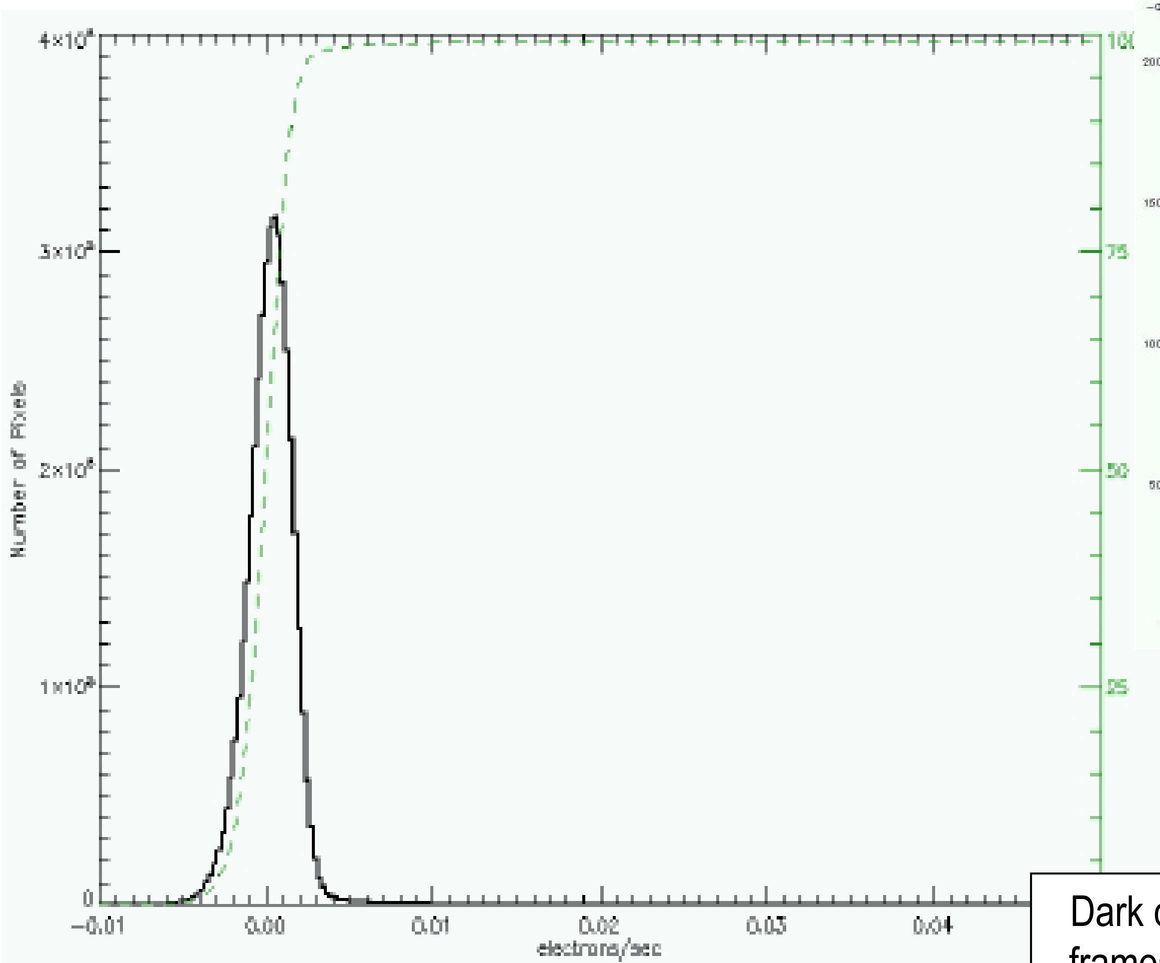

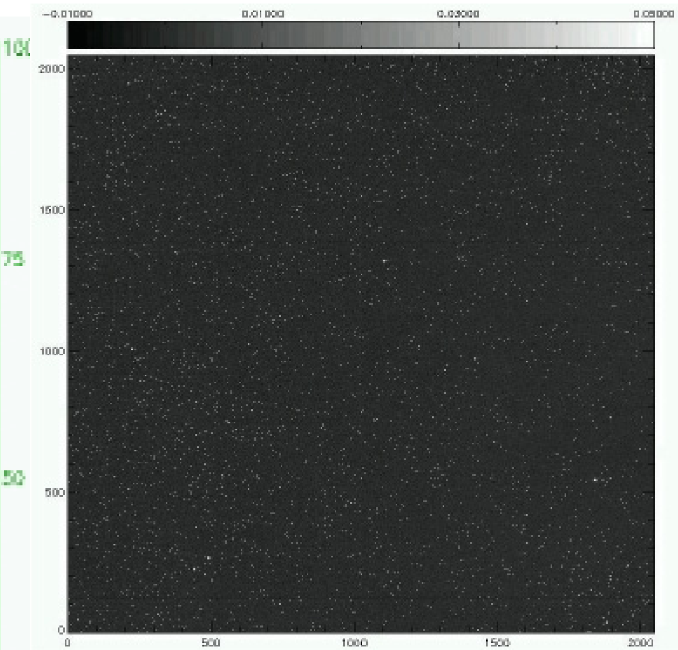

Dark current is sometimes less than Teledyne's measurement limit of ~ 0.005 e-/sec (77K, 2.5 μm cutoff)

Dark current is obtained from the slope from 88 frames "up the ramp", with a frame time of 10.6 seconds, averaged over 50 ramps

Well Depth

Chart 94

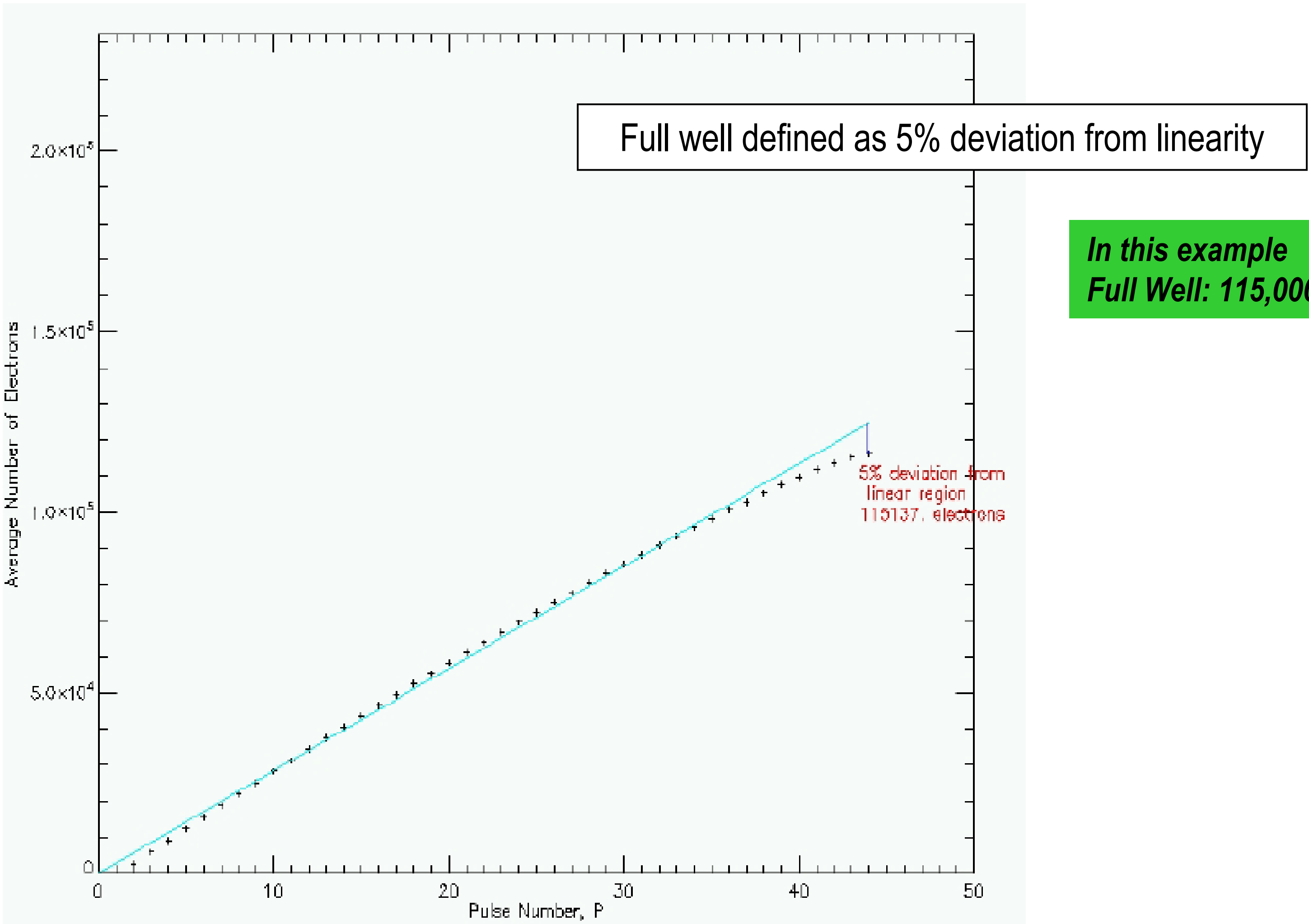

In this example
Full Well: 115,000 e-

Other things to consider with IR arrays

- Source follower (MOSFET) is simplest type of charge-to-voltage converter
- Capacitive Trans-Impedance Amplifier (CTIA), akin to an operational amplifier, has several good properties:
  - VERY linear
  - No inter-pixel capacitance (IPC)
  - Can have very large full well capacity (1–10 million electrons)
- 1.75 micron cutoff H2RG HgCdTe arrays get higher readout noise than 2.5 micron cutoff.
  - 2.5 micron: 12-14 e- single CDS (best is <10 e-)
  - 1.75 micron: 20-25 e- single CDS
- For H2RG, gap between individual sensor chip assemblies (SCAs) is 3 mm on 3-sides, 6 mm on bond pad side

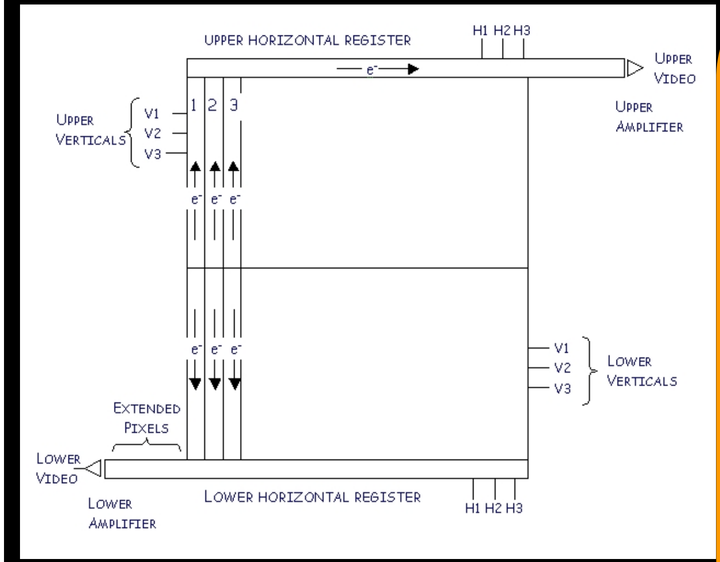

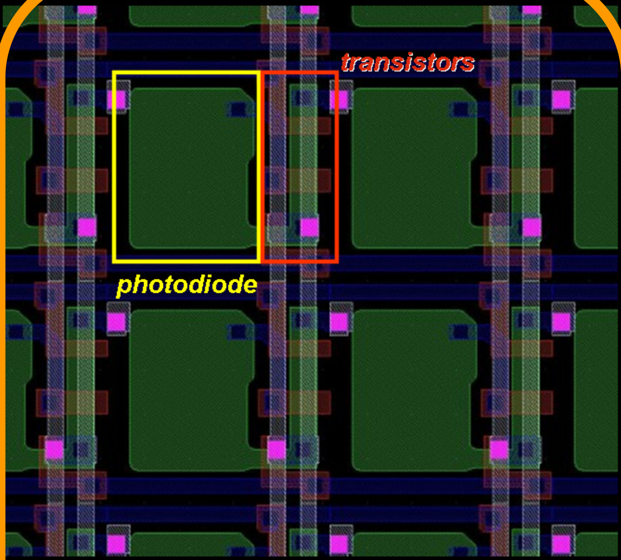

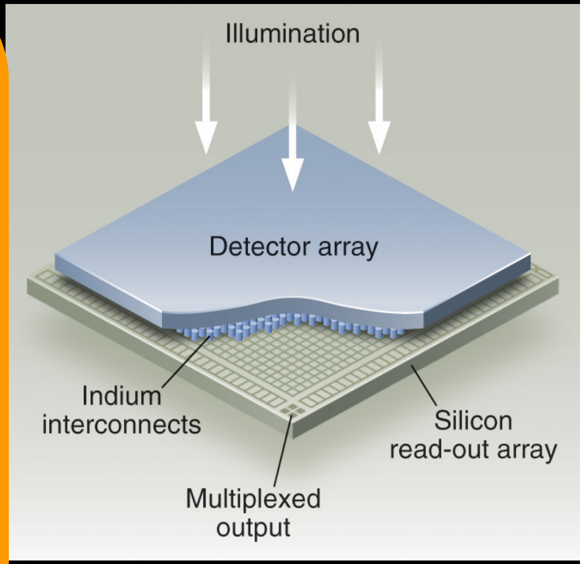

CCD

Monolithic CMOS

Hybrid CMOS

HgCdTe
Visible through IR

Silicon - Visible through near IR

CIS2051 5.5M Pixel Image Sensor

Fairchild Imaging

- 6.5 µm^2 5T pixel architecture
- 2560(H) x 2160(V) imaging array
- Dual gain 11-bit output channels
- 100 fps in rolling shutter readout
- 50 fps in global shutter readout
- Read noise < 2e- rms at 30 fps
- Dynamic range > 83 dB (15000:1)
- QE > 55% at 600 nm
- Dark current at 20ºC 3 pA/cm^2

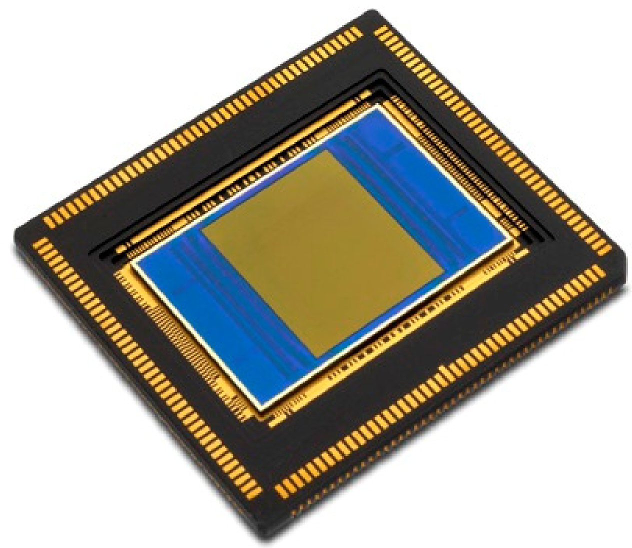

Back-Illuminated CIS2051

Fairchild Imaging

- Imaging area thinned to epi thickness (5 µm)
- QE > 83% at 550 nm
- Dark current at 20ºC < 8 pA/cm^2
- Read noise < 2e$^-$ at 100 MHz

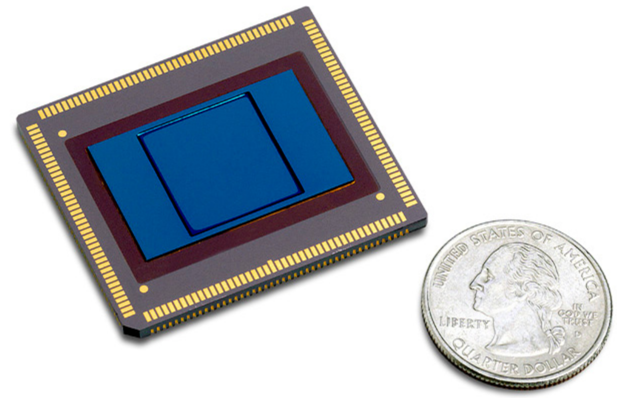

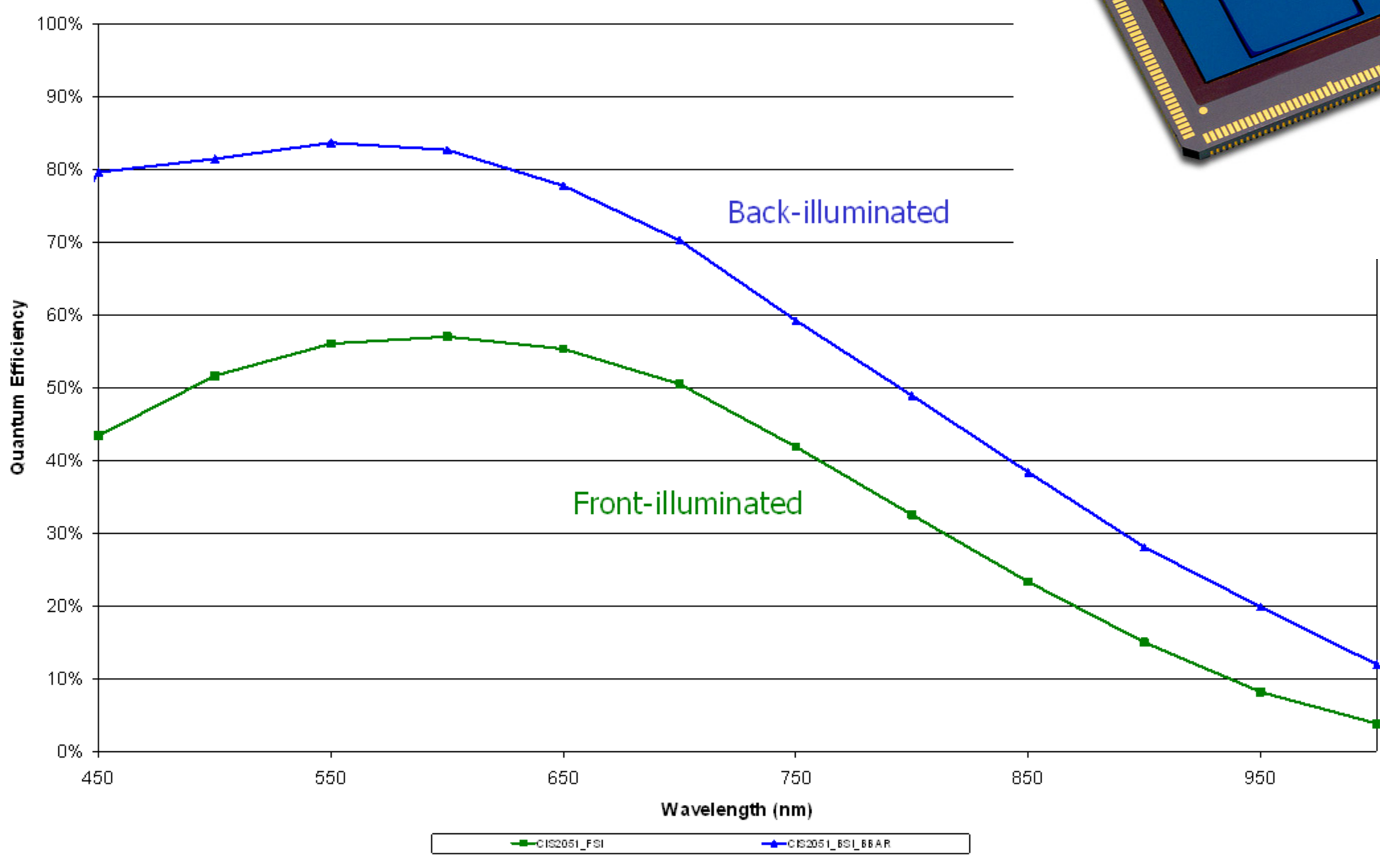

CIS2051 Read Noise Distribution (High gain 100MHz)

Fairchild Imaging

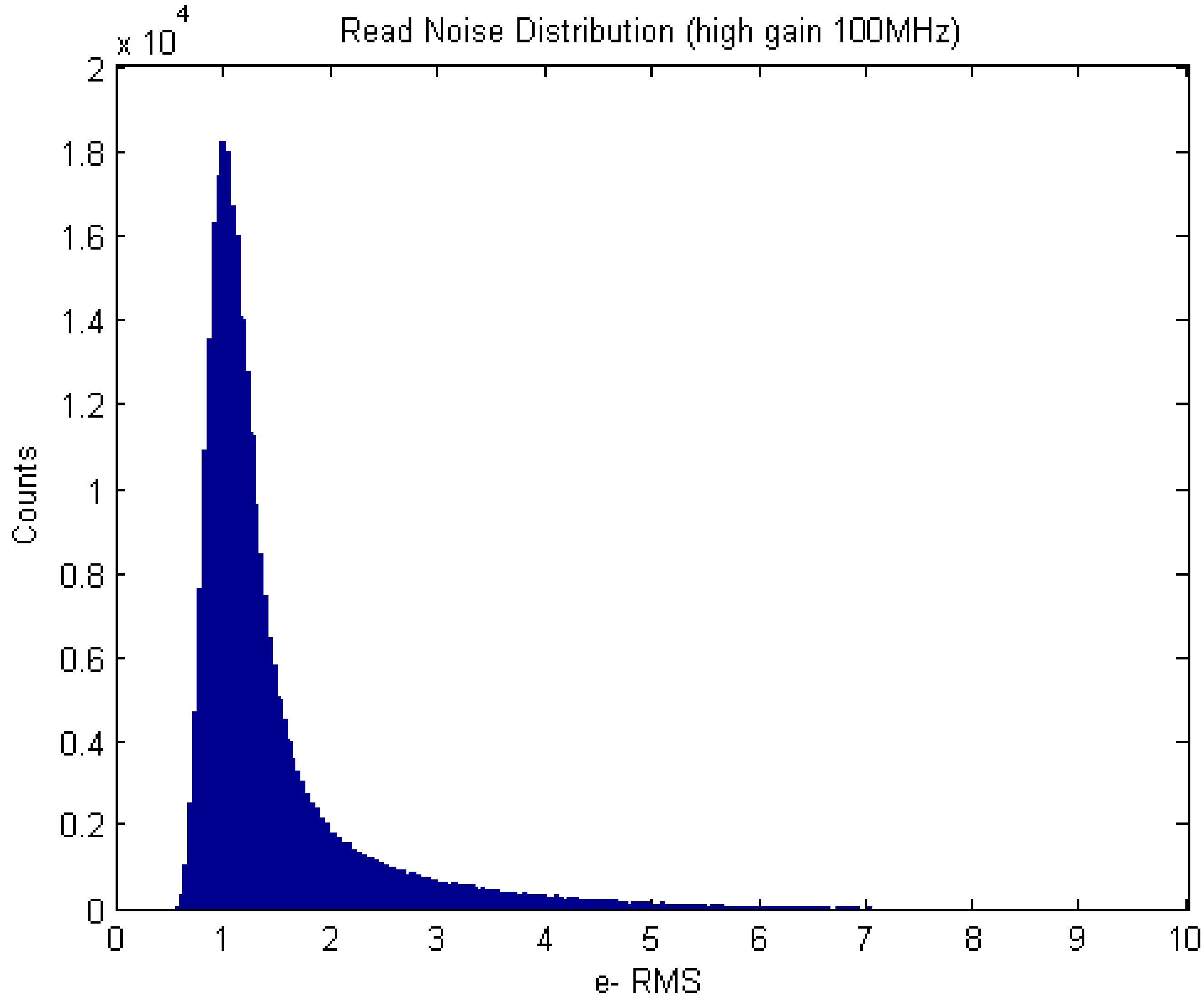

CMOS Backthinning

CMOS Wafers have been thinned from Tower, UMC and IBM. All behave much as expected. The only issue has been the epi starting thickness QE obtained in the red has not yet matched that available from CCDs. We're working with thicker, higher resistivity epi to improve red response

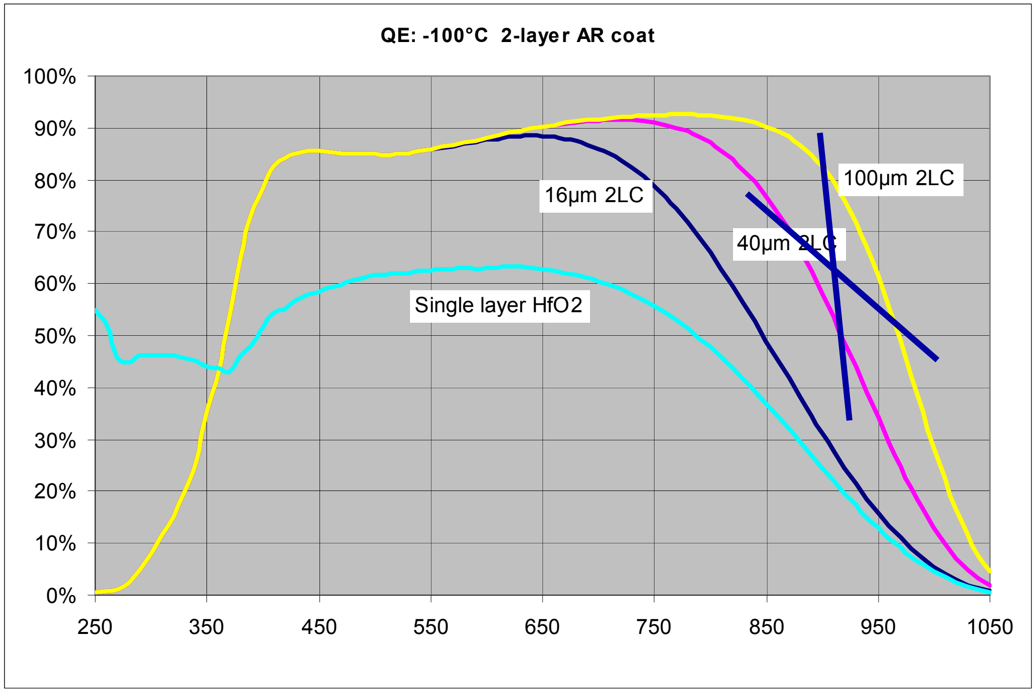

We have space qualified front illuminated CMOS sensors. The next step is to space qualify a backthinned CMOS sensor

Large area Science imager

- Part funded development : Phase 1

- The development sensor is ¼ of the final 12 MPixel device
- Development sensor includes both 3T and 4T pixels (7µm pitch).
- Schematic layout is shown on the following slide
- Each 3 MPixel segment has 4 analogue outputs
  - (Analogue preferred by some customers: more flexible)

- **Timescale**
  - Tape-out was in March 2010
  - Frontside illuminated Silicon available July 2010
  - Backside illuminated silicon characterisation completed in Oct 2010

Large area Science imager

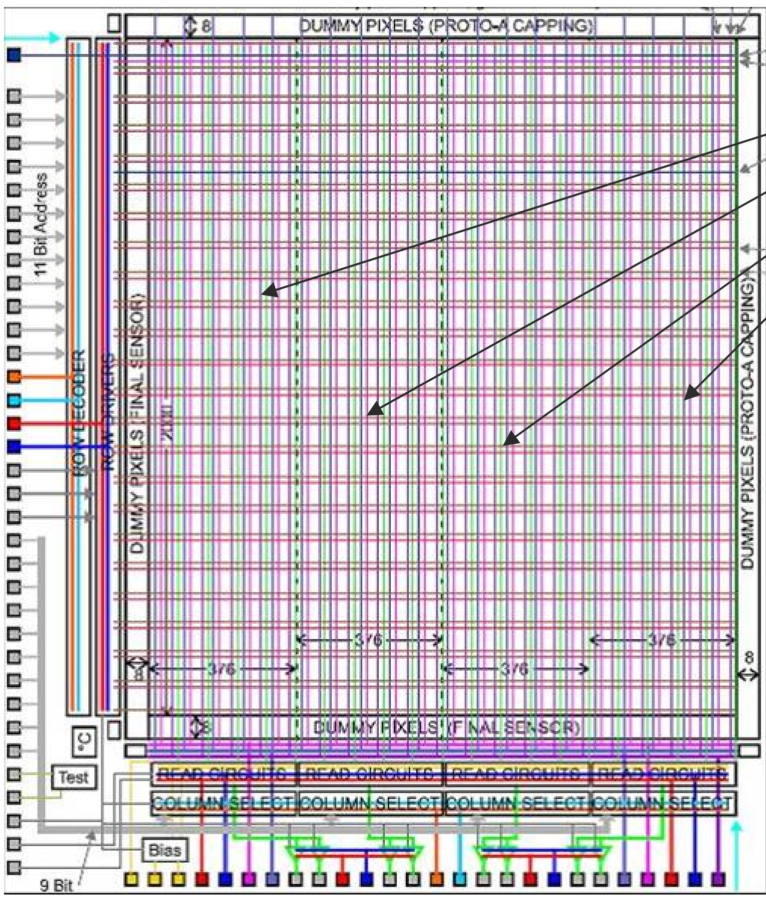

1500 x 2000 pixels.
Different areas have 3T and 4T pixels, with optimisation for low noise or high signal handling,

We expect, for example:
90ke- FWC with 45e- read noise
Or
70ke- FWC with 10e- read noise
Or
15ke- FWC with 5e- read noise

In the PHASE 2 development, this scales up to a full size device

Large area Science imager

Phase 2

The 12MPixel device will be a composite of four 3 MPixel devices

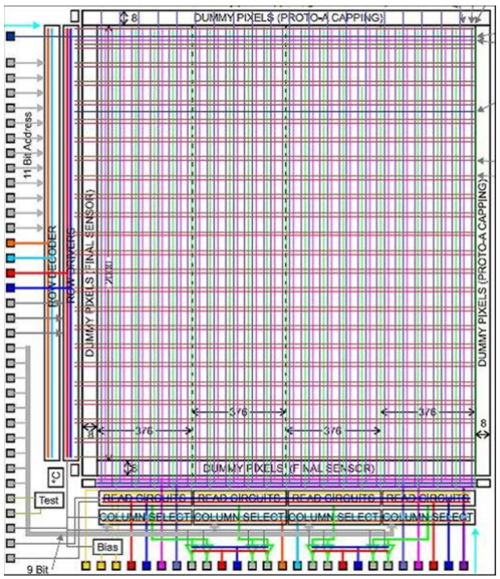

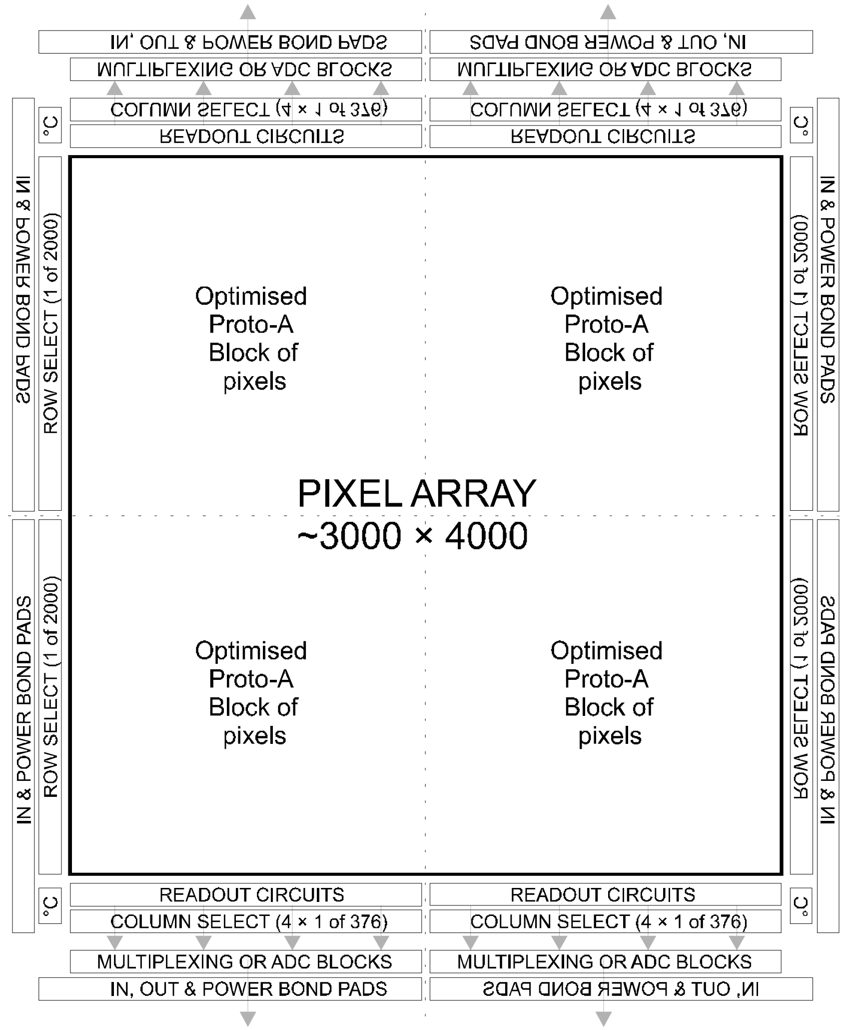

Image Sensors for Planetary Exploration

3 Mega-pixel Wavefront Sensor for the E-ELT

- 1680×1680 pixels
- 24 μm square pixels
- Up to 1000 frames/sec (fps)
- <3e- total noise at 700 fps
- Fully digital sensor
- 40 (9-bit) ADCs per column (a total of 68,000 ADCs)

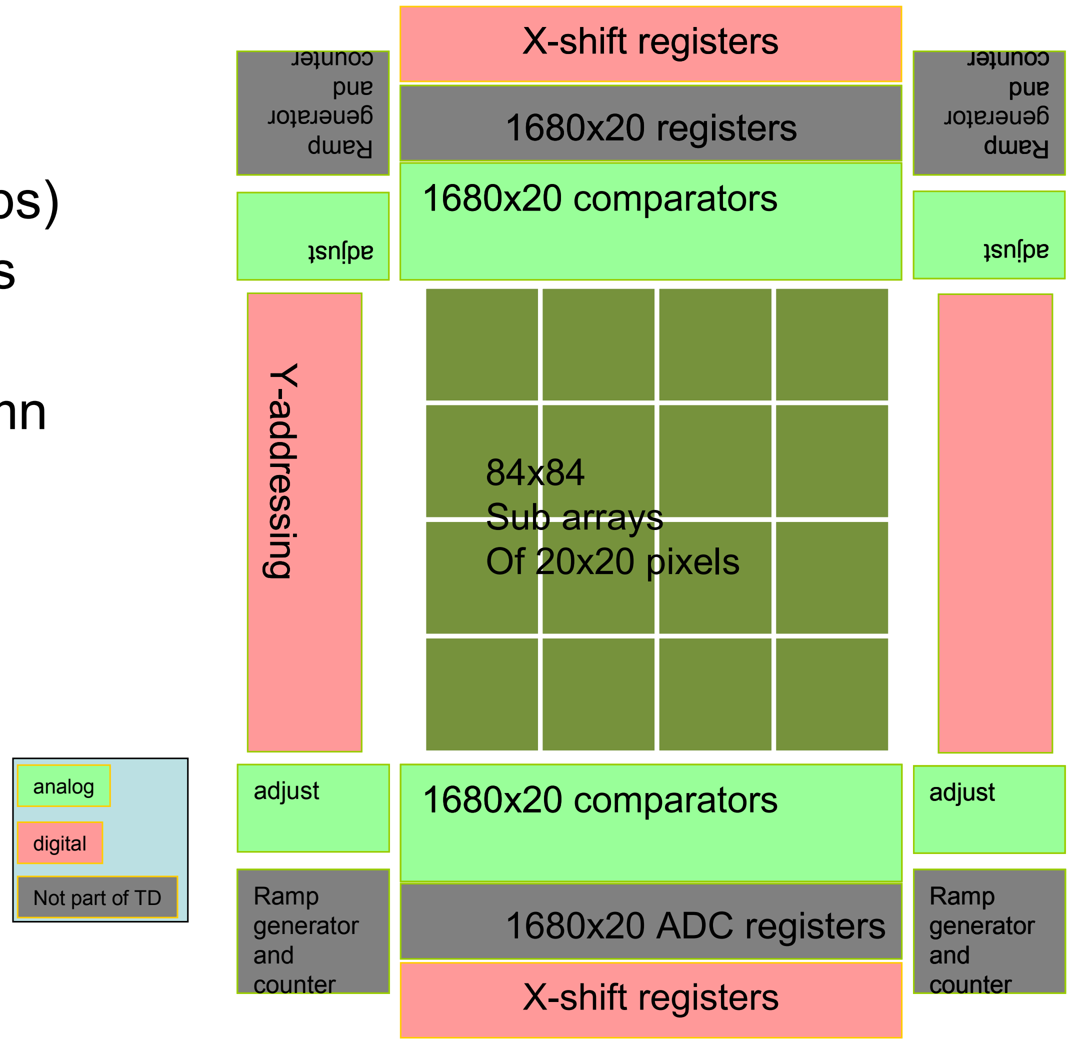

CMOS STITCHING

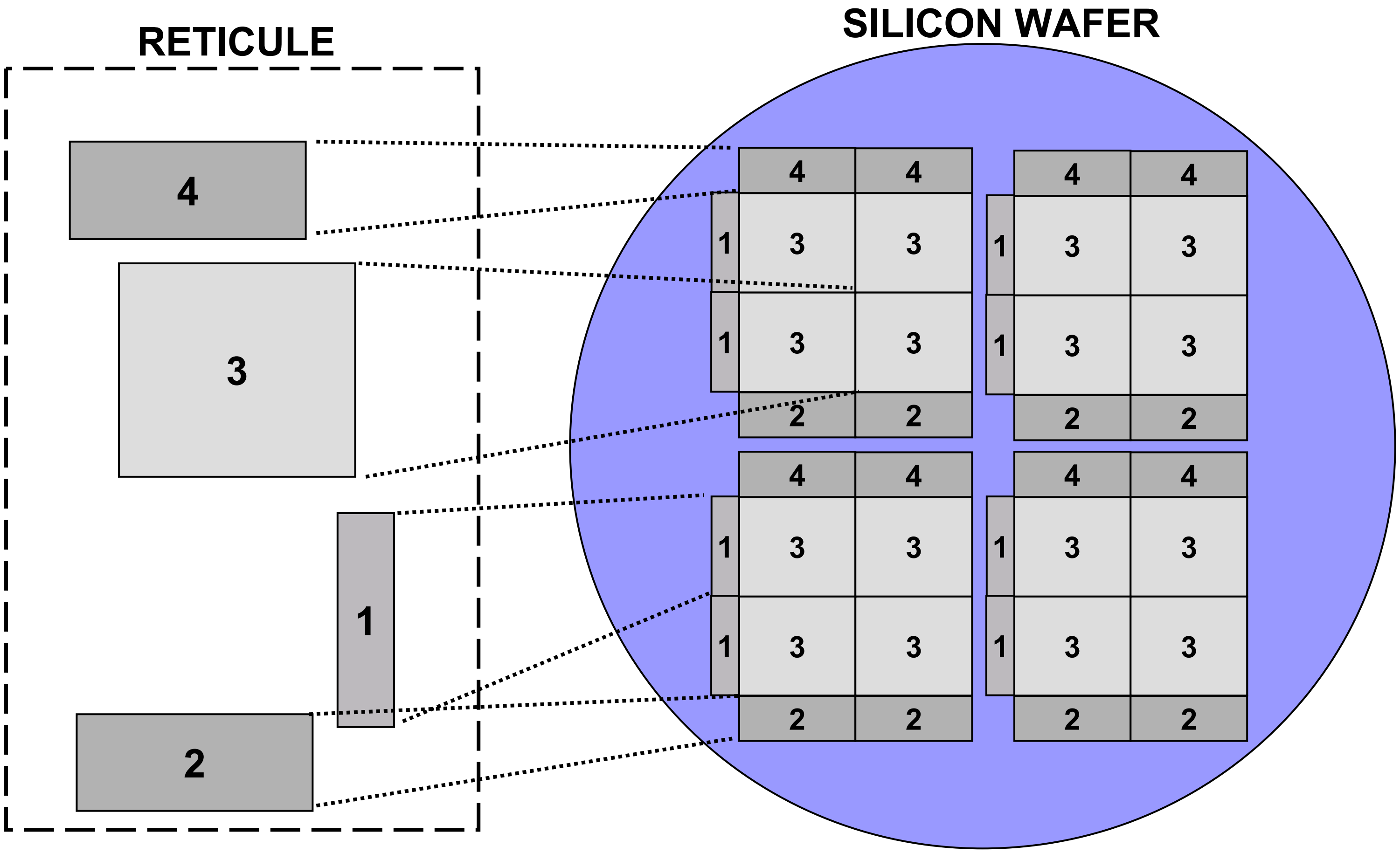

Mk (H) x Nk (V) x 10um IMAGERS

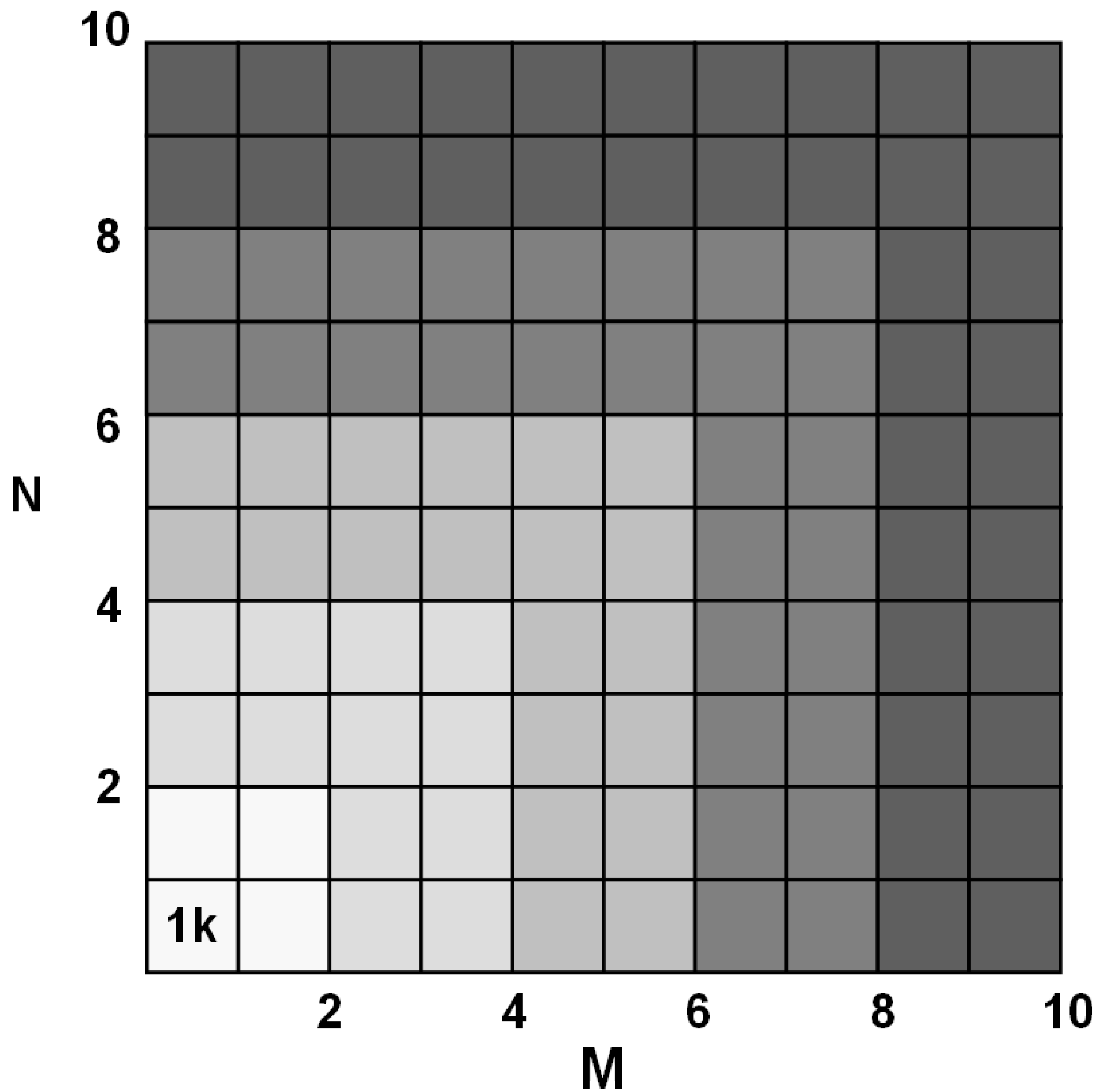

10k x 10k x 10µm COLOSSAL MINIMAL IMAGER CURRENTLY BEING DESIGNED.

Thank you for your attention

Teledyne

Enabling humankind to understand the Universe and our place in it